35e jaargang 2013 nummer 3 issn 1381 - 4842

TIJDSCHRIFT VOOR NUCLEAIRE GENEESKUNDE

^{18}F-methylcholine PET bij prostaatcarcinoom

BelNuc abstracts

^{18}F-labeling van biomoleculen

Rapiscan®
regadenoson

IDB Holland bv
From Atom to Image

Now this won't take a minute...

Rapiscan is the only standard dose, infusion pump-free, selective coronary vasodilator for use as a pharmacological stress agent for radionuclide myocardial perfusion imaging.

- Administer Rapiscan as a full 10 sec IV injection
- Flush immediately with 5 ml saline
- Deliver radiotracer 10-20 seconds after saline flush

Stress simplified by design

RAPISCAN® ▼ (regadenoson)
ABBREVIATED PRESCRIBING INFORMATION

PRESCRIBERS SHOULD READ THE SUMMARY OF PRODUCT CHARACTERISTICS (SPC) Rapiscan vials contain regadenoson (400 microgram solution for injection). Indication: Pharmacological stress agent for radionuclide myocardial perfusion imaging in adult patients which are unable to undergo adequate exercise stress. Dosage and Administration: Each 5 mL vial contains 400 micrograms regadenoson, which is injected over 10 seconds into a peripheral vein followed by 5 mL saline (0.9% sodium chloride) solution flush. The radiopharmaceutical should be administered 10-20 seconds after saline injection. The same catheter may be used for Rapiscan and the radiopharmaceutical. Patients should avoid consumption of any products containing methylxanthines (e.g. caffeine) as well as any medicinal products containing theophylline for at least 12 hours before Rapiscan administration. When possible, dipyridamole should be withheld for at least two days prior to Rapiscan administration. Contra-indications: Hypersensitivity to active substance or excipients; patients with second or third degree AV block or sinus node dysfunction who do not have a functioning artificial pacemaker; unstable angina that has not been stabilised with medical therapy; severe hypotension; decompensated heart failure. Precautions: Rapiscan has the potential to cause serious and life-threatening reactions. Continuous ECG monitoring should be performed and vital signs monitored at frequent intervals until ECG parameters, heart rate and blood pressure have returned to pre-dose levels. Aminophylline may be administered by slow intravenous injection to attenuate severe and/or persistent adverse reactions to Rapiscan. Fatal cardiac arrest, life-threatening ventricular arrhythmias, and myocardial infarction may result from the ischaemia induced by pharmacologic stress agents like regadenoson. Adenosine receptor agonists including regadenoson can depress the sinoatrial (SA) and AV nodes and may cause first, second or third degree AV block, or sinus bradycardia. Adenosine receptor agonists including regadenoson induce arterial vasodilation and hypotension. The risk of serious hypotension may be higher in patients with autonomic dysfunction, hypovolemia, left main coronary artery stenosis, stenotic valvular heart disease, pericarditis or pericardial effusions, or stenotic carotid artery disease with cerebrovascular insufficiency. Adenosine receptor agonists may cause bronchoconstriction and respiratory compromise. For patients with known or suspected bronchoconstrictive disease, chronic obstructive pulmonary disease (COPD) or asthma, appropriate bronchodilator therapy and resuscitative measures should be available prior to Rapiscan administration. Regadenoson stimulates sympathetic output and may increase the risk of ventricular tachyarrhythmias in patients with a long QT syndrome. This medicinal product contains less than 1 mmol sodium (23 mg) per dose. However, the injection of sodium chloride 9 mg/ml (0.9%) solution given after Rapiscan contains 45 mg of sodium. To be taken into consideration by patients on a controlled sodium diet. Undesirable effects: Adverse reactions in most patients were mild, transient (usually resolving within 30 minutes) and required no medical intervention. Rapiscan may cause myocardial ischaemia, hypotension leading to syncope and transient ischaemic attacks, and SA/AV node block requiring intervention. Aminophylline may be used to attenuate severe or persistent adverse reactions. Very common adverse events reported were dyspnoea, headache, flushing, chest pain, electrocardiogram ST changes, gastrointestinal discomfort, and dizziness. Common adverse events reported were paraesthesia, hypoaesthesia, dysgeusia, angina pectoris, atrioventricular block, tachycardia, palpitations, other ECG abnormalities including electrocardiogram QT corrected interval prolonged, hypotension, throat tightness, throat irritation, cough, vomiting, nausea, oral discomfort, back, neck or jaw pain, pain in extremity, musculoskeletal discomfort, hyperhidrosis, malaise, and asthenia. See SPC for details of other undesirable effects. Presentation: One carton contains a single vial of Rapiscan (400 micrograms regadenoson in 5mL solution for injection). Price: Please see your local distributor. ATC code: C01EB21. Legal Classification: UR. Marketing authorization holder: Rapidscan Pharma Solutions EU Ltd, Regent's Place, 338 Euston Road, London, NW1 3BT, United Kingdom. Marketing authorization number: EU/1/10/643/001 Date of preparation: April 2012.

IDB Holland is the exclusive distributor in The Netherlands

IDB Holland bv
Weverstraat 17
5111 PV Baarle-Nassau
The Netherlands

Phone: +31 (0)13 507 9558
Fax: +31 (0)13 507 9912
E-mail: sales@idb-holland.com
Internet: www.idb-holland.com

Date of preparation: April 2012 RPS EU 12-009

For more information please visit www.rapiscan-mpi.com

INHOUD

VAN DE REDACTIE

Door op de ingeslagen weg

In de vorige uitgave van ons Tijdschrift meldden wij enthousiast dat daarin maar liefst twee artikelen waren opgenomen waarin oorspronkelijke bevindingen gepresenteerd en bediscussieerd werden. In het nummer dat voor u ligt zetten we deze lijn voort. Wederom zult u een artikel aantreffen met oorspronkelijke data. In patiënten met prostaatkanker die een verhoogd risico hebben op uitzaaiingen in lymfklieren, worden die lymfklieren door de uroloog via laparoscopische weg uit het bekken genomen. Collega van Os heeft bestudeerd of ^{18}F-methylcholine PET/CT deze rol van de uroloog over kan nemen.

De Belgische Vereniging voor Nucleaire Geneeskunde organiseerde van 24 tot 26 mei jl. een goedbezocht symposium dat plaatsvond in Oostende, in het Thermae Palace hotel. In onze vorige uitgave werd onderstreept dat ook Nederlandse collega's van harte welkom waren, en aan deze oproep is massaal gehoor gegeven. Ruim 80 Nederlanders waren aanwezig bij het symposium, en de reacties waren zeer positief. In deze uitgave vindt u alle zevenendertig abstracts van dit symposium.

^{18}F-FDG PET/CT neemt een centrale plaats in de stagering van lymfoompatiënten. De laatste jaren is ook veel onderzoek gedaan naar de eventuele rol voor FDG PET in een vroege fase van de behandeling van deze patiënten (interim PET/CT). Collegae Zijlstra en Hoekstra hebben de stand van zaken hierover voor u op een rij gezet.

^{18}F-gelabelde PET tracers worden steeds vaker ingezet in klinisch onderzoek. Collegae de Vries en Elsinga betogen dat ^{18}F-gelabelde prosthetische groepen goed bruikbaar zouden kunnen zijn voor binding aan verscheidene functionele groepen van biomoleculen. Deze labelingstechnieken bieden wellicht mogelijkheden om het scala aan ^{18}F-gelabelde tracers uit te breiden.

Recentelijk bereikte ons het bericht dat Dirk Roeda is overleden, op 19 juli 2013. Dirk heeft als radiochemicus op verschillende plekken in Europa gewerkt en een belangrijke bijdrage geleverd aan de verdere ontwikkeling van de radiochemie, voornamelijk ten bate van PET onderzoek. Namens de redactie wensen wij zijn nabestaanden veel sterkte toe in deze moeilijke tijd.

Jan Booij
Hoofdredacteur

Voorblad: PET/CT scan (3D volume-rendered) van een muis met een subcutane pancreas tumor (AR42J) in de rechterflank. De muis is geïnjecteerd met NOTA-octreotide gelabeld met Al^{18}F, een nieuwe ^{18}F-labelingsmethode, zoals ook beschreven staat in het artikel van de Vries en Elsinga.
(met dank aan Dr. P. Laverman, UMC St. Radboud, Nijmegen)

Staging patients with high risk prostate cancer: ^{18}F-methylcholine PET/CT can not replace pelvic lymph node dissection

K.J. van Os[1], MD, E.J. Trip[2], MD, H.H.E. van Melick[2], MD PhD, J.F. Verzijlbergen[1,4], MD PhD, K.C. Kuijpers[3], MD PhD, M.M.C. van Buul[1], MD PhD

[1]Department of nuclear medicine, St. Antonius Hospital, Nieuwegein, the Netherlands
[2]Department of urology, St. Antonius Hospital, Nieuwegein, the Netherlands
[3]Department of pathology, St. Antonius Hospital, Nieuwegein, the Netherlands
[4]Department of nuclear medicine, Erasmus MC, Rotterdam, the Netherlands

Abstract

Van Os KJ, Trip EJ, Van Melick HHE, Verzijlbergen JF, Kuijpers KC, Van Buul MMC. Staging patients with high risk prostate cancer: ^{18}F-methylcholine PET/CT can not replace pelvic lymph node dissection.

Purpose The incidence of (advanced) prostate cancer (PCa) is increasing. In patients with high risk PCa, lymph node (LN) metastasis most commonly involve the internal iliac, external iliac, or obturator nodes. For LN staging, pelvic lymph node dissection (PLND) is the gold standard. The aim of this study was to evaluate if ^{18}F-methylcholine positron emission tomography/computed tomography (FCH PET/CT) could replace invasive PLND.

Materials and methods A consecutive series of 16 patients with high risk PCa according to D'Amico criteria (or cT3, or PSA > 20, or Gleason ≥ 8) and a chance of ≥ 15% to have LN metastasis according to the MSKCC nomogram was prospectively included between May 2011 and July 2012. All patients underwent routine laparoscopic pelvic lymph node dissection (LPLND) after FCH PET/CT. Acquisition started 3-15 minutes after injection of the radiotracer. The blinded reviewed imaging results were compared with histology. Sensitivity, specificity, positive and negative predictive values (PPV, NPV) of FCH PET/CT were calculated.

Results Sixteen patients were included with a mean age of 69 years (60-77 yrs), median PSA 16.4 µg/L (2.8-363 µg/L), mean Gleason score 8.2. Sensitivity, specificity, PPV and NPV were calculated as follows: 63%, 88%, 83%, and 70% respectively. In none of the patients distant metastases were found.

Conclusion In patients with high risk prostate cancer, ^{18}F-methylcholine PET/CT can not replace laparoscopic pelvic lymph node dissection in the staging procedure. These results are comparable with studies in literature in which FCH PET/CT was acquired at 60 minutes pi.

Tijdschr Nucl Geneesk 2013; 35(3):1084-1088

Introduction

In the Netherlands, the incidence of prostate cancer (PCa) is 124 patients /100.000 or 10.166 new cases per year in 2009 (1). Nearly two thirds are diagnosed in men aged 65 years or older, and it is rare before the age of 40. The average age at the time of diagnosis is about 67. In Western men, it is the most common cancer and the second leading cause of cancer death (2). In the early nineties, there was a sharp increase of incidence of PCa due to the rapid diffusion of screening interventions that have the ability to detect asymptomatic disease (3). It has been expected that the rise of incidence of PCa will continue with the increase of ageing population.

Depending on risk stratification, age, co-morbidity and patients preferences, different treatment options exist. The d'Amico risk stratification in low, intermediate and high risk disease is often used and is based on prostate specific antigen (PSA) level, tumour (T)-stage and Gleason score (4).
Depending on the above mentioned factors a choice has to be made between therapies like radical prostatectomy, brachytherapy or external radiotherapy. Active surveillance can be a good option in older patients with low-risk disease. In locally advanced disease there are grossly two options depending on patient health. Radical prostatectomy with pelvic lymph node dissection (PLND) is possible next to a combination of external radiotherapy often with temporary use of androgen deprivation therapy (ADT) (5). In confirmed metastatic disease, treatment has a palliative intent and only ADT is used. Imaging is not very sensitive and specific in diagnosing lymphogenic dissemination, though imaging results do have therapeutic consequences. In order to predict the chance of lymphogenic disseminated disease, the Memorial Sloan-Kettering Cancer Center (MSKCC) Nomogram (http://nomograms.mskcc.org/Prostate/PreTreatment.aspx) is commonly used. In our clinic the cut off point is 15% to perform an additional bilateral PLND including the obturator fossa and the external iliac artery.

Positron emission tomography (PET) has limited utility in clinically localised prostate cancer. Cellular uptake of ^{18}F-FDG is highly variable (6). Although ^{18}F-FDG may accumulate in aggressive and undifferentiated tumours, PCa often presents with poor avidity for ^{18}F-FDG, probably because of the high incidence of well-differentiated tumours (7). Among the different PET tracers evaluated for PCa imaging, carbon-11/ fluor-18 (^{11}C/^{18}F) choline has been particularly investigated. It is widely used for restaging PCa patients (8). Choline is an essential component of phospholipids of the cell membrane. Cell proliferation and upregulation of choline kinase are two mechanisms suggested for the increased uptake of this tracer in PCa (9). This malignancy-induced upregulation of choline kinase leads to the incorporation and trapping of choline in the form of phosphatidylcholine (lecithin) in the tumour cell membrane. Choline uptake in prostate tumours appears not to be correlated with cellular proliferation (10). Both ^{11}C- and ^{18}F-labelled choline are used for imaging. ^{11}C-choline has a shorter half-life of 20 minutes which requires an onsite cyclotron facility. Choline has a rapid renal clearance, therefore a short postinjection time interval seems to be optimal to avoid overprojection of bladder activity.

The aim of this study was to evaluate if ^{18}F-methylcholine positron emission tomography/computed tomography (FCH PET/CT) can replace LPLND (laparoscopic pelvic lymph node dissection) in patients with high risk prostate cancer. Furthermore, it was questioned if a relation could be found between false-negative results and FCH PET/CT uptake in the prostate.

Patients and methods

Between May 2011 and August 2012, a consecutive series of 16 patients with newly diagnosed untreated prostate cancer, was included. All patients were at high risk, according to the D'Amico criteria with cT3 or PSA>20 or Gleason ≥8, and a chance of ≥ 15% to have lymphogenic disseminated disease according to the MSKCC nomogram. All patients were scheduled for LPLND. Before LPLND, patients were referred to the Department of Nuclear Medicine for FCH PET/CT.

^{18}F-methylcholine PET/CT

^{18}F-methylcholine was produced in the VU Medical Centre, Amsterdam, and transported to our hospital.
Patients were prehydrated with 0.5 l water orally before the intravenous administration of the radiotracer, each receiving 2.3 MBq/kg body weight (maximum 400 MBq). Acquisition started 3-15 min after injection of the radiotracer.
PET/CT data were acquired on a Philips Gemini TF-64 PET/CT scanner. A low dose CT scan (64-slice helical, 120 kV, maximum 50 mAs), was acquired from mid-thigh to the skull. PET of the same region was obtained with an acquisition time of 3 min per bed position. CT, PET and fused PET/CT data were analysed on a Hermes Hybrid Viewer Workstation. FCH PET/CT scans were interpreted considering regional and distant metastases. Scans were interpreted by a blinded and independent nuclear medicine physician. Increased uptake in pelvic lymph nodes, higher than muscle activity, was considered to be positive. Assessment was made for both sides separately. Furthermore, a semiquantitative analysis was given for the prostate activity: mild (SUV_{max} < 4.0), moderate (4.0 ≤ SUV_{max} ≥ 10.0) or severe (SUV_{max} > 10.0).

Laparoscopic PLND

All PLNDs were performed laparoscopically (LPLND) and bilateral with a mean of 18 days after FCH (range 1-55 days). An extended template was used including the obturator fossa and the region lateral to the external iliac artery. The cranial border was the ureter and the caudal border the Cloquet node.

Histological examination

After dissection the lymph nodes were examined histologically according to standard protocols. Lymph nodes were dissected from the surrounding fat, counted and cut into slices of 2-3 mm and processed. Sections of 4 µm were stained routinely with haematoxylin and eosin (HE). To confirm the diagnosis based on the HE-slides, in 5 of 16 patients additional immunohistochemical staining with a pankeratin antibody MNF116 and in one patient with a PSA antibody was performed.

Statistical analysis

The results of FCH PET/CT were compared with the histological results of the dissected lymph nodes. Sensitivity, specificity, positive predictive value (PPV) and negative predictive values (NPV) were calculated for patients as well as lymph node specimen. If in a patient one of two dissected specimens was true positive, the patient was considered to be true positive.
In patients with false negative FCH PET/CT-results, the uptake of FCH in the prostate was compared with the histological results.

Results

The characteristics of the patients are summarised in table 1. The mean age of the patients was 69 years (60-77 years). The median PSA at time of the FCH PET/CT was 16.4 µg/L (2.8-363 µg/L), mean Gleason-score 8.1.

LPLND was performed with a mean interval of 19 days (range 1-55 d) after FCH PET/CT.
In total, 31 lymph node specimens could be evaluated in 16 patients. One specimen did not contain any lymph nodes. In another patient, the left fossa could not be investigated because of adhesions due to macroscopic tumour mass. This was considered to be histologically proven.

Out of the 16 patients, FCH PET/CT revealed 5 true positives, 7 true negatives, 1 false positive, and 3 false negatives. The sensitivity, specificity, PPV and NPV were calculated 63%, 88%, 83% and 70%, respectively (tables 2 and 3, figures 1 and 2).

Table 1. Characteristics of 16 patients with high risk prostate cancer

patient	age	T	PSA	Gleason
1	73	cT3	52	9
2	77	cT3	7.6	8
3	64	cT3	16.1	8
4	68	cT3	6.6	9
5	65	cT4	363	7
6	70	cT3	8.3	7
7	60	cT3	11.7	7
8	69	cT1	22.9	9
9	67	cT3	85.3	8
10	60	pT3	14.1	9
11	70	cT3	26.6	8
12	71	pT3	17	9
13	75	cT4	16.7	9
14	69	cT3	2.8	9
15	71	cT3	19.4	8
16	74	cT3	16.1	7
mean **median**	**69**		**42.9** **16.4**	**8.1**

Table 2. Contingency table patient results.
FCH + represents a positive ^{18}F-methylcholine PET/CT scan, and FCH – negative findings on ^{18}F-methylcholine PET/CT.

n=16	histology+	histology-	
FCH +	5	1	6
FCH -	3	7	10
	8	**8**	**16**

Table 3. Contingency table lymph node specimen results
FCH + represents a positive ^{18}F-methylcholine PET/CT scan, and FCH – negative findings on ^{18}F-methylcholine PET/CT.

fossae n=31	histology+	histology-	
FCH +	5	4	9
FCH -	5	17	22
	10	**21**	**31**

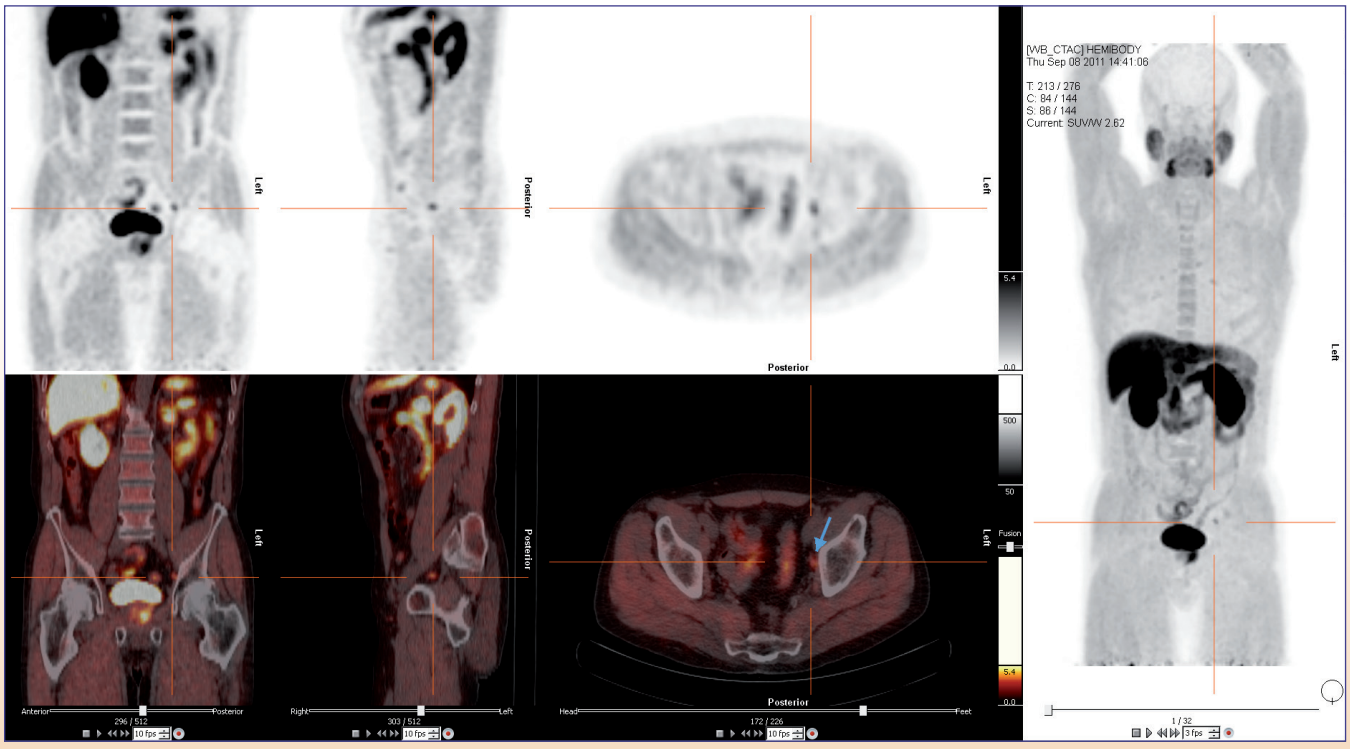

Figure 1. True positive para-iliac lymph node (blue arrow)

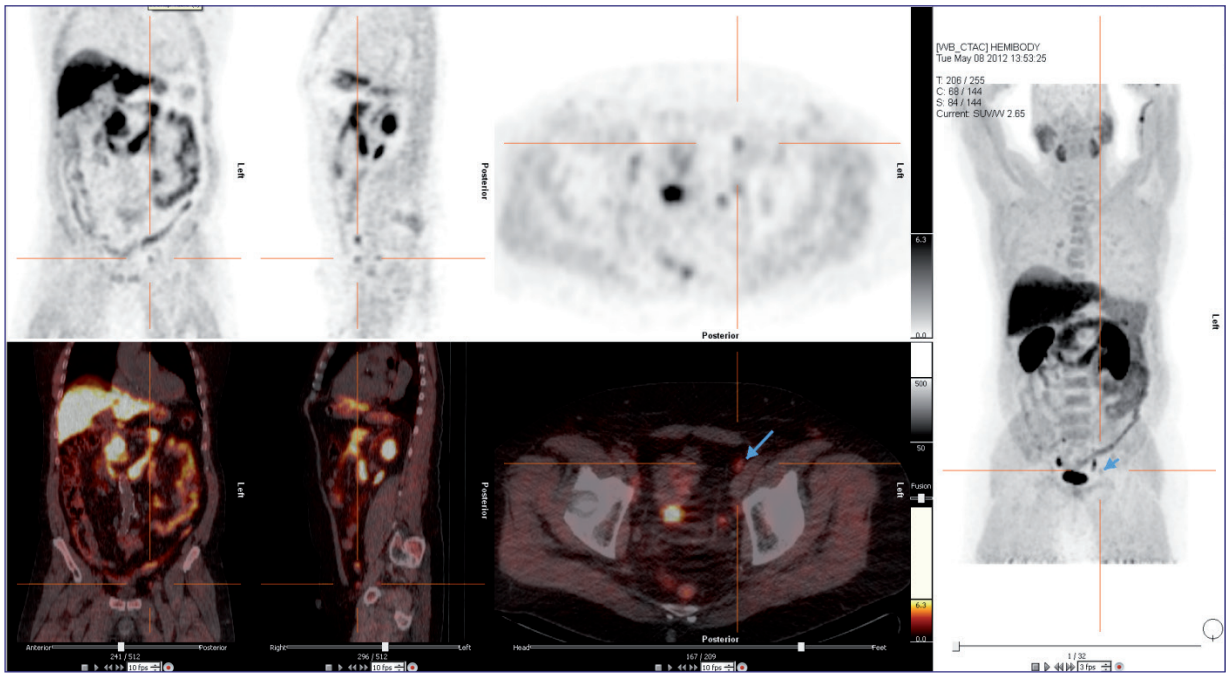

Figure 2. False positive para-iliac lymph node (blue arrows)

Out of 31 dissected lymph node specimens, there were 17 true negatives, 5 true positives, 5 false negatives, 4 false positives. The sensitivity, specificity, PPV and NPV were calculated as 50%, 81%, 56% and 77%, respectively (table 3).

In the five false negative specimens, the prostate uptake was moderate in four and severe in one case (table 4).Therefore, no relation was found between false negative findings and choline uptake in the prostate. In addition, no distant metastases were found.

Discussion

In this small population of patients with high risk prostate cancer, the results were comparable with those of a recent study of Poulsen et al (10). They reported a sensitivity and specificity of 73% and 88%, respectively. In this Danish/German study, patients were scanned 60 minutes after injection of ^{18}F-choline. It was suggested that the low sensitivity was caused by disturbing urine activity in the bladder. However, in our study, we found the same results while patients were scanned within 3-15 minutes post injection (pi). This suggests that bladder activity is of no importance in reviewing the images. Oprea-Lager et al suggested previously that the change in standardised uptake value (SUV) over time in a dual phase FCH PET protocol could discriminate between reactive and malignant lymph nodes. Lymph nodes seen on the scan performed 2 minutes pi and still visible on the scan 30 minutes later were considered malignant, while the lymph nodes with decreasing uptake over time were considered to be benign (12). According to this study, scanning 60 minutes pi, like in the Danish/German study, would not have a negative effect on the sensitivity and specificity for that reason. Because choline is incorporated in the cell membrane no difference in results of different postinjection scanning times is expected. De Jong et al already showed in 2003 promising results while using ^{11}C-choline

Table 4. Relation between maximal choline uptake in the prostate and the lymph node specimen result.

patient	specimen right	specimen left	SUV_{max} prostate	classification
1	TP	TP	7.9	moderate
2	TN	FN	5.1	moderate
3	TN	TP	8.2	moderate
4	FN	TN	4.2	moderate
5	FN	TN	10.2	severe
6	FN	TP	5.2	moderate
7	TN	TN	5.8	moderate
8	TN	TN	7.3	moderate
9	TN	-	19.5	severe
10	TN	TN	3.9	mild
11	TN	TN	7.8	moderate
12	FP	TN	10.3	severe
13	FP	TP	3.9	mild
14	FP	FP	3.0	mild
15	TN	TN	7.0	moderate
16	FN	TN	5.8	moderate

TP = true positive; TN = true negative; FN = false negative; FP= false positive

(13). They reported a sensitivity and specificity of 80% and 93%, respectively. Until recently it was assumed that ^{18}F-choline and ^{11}C-choline were comparable, however, this has never been fully explored. This might be an explanation for the significantly lower sensitivity found in our study compared to the results of De Jong. A point of discussion is the extent of the PLND (10) as well as the terminology of the area dissected, and thereby the comparison of the resected specimen and the positive lymph nodes seen on choline PET/CT. The difficulty of the dissection probably also plays a role. Patient number one for example showed bilateral choline-avid para-iliacal lymph nodes. During LPLND, it was difficult to obtain tissue for histological confirmation, due to many adhesions. Therefore, the surgeons decided to disregard the left side and dissected only the right obturator fossa. One of the reasons was that the tissue appeared macroscopically pathological. Histological examination however showed no malignancy at the right side, which of course is hard to believe since the FHC as well as the examination during surgery was very much suspicious for malignant spread. In our small population, this histologically unproven finding in a macroscopically positive patient negatively influenced the specificity. In our data, no relation was found between the choline uptake in the prostate and the false-negative results in the para-iliac lymph nodes.

Conclusion

In patients with high risk prostate cancer, ^{18}F-methylcholine PET/CT seems not capable of replacing laparoscopic pelvic lymph node dissection in the staging procedure. Our results, with a low sensitivity of 63% and acceptable specificity of 88%, are comparable with the results of studies in literature in which FCH PET/CT was acquired at 60 min pi. Therefore, the suggestion of former investigators that the low sensitivity was caused by disturbing urine activity in the bladder can not be confirmed. In patients with negative FCH PET/CT findings and histologically proven metastasis, no relation could be found with FCH uptake in the prostate.

k.van.os@antoniusziekenhuis.nl

References

1. Nationaal Kompas Volksgezondheid. www.nationaalkompas.nl/gezondheid-en-ziekte/ziekten-en-aandoeningen/kanker/prostaatkanker/cijfers-prostaatkanker-prevalentie-incidentie-en-sterfte-uit-de-vtv-2010-kopie/
2. American Cancer Society. Cancer. Facts & Figures 2012. www.cancer.org
3. Potosky AL, Miller BA, Albertsen PC, Kramer BS. The Role of Increasing Detection in the Rising Incidence of Prostate Cancer. JAMA. 1995;273:548-52
4. D'Amico AV, Whittington R, Malkowicz SB, et al. Biochemical outcome after radical prostatectomy, external beam radiation therapy, or interstitial radiation therapy for clinically localized prostate cancer. JAMA. 1998 16;280:969-74
5. Bolla M, Van Tienhoven G, Warde P, et al. External irradiation with or without long-term androgen suppression for prostate cancer with high metastatic risk: 10-year results of an EORTC randomised study. Lancet Oncol. 2010;11:1066-73
6. Price DT, Coleman RE, Liao RP, et al. Comparison of 18F-fluorocholine and 18F-fluorodeoxyglucose for positron emission tomography of androgen dependent and androgen independent prostate cancer. J Urol. 2002;168:273-280
7. Picchio M, Briganti A, Fanti S, et al. Role of Choline Positron Emission Tomography/ComputedTomography in the Management of Patients with Prostate-SpecificAntigen Progression After Radical Treatment of Prostate Cancer. Eur Urol. 201; 59:51-60
8. Krause BJ, Souvatzoglou M, Tuncel M, et al. The detection rate of 11C-choline-PET/CT depends on the serum PSA-value in patients with biochemical recurrence of prostate cancer. Eur J Nucl Med Mol Imaging. 2008;35:18–23
9. Richter JA, Rodriguez M, Rioja J, et al. Dual tracer 11C-choline and FDG-PET in the diagnosis of biochemical prostate cancer relapse after radical treatment. Mol Imaging Biol. 2010;12:210–7
10. Jadvar H. Prostate Cancer: PET with 18F-FDG, 18F- or 11C-Acetate, and 18F- or 11C-Choline. J Nucl Med. 2011;52:81-9
11. Poulsen M, Bouchelouche K, Høilund-Carlsen P, et al. 18F-fluoromethylcholine (FCH) positron emission tomography/computed tomography (PET/CT) for lymph node staging of prostate cancer: a prospective study of 210 patients. BJU Int. 2012;110:1666-71
12. Oprea- Lager D, Vincent A, van Moorselaar R, et al. Dual-Phase PET-CT to Differentiate 18F-Fluoromethylcholine Uptake in Reactiev and Malignant Lymph Nodes in Patients with Prostate Cancer. PLOS One. 2012; 7, e48430
13. Jong de IJ, Pruim J, Elsinga P, Valburg W, Mensink HJ. Preoperative Staging of Pelvic Lymph Nodes in Prostate Cancer by 11C-Choline PET. J Nucl Med. 2003; 44:331-5

Application of ^{18}F-labelled prosthetic groups for synthesis of radiolabelled biomolecules

Dr. E.F.J. de Vries and Prof. Dr. P.H. Elsinga

Department of Nuclear Medicine and Molecular Imaging, University Medical Center Groningen, University of Groningen, the Netherlands

Abstract

De Vries EFJ, Elsinga PH. Application of ^{18}F-labelled prosthetic groups for synthesis of radiolabelled biomolecules. As complementary to radiopharmaceuticals with radiometals, PET imaging with ^{18}F-labelled biomolecules is a powerful tool. Several ^{18}F-labelled prosthetic groups that can react with a variety of functional groups within biomolecules are now available. In this article several synthesis methods are being discussed, such as acylation, alkylation, formation of oximes and hydrazones, and application of click chemistry. A toolbox of prosthetic groups has become available to properly select the optimal conjugation strategy for the preparation of ^{18}F-biomolecules.
Tijdschr Nucl Geneesk 2013; 35(3):1089-1093

Introduction

Traditionally, larger molecules like peptides, proteins and oligonucleotides were labelled with gamma-emitting radiometals, such as ^{99m}Tc and ^{111}In for planar scintigraphy or SPECT imaging. PET has a higher intrinsic sensitivity than SPECT and planar scintigraphy, because it does not require the use of a collimator. PET can also provide higher resolution images in humans. In the last decade, attention has therefore grown to label larger biomolecules with ^{18}F in order to utilise the favourable properties of this isotope for PET imaging. The ^{18}F-labelled prosthetic groups that are applied for labelling biomolecules are generally neutral and therefore are less likely to affect clearance of the conjugated biomolecule. This is an advantage over radiometal labelling, which generates positively charged molecules, which affect biodistribution and clearance.

Because of the harsh conditions often required for ^{18}F-fluorine labelling (i.e. organic solvents and high temperatures), direct labelling of biomolecules is typically not possible, because this will lead to decomposition or denaturation of the biomolecule. Direct ^{18}F-fluorine labelling is also hampered by the presence of reactive functional groups on biomolecules. Alternatively, the 'prosthetic group' approach is commonly employed.

A prosthetic group can be seen as a *bifunctional ligand* which serves as a linker between the radioactive atom and biomolecule of interest. Ideally, the bifunctional ligand should be stable and regioselectively incorporate the radionuclide with high reactivity. Conjugation of the prosthetic group to the biomolecule should not interfere with the biological activity and specificity of the biomolecule. Versatility is often a key issue, as a prosthetic group with high utility is more likely to find clinical acceptance. The effect of the prosthetic group on the lipophilicity of the conjugated biomolecule should also be taken into account. The hydrophilic or lipophilic character of the labelled compound directs excretion either through the hepatobiliary or the renal-urinary tract, respectively. In case of lipophilic prosthetic groups the overall lipophilicity can be counterbalanced by introduction of sugar moieties.

Biomolecules are (indirectly) radiolabelled in two different ways. In *pre-labelling*, the radionuclide is first incorporated into a ligand, which is subsequently conjugated to the biomolecule. The *post-labelling* approach involves conjugation of a precursor ligand to the biomolecule prior to radioactive labelling.

The Al^{18}F-methodology (see cover) can be considered as a post-labelling approach (1). Until now, most prosthetic groups in ^{18}F-fluorine chemistry are labelled in a pre-labelling fashion. Unfortunately, this means that synthesis of most ^{18}F-based prosthetic groups require multiple steps.

The *natural* functional groups in biomolecules typically involved in conjugations are the amino, carboxylic acid and thiol (sulfhydryl) groups. Conjugation of the ligand via amino groups is the most common approach, since they are common to proteomic systems (that is, the N-terminus of peptides or internal lysine residues). Unfortunately, the high abundance of free amines in peptides and proteins usually results in unselective conjugation.

Natural oligonucleotides do not have functional groups like carboxylic acids or thiols. The amino groups in the bases of oligonucleotides are not suitable for conjugation of prosthetic groups, because they are not very reactive and they play a crucial role in the binding properties of the biomolecule. For radiolabelling, a reactive nucleophilic group is therefore usually attached to the 3' or 5' terminus of the oligonucleotides via a spacer. Frequently used modifications for labelling are hexylamine, hexylthiol and thiophosphate groups. These modified oligonucleotides are nowadays commercially available and can be labelled using the same prosthetic

groups that are used for the labelling of proteins and peptides. Several ^{18}F-labelled prosthetic groups have now been published. These prosthetic groups belong to different classes of molecules. Classification of these prosthetic groups is usually based on the type of conjugation reaction to the biomolecule. Acylation, Michael addition and alkylation are the most common reactions, but a few other reactions have also been applied.

Acylations

Acylations involve reactions of activated esters of ^{18}F-labelled carboxylic acids with free amino groups (e.g. N-terminal or from lysine) to form stable amide bonds. Examples of activated esters are carboxylic succinimides or imidazoles and 4-nitrophenyl or pentafluorophenyl esters. Acylations can be carried out in buffer at slightly basic pH at room temperature.

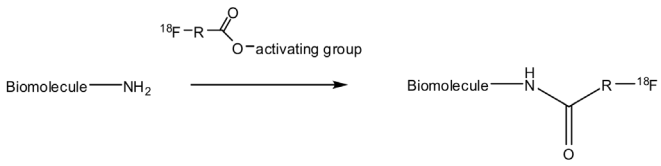

Acylation of a biomolecule amine-moiety using an activated ester.

Acylations are carried out using two different methods: i) reactions in solution and ii) solid-phase reactions. The reactions in solution are more easily carried out and do not require specific equipment or peptide chemistry experience. The disadvantage is that the reaction is not regioselective. The ^{18}F-labelled activated ester reacts potentially with all free amino groups in the biomolecule. The method is especially suitable for radiolabelling of biomolecules that cannot be produced by solid-phase peptide synthesis, such as larger peptides and proteins. Reactions using solid-phase peptide synthesis have the advantage that during the Merrifield-type production of the peptide the ^{18}F-labelled activated ester can be introduced at a specific stage during synthesis, thereby achieving high regioselectivity of the prosthetic group. This method is only suitable for smaller peptides (<20 amino acids).

One of the most common prosthetic groups used in ^{18}F-fluorine labelling of peptides and proteins is N-succinimidyl-4-[^{18}F]-fluorobenzoate ([^{18}F]SFB). In large part, this is due to the high *in vivo* stability and labelling efficiency of [^{18}F]SFB (2-6). The synthetic procedure has been optimised by several groups and can be automated using commercially available synthesis modules. The most critical step is the conversion of 4-[^{18}F]fluorobenzoic acid (FBA) to its N-succinimidyl ester using the reagent TSTU.

The acylation of peptides (at the N-terminal or ε-Lys amino group) is usually carried out in a borate buffer (pH 8.5) at room temperature. Varying amounts of peptides up to 1 mg can be used. The peptide can be purified on a reversed phase HPLC column. Specific activities are in the range of 10-25 GBq/µmol.

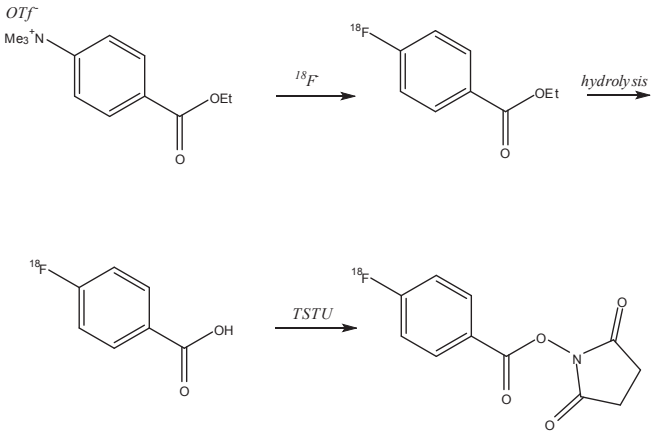

Synthesis of [^{18}F]SFB.

Michael reaction

The Michael reaction is the conjugate addition reaction of a nucleophilic species with an electrophilic multiple bond, like in α,β-unsaturated aldehydes, ketones, esters or nitriles. For the labelling of biomolecules, ^{18}F-fluorine labelled prosthetic groups that are functionalised with a maleimide moiety are very useful. The maleimide group in these reagents can undergo a Michael reaction with the free thiol function of cysteine residues in peptides and proteins or with a hexylthiol modification in oligonucleotides. Thiols are better nucleophiles and therefore more reactive than amines or carboxylic acids. However, free thiol moieties are rare in proteins, since most thiol groups in cysteine residues form disulfide bridges. Therefore, it may be required to break the disulfide bridges with e.g. mercaptoethanol to liberate the thiol groups. When a free thiol group is present in a protein and accessible for the prosthetic group, the maleimide-thiol Michael reaction could provide excellent regio- and chemoselectivity. When necessary, site-directed mutagenesis can be applied to place a cysteine residue at the surface of the protein.

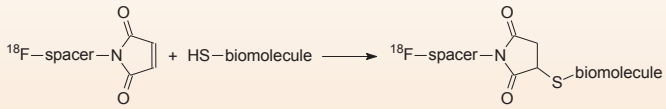

Conjugation of a maleimide prosthetic group with a biomolecule.

Maleimide-base prosthetic groups

Several ^{18}F-fluorine labelled, maleimide-functionalised prosthetic groups have been synthesised and conjugated to peptides, proteins and oligonucleotides. The synthesis of the maleimide-functionalised prosthetic groups generally

consists of two steps, more or less analogous to the synthesis of [^{18}F]SFB: labelling of a reagent with ^{18}F-fluorine, followed by addition of the maleimide functionality. Maleimide functionalisation could be used to convert an amine-reactive prosthetic group into a thiol-reactive one. This might be of interest when higher reactivity or regioselectivity is required. To this purpose, the most frequently used prosthetic group [^{18}F]SFB can be transformed into a maleimide functionalised labelling agent by reaction with N-(2-aminoethyl)maleimide (7).

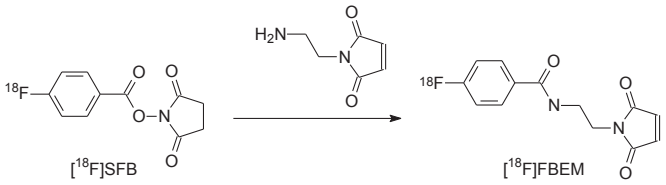

Functionalisation of [^{18}F]SFB with a maleimide moiety.

Conjugation of maleimide-base prosthetic groups

The conjugation of a labelled maleimide-functionalised prosthetic group to the thiol-containing biomolecule is typically performed in PBS or Tris buffer at pH 7 – 8 at room temperature for 10 – 30 minutes. If necessary, the prosthetic group is dissolved in a small amount of organic solvent (DMSO, ethanol) before it is mixed with the biomolecule in aqueous buffer. Labelling yields are generally very high, provided that the concentration of the biomolecule is not too low (>10 – 100 ng/ml depending on the biomolecule and prosthetic group).

Alkylations

Alkylating agents are another class of radiolabelled prosthetic groups that can be conjugated to biomolecules. Alkylations are nucleophilic substitution reactions at an alkyl carbon atom by a nucleophilic group. Amine, hydroxyl, thiol or carboxylic acid groups are nucleophiles in biomolecules that in principle can be alkylated, but the fluorine-18 labelled alkylating agents that have been used so far primarily react with sulphur containing functional groups. ^{18}F-fluorine substituted alkyl halides are usually applied as the alkylating agents in the direct radiolabelling of biomolecules like peptides, proteins and oligonucleotides.

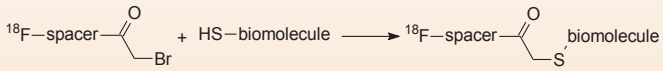

Conjugation of an ^{18}F-labelled α-bromoketone to a sulphur atom in a biomolecule.

Alkylating agents

A vast number of ^{18}F-fluorine labelled alkylating agents have been synthesised for the production of PET tracers. With the exception of the maleimides and the α-bromoketones, hardly any alkylating agent has been specifically investigated as prosthetic groups for the labelling of proteins, peptides or oligonucleotides with ^{18}F-fluorine. In Groningen, we have tested a series of known alkylating agents as potential prosthetic groups for the labelling of thiophosphate-modified oligonucleotides, using adenosine 5'-O-thiomonophosphate as a model compound (8).

In this series, α-bromo-α'-[^{18}F]fluoro-m-xylene ([^{18}F]BFX) showed promising results. So far, [^{18}F]BFX has not been used to label oligonucleotides, probably because high amounts of the expensive oligonucleotide would be required for sufficient labelling yields.

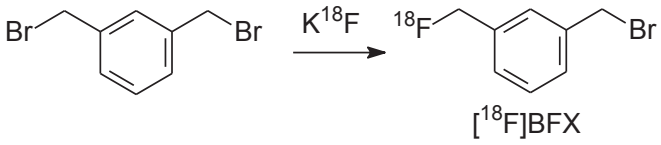

Synthesis of α-bromo-α'-[^{18}F]fluoro-m-xylene

Indirect alkylations

Indirect labelling approaches could be attractive methods when a high regioselectivity is required, for example when a site eligible to conjugation is present at a location crucial for the biological activity of the molecule. Thus, the biologically active molecule is first derivatised at a specific location, which allows selective conjugation at this specific location. For synthetic peptides, this is easily achieved by functionalising the N-terminus with chloroacetic anhydride during peptide synthesis, while the lysine residues are still BOC-protected (9). After deprotection, the peptide with a chloroacetyl function at the N-terminus is suitable for labelling using an alkylation reaction. A series of ^{18}F-fluor-labelled thiol prosthetic groups was prepared for peptide labelling by Glaser et al (9). Overall radiochemical yields (from fluoride to purified peptide) of up to 32% were obtained for a PEG type [^{18}F]fluorothiol. In principle, this approach could also be applied to the labelling proteins and oligonucleotides.

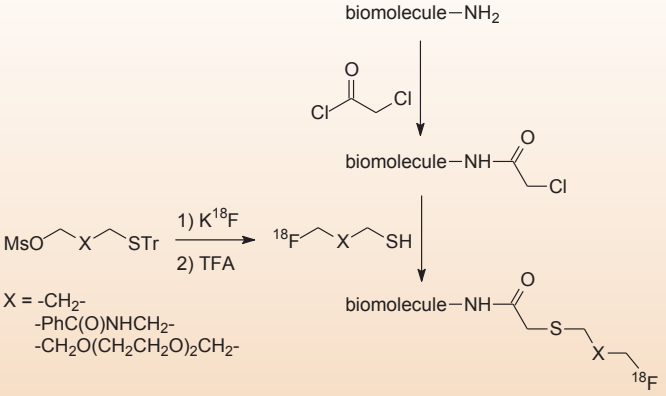

Labelling of a biomolecule via an indirect approach using fluorine-18 labelled thiols.

Other approaches

Oxime and hydrazone formation

Oxime formation is highly chemoselective. The oxime is formed through condensation of an oxoamino and a carbonyl (i.e. aldehyde or ketone) moiety. Oxime bioconjugations have been used in a number of [^{18}F]fluoropeptide preparations, as have hydrazone ligations, which are related carbonyl addition-elimination reactions. The advantage of this method is that a variety of ^{18}F-labelled aldehydes are available. There is choice in size or lipophilicity (e.g. [^{18}F]fluorobenzaldehyde, [^{18}F]FDG, [^{18}F]propionaldehyde), therefore offering the opportunity to steer pharmacokinetics. An obvious disadvantage of this method is that the biomolecules need to be derivatised with an oxoamino or HYNIC group. Native biomolecules do not react with carbonyl groups.

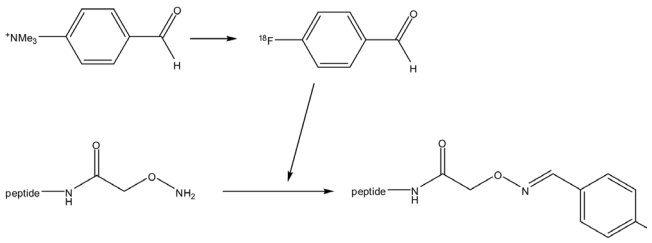

Synthesis of ^{18}F-labelled peptide by oxime formation.

Similar to oxime formation, the formation of hydrazones can be used for chemoselective coupling. Hydrazone formation is a commonly used and highly sensitive analytical method for detection of carbonyl compounds (10). It has been applied to many selective ligation reactions between peptides, proteins, sugars and fatty acid derivatives without side product formation. One hydrazine functionalizing compound is HYNIC (6-hydrazinonicotinic acid), which is widely used in nuclear medicine for ^{99m}Tc-labelling. A few reports have appeared on ^{18}F-labelling of HYNIC conjugated peptides (11-13). The reaction yield is highly dependent on pH, amount of peptide and temperature. A pH value of 4.5 is essential to obtain conjugation efficiencies of >90% with amounts of peptide of 1 mg.

Huisgen cycloaddition

The Huisgen cycloaddition is a relatively new method to prepare ^{18}F-labelled peptides. This ligation involves the 1,3-dipolar cycloaddition of azides and alkynes to form a 1,4-disubstituted 1,2,3-triazole under mild, aqueous conditions. This so-called 'click' reaction has proven very selective, fast and efficient in the presence of a Cu(I) catalyst. Other interesting characteristics of this reaction include simple reaction conditions (insensitive to oxygen and water), readily available starting materials and reagents, the use of benign solvents (such as water) or easily removable solvents, and simple product isolation. Purification, if required, can be done by non-chromatographic methods. In the figure below a schematic overview of the use of click chemistry is shown (14,15). Recently also Cu(I)-free click reactions have been published to prepare ^{18}F-fluoropeptides using extremely reactive cyclooctynes (16).

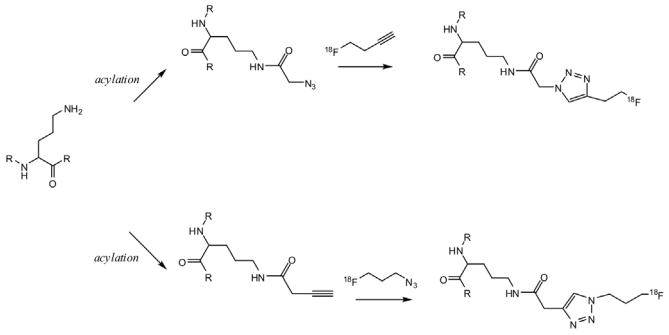

Labelling of peptides via a Huisgen cycloaddition reaction.

Concluding remarks

PET imaging with ^{18}F-labelled biomolecules has become a powerful tool in molecular imaging research. ^{18}F-labelling, however, does not replace other labelling techniques for biomolecules, usually using radiometals, but should be considered a complementary technique. Several ^{18}F-labelled prosthetic groups that can react with a variety of functional groups within biomolecules are now available. This toolbox of prosthetic groups offers the opportunity to properly select the conjugation method of choice. In this manner, care can be taken that the biological activity, kinetics and binding properties of the labelled biomolecules are maintained. Application of ^{18}F-labelled prosthetic groups could further be boosted, if the distribution networks for FDG can be exploited to disseminate the ^{18}F-labelled synthons from sites with a cyclotron to other hospitals.

References

1. Goldenberg DM, Sharkey RM, McBride WJ, Boerman OC. Al^{18}F: a new standard of radiofluorination. J Nucl Med. 2013;54:1170
2. Wester HJ, Hamacher K, Stoecklin G. A comparative study of NCA ^{18}F-fluorine labelling of proteins via acylation and photochemical conjugation. Nucl Med Biol. 1996;23,:365-72
3. Frederiksson A, Johnstrom P, Stone-Elander S et al. Labelling of human C-peptide by conjugation with N-succinimidyl-4-[18F] fluorobenzoate. J Lab Compnds Radiopharm. 2001;44: 509-19
4. Zijlstra S, Gunawan J, Burchert W. Synthesis and evaluation of a ^{18}F-labelled recombinant annexin-V derivative, for identification and quantification of apoptotic cells with PET. Appl Radiat Isot. 2003;58:201-7
5. Wuest F, Hultsch C, Bergmann R, Johannsen B, Henle T. Radiolabelling of isopeptide N$^{\varepsilon}$-(γ-glutamyl)-L-lysine by conjugation with N-succinimidyl-4-[^{18}F]fluorobenzoate. Appl Radiat Isot. 2003;59:43-8
6. Chen X, Park R, Hou Y et al. MicroPET imaging of brain tumor

angiogenesis with ^{18}F-labelled PEGylated RGD peptide. Eur J Nucl Med Mol Imaging. 2004;31:1081-9
7. Cai W, Zhang X, Wu Y, Chen X. A thiol-reactive ^{18}F-labelling agent, N-[2-(4-[^{18}F]-fluorobenzamido)ethyl]maleimide, and synthesis of RGD peptide-based tracer for PET-imaging of $\alpha_V\beta_3$ integrin expression. J Nucl Med. 2006;47:1172-80
8. de Vries EFJ, Vroegh J, Elsinga PH, Vaalburg W. Evaluation of ^{18}F-fluorine-labelled alkylating agents as potential synthons for the labelling of oligonucleotides. Appl Radiat Isot. 2003;58:469-76
9. Glaser M, Karlsen H, Solbakken M et al. ^{18}F-Fluorothiols: A New Approach To Label Peptides Chemoselectively as Potential Tracers for Positron Emission Tomograph. Bioconj Chem. 2004;15: 1447-53
10. Houdier S, Perrier S, Defranq E, Legrand M. A new fluorescent probe for sensitive detection of carbonyl compounds: sensitivity improvement and application to environmental water samples. Anal Chim Acta. 2000; 412: 221-33
11. Lee YS, Jeong JM, Kim HW et al. An improved method of ^{18}F-peptide labelling: hydrazone formation with HYNIC-conjugated c(RGDyK). Nucl Med Biol. 2006;33:677-83
12. Bruus-Jensen K, Poethko T, Schottelius M et al. Chemoselective hydrazone formation betweeb HYNIC-functionalized peptides and ^{18}F-fluorinated aldehydes. Nucl Med Biol. 2006;33:173-83
13. Rennen JJ, Laverman P, van Eerd JM et al. PET imaging of infection with a HYNIC-conjugated LTB4 antagonist labelled with ^{18}F via hydrazone formation. Nucl Med Biol. 2007;34:691-5
14. Glaser M, Arstad E. "Click labelling" with 2-[^{18}F]fluoroethylazide for positron emission tomography. Bioconj Chem. 2007;18:989-93
15. Marik J, Hausner SH, Fix LA, Gagnon MKJ, Sutcliffe JL. Solid-phase synthesis of 2-[^{18}F]fluoropropionyl peptides. Bioconj Chem. 2006;17:1017-21
16. Campbell-Verduyn LS, Mirfeizi L, Schoonen AK et al. Strain-promoted copper-free "click" chemistry for ^{18}F-radiolabelling of bombesin. Angew Chem Int Ed Engl. 2011;50:11117-20

Responscriteria voor ^{18}F-FDG PET/CT bij behandeling van het maligne lymfoom; nieuwe ontwikkelingen

Dr. J.M. Zijlstra[1], Prof. Dr. O.S. Hoekstra[2]

[1]Department of hematology, VU medisch centrum, Amsterdam, the Netherlands
[2]Department of nuclear medicine, VU medisch centrum, Amsterdam, the Netherlands

Abstract

Zijlstra JM, Hoekstra OS. Response assessment in the treatment of malign lymphoma with ^{18}F-FDG PET/CT; new developments. In recent years, advances have occurred in the staging and response assessment of lymphomas. PET combined with CT (PET/CT) has largely replaced PET as stand-alone examination. Progress in imaging is influencing trial design and has impact on clinical practice. Particularly in Hodgkin's lymphoma there seems to be a role for PET/CT in the assessment of response early in the course of chemotherapy to predict treatment outcome. International trials are underway to test image based response–adapted treatment guided by early interim PET/CT. Efforts have been made to standardise PET/CT image acquisition and interpretation in these ongoing trials and these guidelines are increasingly applied in clinical practice. The International Workshops on PET in Lymphoma held in Deauville and Menton, France, were the basis of the so-called Deauville criteria for assessment of interim PET/CT. This 5-point scale better represents different levels of residual uptake in initially involved sites. The aim was to design a reproducible method of scoring without loss of important information about the degree of response. For clinical trials this Deauville score has the ability to change the cut-off between good and poor response according to the clinical context.
Tijdschr Nucl Geneesk 2013; 35(3):1094-1097

Inleiding

In 2007 werd door de International Harmonization Project (IHP) Group, bestaande uit hematologen, nucleair geneeskundigen en klinisch fysici, nieuwe responscriteria geformuleerd waarbij voor het eerst ^{18}F-fluorodeoxyglucose (^{18}F-FDG) positron emission tomography (PET) en computed tomography (CT) werden geïntegreerd (1,2). Deze zogenaamde 'revised Cheson-criteria' vervingen de International Workshop Criteria (IWC) uit 1999 (3). De 2007 criteria zijn bedoeld voor gebruik van ^{18}F-FDG PET ná behandeling.
Direct gekoppeld aan deze publicatie verscheen tevens een artikel over de operationalisatie van ^{18}F-FDG PET (1). Naast aanbevelingen voor de voorbereiding en uitvoering van ^{18}F-FDG PET bij patiënten met maligne lymfoom bevatte deze laatste publicatie ook criteria voor de beoordeling van ^{18}F-FDG PET (bij toepassing ervan na afloop van behandeling; 'end-of-treatment' PET). Men ging daarbij uit van visuele beoordeling. ^{18}F-FDG PET-positiviteit werd gedefinieerd als ^{18}F-FDG opname hoger dan mediastinale "blood pool" activiteit in lymfklieren die op de CT scan groter zijn dan 2 cm.
^{18}F-FDG opname gelijk aan of minder dan mediastinale blood pool werd beoordeeld als PET-negatief. Voor lesies < 2 cm werd PET-positiviteit gedefinieerd als de ^{18}F-FDG opname meer was dan de lokale achtergrond. De classificatie complete remission undetermined (CRu) van de IWC 1999 verdween daarmee, en de daardoor ontstane dichotomie in de responsbeoordeling was een grote vooruitgang (2). Het IHP responssysteem is gevalideerd door toepassing ervan op destijds bestaande datasets. Het 2 cm afkappunt berustte op een consensus over partial volume effecten bij de destijds vigerende scanners en beeldreconstructieparameters.

Sinds 2007 zijn er belangrijke ontwikkelingen geweest op het gebied van beeldvorming. PET in combinatie met CT (PET/CT) heeft grotendeels de PET 'stand alone' vervangen. Verder is de kwaliteit van de PET beelden o.a. door introductie van time-of-flight veranderd, waardoor vooral het criterium bij beoordeling van lymfklieren < 2 cm gecompromitteerd leek te worden ('het werd steeds moeilijker voor lymfklieren om negatief te worden'). Naast gebruik van PET/CT voor responsevaluatie ná behandeling, wordt PET/CT heden ten dage in studieverband steeds frequenter gebruikt voor evaluatie van respons tijdens behandeling (interim PET, i-PET). Daarnaast wordt PET/CT in de dagelijkse praktijk niet alleen gebruikt voor stadiëring en responsevaluatie van Hodgkin lymfoom en agressief non-Hodgkin lymfoom (NHL), maar ook voor beoordeling van het indolente (voorheen laaggradige) folliculaire NHL. Al met al voldoende redenen om het toepassingsgebied en de criteria uit 2007 te willen herzien.

Sinds 2009 zijn er jaarlijks 'International Workshops on interim PET' gehouden, aanvankelijk in het Franse Deauville, later in Menton bij Nice. Deze workshops zijn het initiatief van prof. dr. Michel Meignan, waarbij hematologen, nucleair geneeskundigen en klinisch fysici met expertise op het gebied van PET/CT bij maligne lymfoom werden uitgenodigd. De voorziene herziening van de responscriteria zijn grotendeels voortgevloeid uit de

discussies tijdens deze workshops (4). Het is nu wachten op IHP 2.0-richtlijnen, die naar alle waarschijnlijkheid net als in 2007 in combinatie met herziene klinische richtlijnen gepubliceerd zullen worden.

i-PET: visuele beoordeling

Beoordeling van respons tijdens behandeling met chemo-immunotherapie wordt zowel in de klinische trials als in de dagelijkse praktijk toegepast. Het doel van deze vroege responsbeoordeling is de effectiviteit vaststellen van de gegeven therapie (chemosensitiviteit) en uitsluiten van ziekteprogressie tijdens behandeling. Voorheen werd hierbij een CT scan gemaakt na 3-4 kuren, maar momenteel steeds vaker een ^{18}F-FDG PET/CT. PET/CT toont metabole veranderingen nog voordat anatomische respons duidelijk zichtbaar wordt, en heeft derhalve de potentie om de CT scan te vervangen. Diverse publicaties hebben aangetoond dat interim PET/CT nauwkeuriger is dan CT scan alleen bij vroege responsbeoordeling (5-9). Tevens blijkt i-PET/CT een belangrijke prognostische waarde te hebben bij zowel Hodgkin lymfoom als diffuus grootcellig B-cel NHL (DLBCL). Op grond van deze bevindingen wordt het mogelijk om i-PET/CT gestuurde behandelstrategieën (escalatie of de-escalatie) in studieverband te gaan toepassen. Echter, momenteel zijn er nog onvoldoende gegevens die aantonen dat aanpassing van de behandeling op basis van i-PET de uitkomst van behandeling verbetert (10). Dit concept wordt momenteel in diverse klinische studies zowel bij Hodgkin lymfoom als DLBCL onderzocht (11). Aanvankelijk werden de IHP of 'revised Cheson criteria' ook toegepast bij interim PET, maar deze wijze van beoordeling bleek minder accuraat bij een dergelijke, vroege responsbeoordeling van metabole veranderingen. ^{18}F-FDG PET scans na 2-4 kuren tonen vaak nog geringe ^{18}F-FDG opname, vaak geduid als gevolg van 'ongoing response', waarbij de dichotome beoordeling negatief vs positief onvoldoende nuance biedt (6).
Tijdens de eerste 'International Workshop on Interim PET' in 2009 in Deauville werd een visuele beoordeling in vijf categorieën voorgesteld (5-point scale, 5PS), later de Deauville score (DS) genoemd (4) (zie tabel 1). Het doel was om een reproduceerbare wijze van beoordeling te ontwikkelen, die tevens de mogelijkheid bood om afhankelijk van de klinische context en behandelopties de cut-off tussen goede en slechte cq onvoldoende respons te variëren. Afhankelijk van de vraagstelling cq klinische beleidsconsequentie is het mogelijk de cut-off zodanig te variëren dat gestreefd kan worden naar hoge positief voorspellende waarde (PPV) dan wel hoge negatief voorspellende waarde (NPV) van de i-PET/CT. Hodgkin patiënten hebben momenteel een uitstekende progressievrije overleving na behandeling met chemo- en radiotherapie. Gezien de late toxiciteit van radiotherapie bij deze jonge patiënten is het relevant te onderzoeken of een deel van deze patiënten zonder radiotherapie ook goed behandeld kan worden. In studieverband (RAPID studie UK, HD16 studie GHSG) wordt dit concept momenteel onderzocht. Gezien de de-escalatie van therapie is in deze context een hoge NPV gewenst. In deze studies wordt PET-negativiteit daarom gedefinieerd als DS 1-2. Uit onderzoek bleek een goede interobserver variatie en de DS werd gevalideerd in patiënten met zowel Hodgkin als agressief NHL (12,13). In de Britse RATHL studie voor patiënten met uitgebreid stadium Hodgkin lymfoom wordt behandeling gestart met ABVD kuren. Voor patiënten met een positieve PET scan na twee kuren volgt randomisatie tussen ABVD of de intensievere BEACOPP kuren. In deze studie is een hoge PPV gewenst en derhalve wordt PET-positief in deze studie gedefinieerd als DS 4-5. Voor een correcte visuele i-PET beoordeling is een adequate vergelijking met de uitgangssituatie essentieel. Om die reden wordt in de nieuwe responscriteria een stadiëring PET/CT scan verplicht gesteld.

Tabel 1. Deauville score (DS) system

1. no uptake
2. uptake < mediastinal bloodpool
3. uptake > mediastinal bloodpool but < liver
4. uptake moderately higher than liver
5. uptake markedly higher than liver and/or new lesions

X. new areas of uptake unlikely to be related to lymphoma

Aanwijzingen voor de praktijk

- voor stadiëring van patiënten met Hodgkin lymfoom of DLBCL dient een PET/CT verricht te worden;
- voor visuele beoordeling van interim PET/CT en PET/CT bij evaluatie na behandeling wordt de Deauville score (DS) aanbevolen;
- er is momenteel nog onvoldoende bewijs dat aanpassing van behandeling op basis van een interim PET verbetering van prognose geeft; dit is momenteel alleen aanbevolen in de context van een klinische trial;
- voor kwantitatieve responsbeoordeling in klinische studies is een EARL accreditatie essentieel.

i-PET/CT: semikwantitatieve beoordeling

Visuele beoordeling van i-PET/CT toont in het algemeen een goede NPV, maar variabele PPV. Het is mogelijk dat de huidige standaard van chemo-immunotherapie (met toevoeging van Rituximab, monoclonale antistof tegen CD20, aan het standaard chemotherapieschema CHOP bij NHL) en/of toepassing van groeifactoren (Neupogen®/ Neulasta®) deze variabele PPV veroorzaken door inflammatie en verandering van de ^{18}F-FDG biodistributie. Of SUV veranderingen de visuele beoordeling verbeteren, is vooral onderzocht bij patiënten met DLBCL (14). De verandering in SUV_{max} (SUV in deze context meestal gecorrigeerd voor lichaamsgewicht) in aangedane lymfeklieren vóór en na 2-4 kuren is het meest frequent onderzocht. ROC analyse, bij 92 patiënten met DLBCL gescand na 2 kuren en 80 patiënten gescand na 4 kuren, toonde een optimale ΔSUV van 66% na 2 kuren en 70% na 4 kuren ten aanzien van voorspellen van Event-free Survival (15). Momenteel wordt in Groot-Brittannië

een prospectieve studie verricht met een geblindeerde i-PET waarbij visuele en semikwantitatieve beoordeling met elkaar worden vergeleken. Ook in de Nederlandse HOVON84 trial (waarvan de inclusie in 2012 werd voltooid) wordt bij een deel van de patiënten de visuele beoordeling vergeleken met ΔSUV. Uit deze analyses zal blijken of PPV en NPV verder verbeterd kunnen worden met een semikwantitatieve beoordeling. Voor de correcte toepassing van semikwantitatieve beoordeling van i-PET is standaardisatie van patiëntenvoorbereiding en PET acquisitie essentieel. Mede op instigatie van de Nederlandse HOVON-imaging werkgroep (www.hovon.nl/werkgroepen/technische-commissies/imaging-werkgroep) zijn sinds 2008 richtlijnen opgesteld voor de uitvoering van ^{18}F-FDG PET in de klinische praktijk en in studieverband (16). De uit die activiteiten voortgevloeide Europese richtlijnen impliceren onder meer dat scanners gekalibreerd dienen te worden (17). Via de EANM wordt dit geleidelijk in Europa uitgerold onder de vlag van EARL (EANM Research Ltd, http://earl.eanm.org). Voor de komende klinische trials bij Hodgkin en NHL met SUV responsbeoordeling zal een EARL-accreditatie dan ook voorwaarde zijn voor deelname van een ziekenhuis aan deze studies. Omdat bij diagnosestelling vaak nog onduidelijk is of patiënten aan zo'n trial mee gaan doen, is toepassing van de EANM richtlijn in de dagelijkse klinische praktijk nodig. Een ondeugdelijke uitgangsscan maakt immers een betrouwbare SUV meting onmogelijk.

PET/CT na behandeling

Visuele beoordeling van respons na behandeling is nauwkeuriger met PET/CT dan met CT scan alleen, met name bij radiologische partiële remissie (PR) of 'complete remissie undetermined' (CRu). Op basis van deze bevinding is in de revised Cheson criteria van 2007 complete remissie gedefinieerd als PET-negativiteit, onafhankelijk van eventueel aanwezige restmassa op de CT scan. Deze diameterafhankelijke beoordeling is in de dagelijkse praktijk niet goed hanteerbaar, daar de nieuwste generatie PET/CT scanners dermate sensitief is dat kleine lymfeklieren zeer vaak FDG-aviditeit boven de lokale achtergrond tonen en dan als positief geduid moeten worden. In de voorgenomen herziening van de richtlijnen worden voor zowel interim PET als end-of-treatment PET de Deauville criteria gebruikt. Waar voorheen in de IHP criteria opname minder dan mediastinale blood pool als negatief werd gedefinieerd, wordt in de Deauville score in het algemeen ^{18}F-FDG-aviditeit minder dan die in de lever als PET-negatief benoemd. In de setting van PET/CT evaluatie ná therapie wordt Deauville score 1, 2 en 3 geduid als complete metabole respons (CMR).

PET/CT beoordeling voor autologe stamceltransplantatie

De prognostische waarde van ^{18}F-FDG PET bij patiënten met recidief of refractair Hodgkin of DLBCL na reïnductietherapie en voor autologe stamceltransplantatie wordt door vele publicaties bevestigd (18-20). Een recente meta-analyse (12 studies, 630 patiënten) toonde een sensitiviteit van 69% (95% CI 56-81%) en een specificiteit van 81% (95% CI 73-87%) (21). Belangrijker is dat PET status vóór autologe stamceltransplantatie (ASCT) voorspellend is voor de progressievrije overleving (PFS) na ASCT. Bij PET-positiviteit na reïnductietherapie bleek de 3-jaars PFS 31-41%, PET-negativiteit voor ASCT resulteerde in een PFS van 75-82% (22). Met PET/CT kan een surrogaat eindpunt worden gedefinieerd voor fase II studies, zoals in de binnenkort te starten BRaVe Transplant studie voor patiënten met recidief of refractair Hodgkin lymfoom waarbij aan de standaard chemotherapie met DHAP het nieuwe antilichaam conjugaat brentuximab wordt toegevoegd, teneinde het aantal patiënten in complete remissie vóór autologe stamceltransplantatie te verhogen.

PET/CT in de follow-up

Bij patiënten met een negatieve PET/CT scan na behandeling wordt geadviseerd om in de fase van controles na behandeling geen standaard PET/CT te verrichten, gezien de in het algemeen goede kans op PFS (cq lage prevalentie van ziekte en daarmee gepaard gaande grote kans op fout-positiviteit), de stralenbelasting en kosten. In onderzoek dat onlangs bij ASCO gepresenteerd werd, bleken bij toepassing van routinematige PET vrijwel alle recidieven toch ontdekt te worden via klinische symptomen en niet via PET. Bij patiënten met ^{18}F-FDG-positieve restafwijkingen die mogelijk wijzen op actieve restziekte (in het algemeen DS 3), maar niet eenvoudig voor histologische diagnostiek toegankelijk zijn (mediastinale en retroperitoneale klieren), wordt geadviseerd PET/CT te herhalen na 6-8 weken; (al dan niet sarcoid-like) inflammatoire ^{18}F-FDG opname als mogelijke oorzaak van PET-positiviteit na behandeling neemt in de maanden na behandeling immers geleidelijk af, in tegenstelling tot residueel lymfoom.

PET/CT bij folliculair lymfoom

Het folliculair lymfoom (FL) is een frequent voorkomende entiteit (circa 30% van alle NHL) die zich vaak kenmerkt door een indolent gedrag. Voorheen werd dit type laaggradig NHL genoemd. Het FL is vrijwel altijd ^{18}F-FDG-avide, maar heeft duidelijk minder intense ^{18}F-FDG opname dan bijvoorbeeld het HL of DLBCL (23). Recentelijk bleek in een retrospectieve studie dat ook bij het folliculair lymfoom de PET/CT scan na behandeling voorspellend is voor de progressievrije overleving (24). Deze PFS bleek voor patiënten met een positieve PET/CT scan na behandeling aanmerkelijk ongunstiger dan voor de PET/CT negatieve populatie (PFS 42 maanden 33% vs 71%). Deze resultaten werden bevestigd in een prospectieve studie van de Franse GELA, waarbij de PET/CT scan ná behandeling een betere voorspeller van uitkomst bleek dan de interim PET/CT na 4 kuren (25). Bij 6 patiënten bleek de interim scan negatief, maar de PET/CT scan na 8 kuren evenwel positief. Bij de helft van deze patiënten werd transformatie naar een agressief NHL histologisch vastgesteld. Momenteel loopt in Nederland de HOVON110 studie waarbij zowel stadiëring als evaluatie na behandeling plaatsvindt met PET/CT. Hopelijk zal deze studie bovenstaande resultaten bevestigen.

Conclusie

De afgelopen jaren zijn er grote veranderingen geweest in de uitvoering en toepassing van PET/CT bij maligne lymfoom. Dit maakt verdere verfijning in standaardisatie van beoordeling noodzakelijk. Naast de waarde van PET/CT ná behandeling lijkt er voor een aantal subtypes lymfoom ook toegevoegde waarde voor de interim PET/CT. Momenteel wordt in meerdere internationale trials onderzocht of 'response adapted therapy' verbetering van behandeling en/of vermindering van toxiciteit tot gevolg heeft. Voorheen waren de responscriteria voor de diverse trials vaak niet uniform. Met de komst van de 'revised Cheson criteria' en de introductie van de Deauville score is aan dit manco tegemoetgekomen. Deze nieuwe ontwikkelingen zijn een grote stap in de goede richting voor de behandeling van patiënten binnen, maar op termijn ook buiten studieverband.

Referenties

1. Juweid ME, Stroobants S, Hoekstra OS, et al. Use of positron emission tomography for response assessment of lymphoma: Consensus of the Imaging Subcommittee of International Harmonization Project in lymphoma. J Clin Oncol. 2007;25:571-8
2. Cheson BD, Pfistner B, Juweid ME, et al. Revised response criteria for malignant lymphoma. J Clin Oncol. 2007;25:579-86
3. Cheson BD, Horning SJ, Coiffier B, et al. Report of an international workshop to standardize response criteria for non-Hodgkin's lymphomas. J Clin Oncol. 1999;17:1244
4. Meignan M, Gallamini A, Meignan M, et al. Report on the First International Workshop on Interim-PET-Scan in Lymphoma. Leuk lymphoma. 2009;50:1257-60
5. Gallamini A, Hutchings M, Rigacci L, et al. Early interim 2- F-18 Fluoro-2-Deoxy-D-Glucose positron emission tomography is prognostically superior to international prognostic score in advanced-stage Hodgkin's lymphoma: A report from a joint Italian-Danish study. J Clin Oncol. 2007;25:3746-52
6. Hutchings M, Loft A, Hansen M, et al. FDG PET after two cycles of chemotherapy predicts treatment failure and progression-free survival in Hodgkin lymphoma. Blood. 2006;107:52-9
7. Cerci JJ, Pracchia LF, Linardi CCG, et al. (18)F-FDG PET After 2 Cycles of ABVD Predicts Event-Free Survival in Early and Advanced Hodgkin Lymphoma. J Nucl Med. 2010;51:1337-43
8. Juweid ME, Wiseman GA, Vose JM, et al. Response assessment of aggressive non-Hodgkin's lymphoma by integrated International Workshop Criteria and fluorine-18-fluorodeoxyglucose positron emission tomography. J Clin Oncol. 2005;23:4652-61
9. Safar V, Dupuis J, Itti E, et al. Interim [18F]fluorodeoxyglucose positron emission tomography scan in diffuse large B-cell lymphoma treated with anthracycline-based chemotherapy plus rituximab. J Clin Oncol. 2012;30:184-90
10. Hutchings M, Barrington SF. PET/CT for therapy response assessment in lymphoma. J Nucl Med. 2009;50 Suppl 1:21S-30S
11. Duhrsen U, Huttmann A, Jockel KH, et al. Positron emission tomography guided therapy of aggressive non-Hodgkin lymphomas - the PETAL trial. Leuk lymphoma. 2009;50:1757-60
12. Biggi A, Gallamini A, Chauvie S, et al. International Validation Study for Interim PET in ABVD-Treated, Advanced-Stage Hodgkin Lymphoma: Interpretation Criteria and Concordance Rate Among Reviewers. J Nucl Med. 2013;54:683-90
13. Itti E, Meignan M, Berriolo-Riedinger A, et al. An international confirmatory study of the prognostic value of early PET/CT in diffuse large B-cell lymphoma: comparison between Deauville criteria and ΔSUVmax. Eur J Nucl Med Mol Imaging 2013 May 7. [Epub ahead of print]
14. Lin C, Itti E, Haioun C, et al. Early 18F-FDG PET for prediction of prognosis in patients with diffuse large B-cell lymphoma: SUV-based assessment versus visual analysis. J Nucl Med. 2007;48:1626-32
15. Casasnovas RO, Meignan M, Berriolo-Riedinger A, et al. SUVmax reduction improves early prognosis value of interim positron emission tomography scans in diffuse large B-cell lymphoma. Blood. 2011;118:37-43
16. Boellaard R, Oyen WJG, Hoekstra CJ, et al. The Netherlands protocol for standardisation and quantification of FDG whole body PET studies in multi-centre trials. Eur J Nucl Med Mol Imaging. 2008;35:2320-33
17. Boellaard R, O'Doherty MJ, Weber WA, et al. FDG PET and PET/CT: EANM procedure guidelines for tumour PET imaging: version 1.0. Eur J Nucl Med Mol Imaging Imaging. 2010;37:181-200
18. Moskowitz AJ, Yahalom J, Kewalramani T, et al. Pretransplantation functional imaging predicts outcome following autologous stem cell transplantation for relapsed and refractory Hodgkin lymphoma. Blood. 2010;116:4934-7
19. Schot BW, Zijlstra JM, Sluiter WJ, et al. Early FDG PET assessment in combination with clinical risk scores determines prognosis in recurring lymphoma. Blood. 2007;109:486-91
20. Svoboda J, Andreadis C, Elstrom R, et al. Prognostic value of FDG PET scan imaging in lymphoma patients undergoing autologous stem cell transplantation. Bone Marrow Transplantation. 2006;38:211-6
21. Terasawa T, Dahabreh IJ, Nihashi T. Fluorine-18-Fluorodeoxyglucose Positron Emission Tomography in Response Assessment Before High-Dose Chemotherapy for Lymphoma: A Systematic Review and Meta-Analysis. Oncologist. 2010;15:750-9
22. Moskowitz CH, Matasar MJ, Zelenetz AD, et al. Normalization of pre-ASCT, FDG PET imaging with second-line, non-cross-resistant, chemotherapy programs improves event-free survival in patients with Hodgkin lymphoma. Blood. 2012;119:1665-70
23. Schoder H, Noy A, Gonen M, et al. Intensity of 18fluorodeoxyglucose uptake in positron emission tomography distinguishes between indolent and aggressive non-Hodgkin's lymphoma. J Clin Oncol. 2005;23:4643-51
24. Trotman J, Fournier M, Lamy T, et al. Positron Emission Tomography-Computed Tomography (PET/CT) After Induction Therapy Is Highly Predictive of Patient Outcome in Follicular Lymphoma: Analysis of PET/CT in a Subset of PRIMA Trial Participants. J Clin Oncol. 2011;29:3194-200
25. Dupuis J, Berriolo-Riedinger A, Julian A, et al. Impact of [18F] Fluorodeoxyglucose Positron Emission Tomography Response Evaluation in Patients With High-Tumor Burden Follicular Lymphoma Treated With Immunochemotherapy: A Prospective Study From the Groupe d'Etudes des Lymphomes de l'Adulte and GOELAMS. J Clin Oncol. 2012;30:4317-22

Breast uptake of ^{131}I in a post-menopausal woman treated for thyroid cancer

Dr. E.M. van der Zwaal, Prof. Dr. J. Booij, Dr. H.J. Verberne

Department of Nuclear Medicine, Academic Medical Center, University of Amsterdam

Abstract

Van der Zwaal EM, Booij J, Verberne HJ. Breast uptake of ^{131}I in a post-menopausal woman treated for thyroid cancer. We present the case of a 60-year old woman treated for papillary thyroid cancer who showed breast uptake of ^{131}I on her post-therapy scan. As thyroid cancer rarely metastasises to mammary tissue and the observed breast uptake was bilateral, pathological uptake due to malignancy was considered unlikely. On the other hand, physiological breast uptake of ^{131}I has mostly been reported in lactating women and is uncommon outside the post-partum period. In this particular case, however, the patient was being treated with antipsychotics that may induce hyperprolactinemia and galactorroe due to their anti-dopaminergic effects. Therefore, the bilateral breast uptake in this patient was most likely secondary to drug-induced hyperprolactinemia, and not related to breast malignancy.

Tijdschr Nucl Geneesk 2013; 35(2):1098-1100

Case report

A 60-year old woman was presented to our department for treatment with ^{131}I for thyroid cancer. She was diagnosed with papillary thyroid cancer (T3N1M0) in 1999 for which she was initially treated with a total thyroidectomy and a subsequent ablation dose of ^{131}I, followed by a therapeutic doses of 5500 MBq ^{131}I in 2000. Her post-ablation images showed uptake in a fairly large thyroid remnant, which was only just visible on the following post-therapy scan. Subsequently, unstimulated and stimulated thyreoglobulin (Tg) levels remained undetectable for ten years. In 2010 Tg levels increased to 4 pmol/l (thyroid stimulating hormone (TSH) 88 mE/l) and a second therapeutic dose of ^{131}I was administered, with post-therapy images revealing moderate uptake in the left paratracheal area. Subsequently, Tg levels temporarily declined to undetectable levels again. Current treatment (in 2012) with 5500 MBq ^{131}I was indicated because Tg levels rose again, up to 2 pmol/l (TSH 48 mE/l), and a suspicious lesion was detected by follow-up ultrasound in the left paratracheal area. Co-morbidity at the time of treatment included diabetes mellitus, hypertension, dyslipidemia and a psychiatric disorder, for which she was being treated with glimepiride, insuline, metformine, nifedipine, lisinopril, atorvastatin, and the antipsychotics quetiapine and risperidone, respectively.

Whole-body images acquired seven days after administration of ^{131}I failed to show any pathological uptake of ^{131}I in the neck. However, in addition to physiological uptake in the liver, bladder, nasal and oral cavities, bilateral uptake was observed at the level of the lower chest (figure 1). Additional

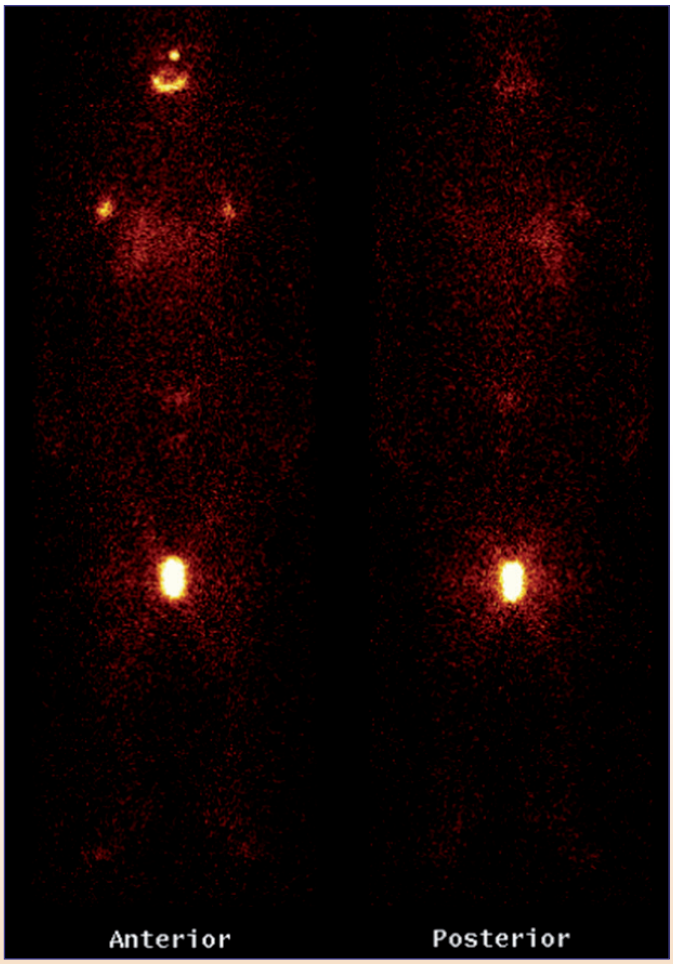

Figure 1: Whole body images obtained 7 days after treatment with 5500 MBq ^{131}I (with a reference standard placed between the legs) showed uptake of ^{131}I in the lower thoracic region.

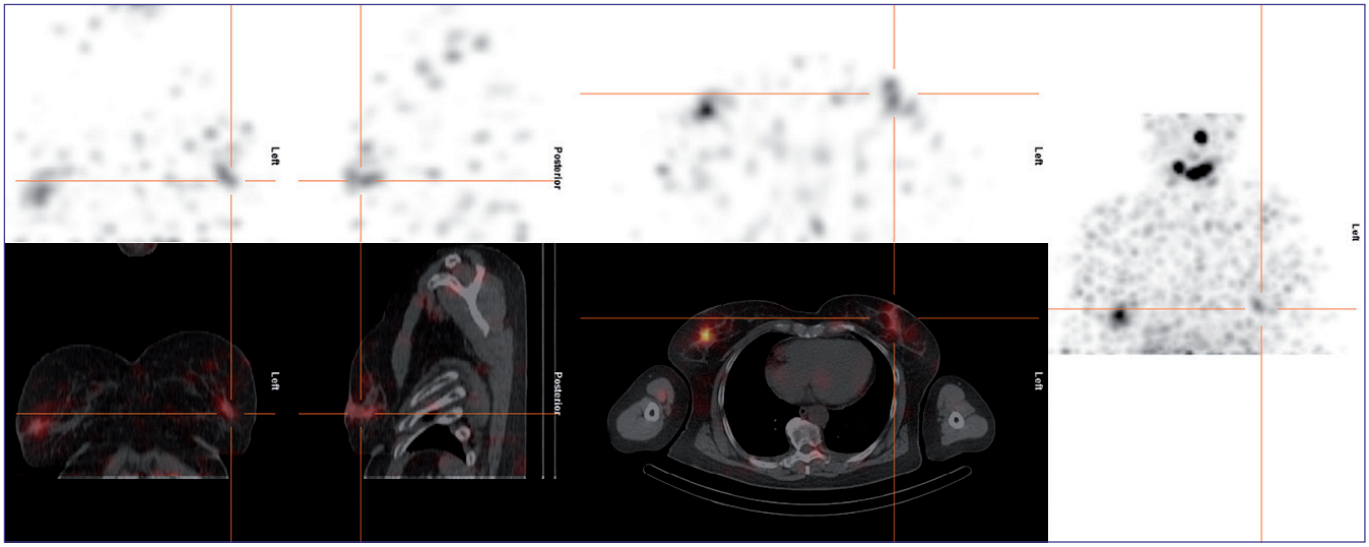

Figure 2: Additional SPECT/CT images revealed ^{131}I uptake in both mammary glands.

SPECT/CT imaging revealed that this was due to uptake in the mammary glands, especially in the retro-areolar area and more prominent on the right than on the left side (figure 2). No anatomical abnormalities were observed on the low-dose CT images of the breasts. Although not visible on the whole body images, SPECT/CT images also revealed minor uptake in the left paratracheal area (image not shown). This correlated with the lesion identified with the follow-up ultrasound, as well as the previous post-therapy scan in 2010, indicating persistence/recurrence of papillary thyroid cancer in this area.

Discussion

It has been known for many years that iodine is secreted in breast milk to provide new-borns with the iodine necessary for normal thyroid function. After the power-plant accident in Chernobyl, the same mechanism resulted in high levels of ^{131}I in cow's milk, which eventually caused an increase in thyroid cancer in the surrounding area (1,2). To enable secretion of iodine in breast milk, concentration of iodine in breast tissue occurs by the mammary gland Na/I Symporter (mNIS), a transmembrane transporter similar to the NIS that is expressed in the thyroid gland (tNIS) (3). In contrast to the tNIS, which is expressed constitutively in the thyroid gland, the mNIS is generally absent in breast tissue, and only expressed during gestation and lactation (4,3). Both oxytocin and prolactin appear to play a role in the temporary expression of mNIS (4). Considering the hormonal regulation of lactation and iodine uptake in breast tissue, one might expect physiological uptake of ^{131}I in breast tissue to be fairly symmetrical and diffuse. However, Bakheet et al reported that breast uptake of ^{131}I in lactating women was symmetrical in only 25% of cases. In the remaining cases, uptake was asymmetrical (60%) or unilateral (15%). He also described four distinct patterns of ^{131}I uptake: full, focal, crescent and irregular (5). Thus, different patterns of physiological uptake of ^{131}I in breast tissue can be observed. Furthermore, ^{131}I uptake may persist for up to five weeks after cessation of breast feeding (6).

In addition to the physiological expression of the mNIS in lactating breast tissue, pathological expression of the mNIS has been reported in breast cancer specimens. In one study, up to 87% of human breast cancer tissue specimens expressed mNIS as well as breast cancer specimens obtained from mice with Her2/Neu overexpression(3). Interestingly, in breast cancer specimens mNIS is expressed throughout the plasma membrane as well as intracellularly, whereas physiological expression of mNIS occurs at the basolateral membrane only (3). However, as mNIS expression has also been observed in benign fibroadenoma, focal uptake of ^{131}I in breast tissue is not an exclusive marker for malignancy (7). Nevertheless, if focal uptake is seen in breast tissue on a ^{131}I post-therapy scan, the possibility of a second primary malignancy of the breast should be considered.

Although metastases of differentiated thyroid cancer in mammary tissue have been reported, it is considered extremely rare (8). Furthermore, in the present case, fairly diffuse uptake was seen in both breasts. This is not a common pattern for either metastases of thyroid cancer or a primary breast malignancy. In this particular case the patient was being treated with two antipsychotics: risperidone (Risperdal®) and quetiapine (Seroquel®). Both these drugs act as dopamine antagonists and may cause hyperprolactinemia and galactorroea as a side effect (9). Normally, the release of prolactin from the pituitary gland is tonically inhibited by dopaminergic input from the hypothalamus. Interruption of this tonic inhibition is thought to underlie the hyperprolactinemia associated with many antipsychotic drugs (10). Risperidone has the highest propensity to do so and hyperprolactinemia is observed in nearly all patients (9). Considering the role of prolactin in the expression of mNIS, it is not surprising that drugs that cause hyperprolactinemia may cause transient breast uptake of ^{131}I. This has indeed been

reported previously for the antipsychotics risperidone and amisulpiride (11,12). As mentioned above, physiological breast uptake in lactating women is symmetrical only in a minority of cases. Therefore, even though it was slightly asymmetrical, the bilateral breast uptake of ^{131}I in the present case was most likely secondary to drug-induced hyperprolactinemia, and not caused by malignancy in the breast tissue. This case illustrates the contribution of a complete medical history, including drug treatment, in the interpretation of certain nuclear scans.

Reference List

1. Nishizawa K, Takata K, Hamada N et al. 131I in milk and rain after Chernobyl. Nature. 1986;324:308
2. Balter M. Chernobyl's thyroid cancer toll. Science. 1995;270:1758-9
3. Tazebay UH, Wapnir IL, Levy O et al. The mammary gland iodide transporter is expressed during lactation and in breast cancer. Nat Med. 2000;6:871-8
4. Cho JY, Leveille R, Kao R et al. Hormonal regulation of radioiodide uptake activity and Na+/I- symporter expression in mammary glands. J Clin Endocrinol Metab. 2000;85:2936-43
5. Bakheet SM, Hammami MM. Patterns of radioiodine uptake by the lactating breast. Eur J Nucl Med. 1994;21:604-8
6. Hsiao E, Huynh T, Mansberg R et al. Diagnostic I-123 scintigraphy to assess potential breast uptake of I-131 before radioiodine therapy in a postpartum woman with thyroid cancer. Clin Nucl Med. 2004;29:498-501
7. Berger F, Unterholzner S, Diebold J et al. Mammary radioiodine accumulation due to functional sodium iodide symporter expression in a benign fibroadenoma. Biochem Biophys Res Commun. 2006;349:1258-63
8. Song HJ, Xue YL, Xu YH et al. Rare metastases of differentiated thyroid carcinoma: pictorial review. Endocr Relat Cancer. 2011;18:R165-74
9. Bushe C, Shaw M, Peveler RC. A review of the association between antipsychotic use and hyperprolactinaemia. J Psychopharmacol. 2008;22:46-55
10. Petty RG. Prolactin and antipsychotic medications: mechanism of action. Schizophr Res. 1999;35 Suppl:S67-73
11. Ahn JH, Kim SY, Kim YJ, et al. Hyperprolactinemia-Associated Breast Uptake of Radioiodine Following 131I Postablation Scan in Differentiated Thyroid Cancer. Endocrinol Metab. 2011;26:345-7
12. Ronga G, Bruno R, Puxeddu E et al. Radioiodine uptake in non-lactating mammary glands: evidence for a causative role of hyperprolactinemia. Thyroid. 2007;17:363-6

In memoriam Dr. Dirk Roeda

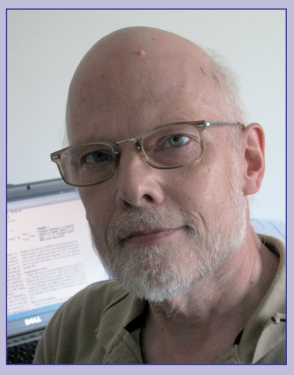

Op 19 juli overleed dr. Dirk Roeda, radiochemicus bij het Service Hospitalier Frédéric Joliot in Orsay (Frankrijk). Dirk studeerde organische chemie aan de Vrije Universiteit te Amsterdam, waar hij in 1982 promoveerde op radiosynthese en toepassing van koolstof-11 gelabeld fosgeen. Een gedeelte van dit onderzoek werd uitgevoerd bij dr. Comar in het Service Hospitalier Frédéric Joliot in Orsay. Na zijn promotie verhuisde Dirk naar Finland om te gaan werken bij het Turku Medical Cyclotron Project aan de Universiteit van Turku, de basis van het huidige Finse nationale PET centrum. In 1986 vertrok hij naar de groep van prof. John Mallard aan de Universiteit van Aberdeen (Schotland) om mee te werken aan de bouw van een nieuw PET centrum, inclusief de installatie van een CS30 cyclotron en bijbehorende laboratoria. In 1993 keerde Dirk terug naar Orsay om in de radiochemie groep van prof. Crouzel te gaan werken. Later werkte hij onder leiding van prof. Dollé aan de verdere ontwikkeling van koolstof-11 en fluor-18 syntheses. Dirk werkte graag in de luwte maar heeft een belangrijke bijdrage geleverd aan de radiochemie, met name aan koolstof-11 chemie. Wij zullen hem missen, om zijn werk en om zijn innemende persoonlijkheid.

Dr. Peter Laverman
namens de Nederlandse Klinisch Radiochemische Vereniging (NKRV)

2QUART BV MEDICAL

Een nieuw bedrijf in de markt van Nucleaire Geneeskunde.

Wij zijn Technetium sponsor van de NVNG en vertegenwoordigen sinds kort Comecer Spa en Scintomics GmbH.

COMECERGROUP

Comecer SpA levert:

- Diverse LAF kasten voor PET- en Single Photon isotopen
- Radiochemie kasten voor NM lab en research
- Meubel inrichting voor Medische laboratoria
- Volautomatische dispensing systemen
- Stralings afscherming accessoires
- Speciaal maatwerk voor unieke projecten

Comecer producten onderscheiden zich ondermeer door gebruik van hoogwaardige kwaliteitsmaterialen en automatisering van processen.

Voor meer informatie: www.comecer.com

SCINTOMICS

Scintomics GmbH levert:

- Labeling modules
- Geïntegreerde HPLC unit
- Volautomatisch dispensing systeem
- Gebruiksklare GMP disposable cassette & reagens labelings kits (FDG, FET, FMC, FLT, FMISO, Fluoride, Ga-/Lu-/Y-peptides...)
- Innovatieve en exclusieve introductie van PET Radiopharmca (Pentixafor (CXCR4), TRAP (RGD)3,...)
- Advies (samenwerking) voor ontwikkeling van unieke labelingen processen.

Scintomics producten onderscheiden zich door het compacte ontwerp van de modules, betrouwbaarheid, flexibiliteit in labeling processen en scherpe prijsstelling.

Voor meer informatie: www.scintomics.com en/of info@scintomics.com

Wij verwelkomen u graag tijdens het EANM 2013 op onze stand in THE PAVILION

Mathijs Faber | 2Quart Medical B.V. | Postbus 64, 1740 AB Schagen, Nederland | Telefoon: +31 (0) 6 2377 0886 | e-Mail: easy@planet.nl

PROEFSCHRIFT

Dr. H.J. Veenstra

18 april 2013
Antoni van Leeuwenhoek-ziekenhuis Amsterdam
Universitair Medisch Centrum Utrecht

Promotor:
Prof. dr. A.J.M. Balm

Co-promotores:
Dr. O.E. Nieweg
Dr. W.M.C. Klop
Dr. R.A. Valdés Olmos

Melanoma surgery and the impact of sentinel node biopsy

Het in dit proefschrift beschreven onderzoek evalueert schildwachtklierprocedures bij melanoompatiënten en analyseert de lymfeklierdrainage in het hoofd-halsgebied. Het belangrijkste doel van deze procedure is het identificeren van patiënten met uitzaaiingen in de lymfeklieren, zodat deze vroegtijdig aanvullende behandeling ondergaan met een verbeterde kans om te overleven.

Recente studies hebben aangetoond dat patiënten met een tumorpositieve schildwachtklier en vroeg aanvullende klierdissectie mogelijk een verhoogde kans hebben op het ontwikkelen van in-transitmetastasen ten opzichte van patiënten die klierdissectie ondergaan vanwege een palpabele lymfeklier metastase. Dit proefschrift verwerpt deze suggestie.

Schildwachtklierbiopsie bij melanoompatiënten is een nuttig en vrij nauwkeurig diagnostisch instrument voor het vroegtijdig opsporen van lymfekliermetastasen. Het gegeven van 29% foutnegatieve procedures in het eerste jaar nadat schildwachtklierbiopsie werd geïntroduceerd, geeft aan dat er sprake is geweest van een leerfase. Het percentage foutnegatieve procedures is nadien afgenomen tot 5.7%.

Bij 35 niet geselecteerde melanoompatiënten met een indicatie voor schildwachtklierbiopsie werd naast conventionele lymfoscintigrafie aanvullend een SPECT/CT verricht. SPECT/CT verschafte relevante additionele informatie bij in totaal 16 van de 35 patiënten (46%). Op grond van deze bevinding wordt, naast conventionele lymfoscintigrafie, routinegebruik van SPECT/CT geadviseerd voor melanoompatiënten die een schildwachtklierbiopsie ondergaan.

Aanvullende lymfeklierdissectie bij patiënten met een tumorpositieve schildwachtklier is een procedure met aanzienlijke comorbiditeit. Daarom werd bestudeerd of alle patiënten met een positieve schildwachtklier daadwerkelijk aanvullende behandeling nodig hebben. Er werden 16 melanoompatiënten met een Starz-I tumorpositieve schildwachtklier, waar aanvullende lymfeklierdissectie achterwege werd gelaten, gevolgd. Geen van deze patiënten ontwikkelde een lymfeklierrecidief gedurende de mediane follow-up van vijf jaar. Dit suggereert dat in overweging kan worden genomen een aanvullende klierdissectie in deze gevallen achterwege te laten.

Een belangrijk deel van dit proefschrift betreft het hoofd-halsgebied. Bij lymfekliermetastasering van een hoofd-halsmelanoom wordt halsklierdissectie verricht, maar uitgebreidheid van de ingreep is reeds lang onderwerp van discussie. We brachten lymfedrainagepatronen van melanomen in het hoofd-halsgebied in kaart, gebaseerd op locaties van schildwachtklieren. Hoofd-halsmelanomen vertonen meestal een voorspelbaar metastaseringspatroon, maar toch worden er frequent schildwachtklieren gelokaliseerd buiten dit verwachte gebied. Deze schildwachtklieren kunnen tumorcellen bevatten. Het individuele metastaseringspatroon van een patiënt is daarom van belang en tweede-echelonklieren kunnen ons mogelijk gaan helpen dit nog beter te voorspellen.

Het suboccipitale gebied is een belangrijke regio voor lymfedrainage van maligne huidlaesies op de schedelhuid. De anatomie van de suboccipitale regio werd onderzocht in vijf menselijke kadavers. Het bleek dat suboccipitale lymfeklieren klein zijn en voornamelijk in het subcutane weefsel liggen, met een minderheid net onder de oppervlakkige fascie van de musculus trapezius. Deze anatomische kennis werd gebruikt om het ontwerp van de suboccipitale dissectie verder te verfijnen.

De lymfedrainage van melanomen gelegen op de craniale zijde van de romp is vaak complex en kan een onverwacht patroon laten zien. Soms zien we zelfs directe lymfedrainage van dit gebied naar cervicale lymfeklieren. Het patroon van cervicale lymfedrainage van patiënten met een melanoom op de schouder of romp werd in kaart gebracht. Bij slechts een klein deel van de patiënten was er sprake van lymfedrainage naar cervicale klieren, met een voorkeursdrainage naar level IV en Vb.

E-mail: h.veenstra@nki.nl

Dr. B.B. Koolen

April 26th 2013
Netherlands Cancer Institute - Antoni van Leeuwenhoek Hospital
University of Amsterdam

Promotor:
prof. dr. E.J.Th. Rutgers

Co-promotores:
dr. R.A. Valdés Olmos
dr. M.J.T.F.D. Vrancken Peeters

PET/CT and dedicated PET in breast cancer

Implications for classification, staging, and response monitoring

Introduction

Breast cancer is the most frequent type of cancer in women all over the world. Progressive insight in breast cancer and its various appearances has changed generalised breast cancer treatment into today's individualised or patient-tailored therapy, which is guided by a combination of patient and tumour characteristics. In order to select patients optimally benefiting from the assigned therapy, several imaging procedures and clinical/pathological assessments are currently available. The core of this thesis is dedicated to the value of PET/CT, i.e. positron emission tomography (PET) in combination with computed tomography (CT), and a dedicated breast PET in breast cancer, particularly aiming for an improvement in patient selection and care by increasing personalised management.

Classification and staging with pre-treatment PET/CT

The first part of this thesis describes the value of pre-treatment PET/CT in breast cancer patients. This was mainly investigated in stage II-III breast cancer patients scheduled for neoadjuvant chemotherapy; a smaller proportion addresses its use in early breast cancer.

In stage II-III breast cancer increased primary tumour fluorodeoxyglucose (FDG) uptake was seen in 95% of the patients. Significantly higher maximum standardised uptake value (SUV_{max}) was observed in patients with unfavourable tumour characteristics. No subgroup of patients with consistently low tumour FDG uptake, in whom a PET/CT could safely be omitted, could be identified. Regarding the detection of axillary lymph node metastases, the positive predictive value was excellent (98%), indicating that an immediate axillary lymph node dissection instead of a sentinel lymph node biopsy would be reasonable in case of an FDG-avid node (figure 1). Sensitivity and negative predictive value, however, were suboptimal (82 and 53%, respectively). PET/CT detected occult N3-disease (either in the internal mammary chain or periclavicular area) in 16% of patients and was found to be valuable for selection of breast cancer patients at high risk for locoregional recurrence (23% of patients were upstaged to the high-risk group) and postoperative radiotherapy planning (figures 1 and 2). Further, PET/CT was found to be superior to conventional imaging techniques for the detection of distant metastases (figure 2). Of twenty patients with confirmed metastases, additional lesions were exclusively seen with PET/CT in 16 of them, leading to a change in treatment in 13. Although sensitivity of PET/CT was

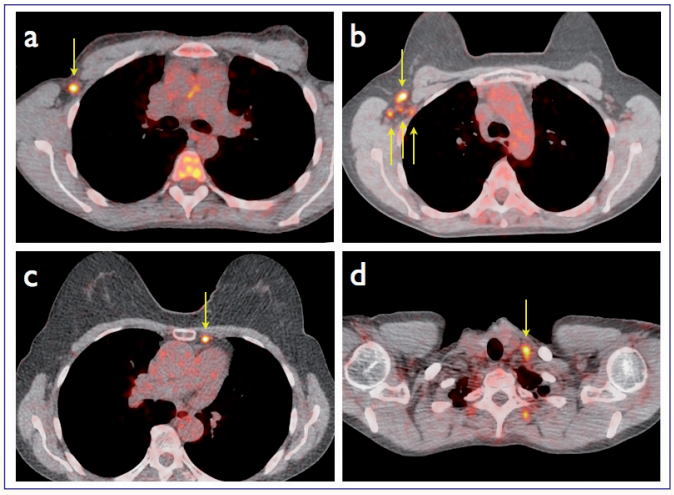

Figure 1. Fused PET/CT images depicting a single FDG-avid axillary node (a), 4 FDG-avid axillary nodes (b), an FDG-avid node in the internal mammary chain (c), and an FDG-avid supraclavicular node (d).

100%, it was false positive in five patients. Therefore, no change in treatment should be made before microscopic verification of suspect lesions is attained.

In T1 breast cancer the primary tumour was visible with PET/CT in 87% of patients when using the hanging breast technique in prone position. It increased from 58% in tumours ≤10 mm to 98% in tumours over 10 mm. Again, regarding axillary lymph node metastases, sensitivity was suboptimal (73%) and specificity was high (100%). Of twelve FDG-avid lesions outside the breast and locoregional lymph node basins, one was

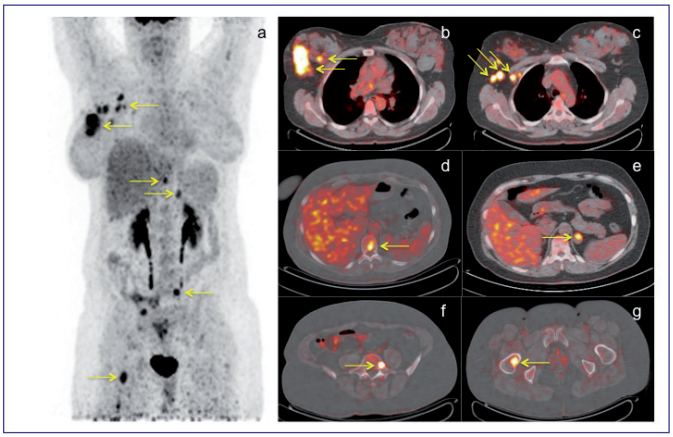

Figure 2. Maximum intensity projection (MIP) (a) and corresponding axial fused PET/CT images (b-g) of a 48-year-old woman with breast cancer scheduled for neoadjuvant chemotherapy: large and multifocal primary tumour (b), multiple axillary and retropectoral lymph nodes (c) and lesions suspect for a bone metastases in the 10th thoracic vertebra (d), a metastases in the left adrenal gland (e) and bone metastases in the 5th lumbar vertebra (f) and the right femur (g).

confirmed to be a lung metastasis, three were false positive findings, and eight were new primary proliferative lesions.

Response monitoring of primary tumour and axillary metastases with hanging breast PET/CT

Neoadjuvant chemotherapy (NAC) has become standard care in locally advanced breast cancer and is increasingly used in large and/or node-positive disease. The second part of this thesis evaluates the use of hanging breast PET/CT during neoadjuvant chemotherapy for prediction of complete pathological response (pCR) to chemotherapy.
First, PET/CT response monitoring of the primary tumour during NAC is dependent on the breast cancer subtype: PET/CT may accurately predict pathologic response in triple negative and ER-positive/HER2-negative breast cancer, but was found less accurate in HER2-positive disease. For this purpose, a PET/CT after three cycles of chemotherapy was found to be superior to a PET/CT after one cycle. Second, response monitoring of axillary lymph node metastases was feasible, accurately identifying axillary pCR in 12 of 25 pathological responders in whom less invasive axillary treatment could be appropriate. Finally, PET/CT and MRI showed complementary potential to predict response to NAC.

Improving primary tumour characterisation using hanging breast imaging with PET/CT and dedicated breast PET

Based on intratumour heterogeneity, PET/CT information may enable tumour sampling from the most aggressive part of the tumour (area with highest degree of FDG uptake). Non-correspondence between the ultrasound-guided tumour sampling location and SUV_{max} area was seen in 14% of tumours, mainly in large, diffuse and multifocal tumours, in which PET/CT information and possibly FDG-guided biopsies are most likely to improve pre-treatment tumour sampling.
Based on limitations due to limited spatial resolution, breast tissue compression, blurring due to the breathing motion of the thorax, and the long path from source to detector, PET/CT is currently not advised for primary tumour detection. Therefore, in the last part of this study, a newly developed, high-resolution dedicated breast PET for hanging breast molecular imaging (MAMMI PET) was evaluated (figure 3). It visualised 97% of stage II and III tumours before neoadjuvant chemotherapy and detected intratumour heterogeneity in a large proportion of patients. As compared with other dedicated breast PET devices it generates true 3D images (directly comparable with MRI), enables visualisation of tumours close to the pectoral muscle, and uses lower FDG dosages.

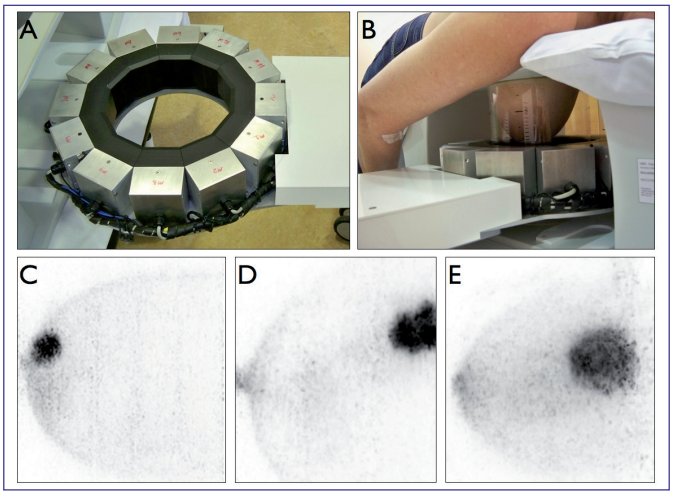

Figure 3. MAMMI PET ring detector with 12 detectors in dodecagon configuration connected to the console (A), patient in prone position with the arm in adduction for image acquisition (B) and transversal MAMMI PET images with maximum intensity projection (MIP) showing an FDG-avid breast carcinoma (C-D-E); note the heterogeneous FDG uptake (E).

Conclusions

The results described in this thesis have expanded our knowledge on the use of PET/CT in breast cancer and have provided a rationale for extending the use of PET/CT to primary breast cancer patients. Based on these results, we recommend performing a PET/CT before NAC in all stage II-III breast cancer patients for staging purposes. In T1 breast cancer its standard use is not recommended.
Response monitoring with PET/CT during NAC generated promising results, both for the primary tumour and axillary metastases. Further, a complementary potential with MRI was found.
Finally, dedicated breast PETs could offer more accurate molecular imaging of breast tumours and might be a valuable addition to conventional imaging modalities.

E-mail: b.koolen@nki.nl

Dr. A.G.T. Terwisscha van Scheltinga

13 mei 2013
Rijksuniversiteit Groningen

Promotores:
Prof.dr. E.G.E. de Vries
Prof.dr. J.G.W. Kosterink

Co-promotores:
Dr. M.N. Lub-de Hooge
Dr. C.P. Schröder

Molecular imaging of tumor characteristics to support targeted cancer therapies

A preclinical focus on HER2, HER3, c-Met, IGF-1R and VEGF-A imaging

In de afgelopen decennia zijn door onderzoek op het gebied van de tumorbiologie nieuwe moleculaire tumorkenmerken geïdentificeerd. Inzicht in deze kenmerken krijgt een steeds grotere invloed op de ontwikkeling van nieuwe geneesmiddelen. Er zijn moleculair gerichte antikankergeneesmiddelen ontwikkeld die specifiek gericht zijn op doelen op of in de tumorcel, doelen in de extracellulaire matrix of op de bloedvaten in de tumor. Voorbeelden van doelen waartegen medicijnen gericht zijn en welke ook relevant zijn voor dit proefschrift, zijn de receptoren voor groeifactoren 'human epidermal growth factor receptor (HER) family', de 'insulin-like growth factor receptor 1' (IGF-1R) en de 'mesenchymal-epithelial transition factor' (c-Met) receptor. Ook de pro-angiogene 'vascular endothelial growth factor' (VEGF), het chaperone eiwit 'heat shock protein-90' (Hsp90) en het intracellulaire doel 'mammalian target of rapamycin' (mTOR) zijn onderzocht als mogelijk target voor geneesmiddelen.

Een belangrijke groep van specifiek tumorgerichte geneesmiddelen zijn de therapeutische monoklonale antilichamen. Moleculaire beeldvorming waarbij gebruik wordt gemaakt van radioactief gelabelde antilichamen als tracer kan de aanwezigheid van het doel waartegen het antilichaam gericht is identificeren. Ook kan het potentieel informatie geven over de tumoropname en verdeling van de antilichamen in het lichaam. Daarnaast kunnen deze radioactief gelabelde antilichamen gebruikt worden om de tumorstatus van een bepaalde eigenschap te monitoren tijdens behandelingen, waarbij receptoren of liganden als biomarker gebruikt worden.

Immuno positron emissie tomografie (immuno-PET) is een techniek die gebruikt kan worden voor het volgen en kwantificeren van radioactief gelabelde antilichamen met PET in levende organismen. Een sinds enige jaren beschikbaar radio-isotoop voor PET beeldvorming is zirconium-89 (^{89}Zr), dat gezien de halfwaardetijd van 78,4 uur geschikt is voor antilichaambeeldvorming. ^{89}Zr is gelabeld aan verschillende antilichamen zowel preklinisch als klinisch getest. Ook kunnen fluorescent gelabelde antilichamen zichtbaar gemaakt worden met optische beeldvorming. Deze benadering geeft geen afbeelding van laesies in het hele lichaam maar heeft als voordeel dat geen radioactiviteit nodig is en het een hogere resolutie geeft. Hiermee wordt lokale tumorbeeldvorming, met behulp van de verschillende doelen in de tumor waartegen geneesmiddelen gericht zijn, in de toekomst mogelijk.

Uit het onderzoek beschreven in dit proefschrift is gebleken dat ^{89}Zr-PET de orgaandistributie en tumoropname van nieuwe geneesmiddelen gericht tegen HER3 of c-Met zichtbaar kon worden gemaakt. We vonden specifieke HER3 gedreven opname van een met ^{89}Zr gelabeld anti-HER3 antilichaam in tumormodellen met HER3-expressie. Op basis van deze preklinische resultaten wordt de tracer momenteel toegepast in een klinische studie waarbij de distributie en tumoropname van dit antilichaam bepaald wordt in patiënten met HER3-tumorexpressie.

Moleculaire beeldvorming kan mogelijk gebruikt worden als vroege voorspeller van de antitumoreffecten van andere geneesmiddelen. Het effect van een remmer van het eiwit 'mammalian target of rapamycin' (mTOR) op VEGF-A is bestudeerd. Het eiwit mTOR heeft een functie bij de translatie van verschillende oncogenen waaronder bij de angiogenese betrokken factoren. Door het remmen van mTOR door everolimus kan de tumorcel minder VEGF-A produceren. Monitoring van de VEGF-A expressie zou daarom

een vroege uitleesmogelijkheid kunnen zijn om te bepalen of de mTOR-remmer werkzaam is. VEGF-A spiegels kunnen uitgelezen worden door middel van een PET scan met het ^{89}Zr gelabelde antilichaam bevacizumab, dat bindt aan VEGF-A. Muizen met humane ovariumtumoren werden voor en tijdens behandeling met everolimus gescand na injectie van ^{89}Zr-bevacizumab. Behandeling met everolimus deed de ^{89}Zr-bevacizumab opname met 21% afnemen. In klinische studies wordt nu gekeken of ^{89}Zr-bevacizumab PET waardevol is als vroeg predictieve biomarker voor de antitumoreffectiviteit van mTOR-remmers in kankerpatiënten.

De rol die fluorescente beeldvorming kan spelen bij lokale beeldvorming van tumoren, bijvoorbeeld voor intra-operatieve tumorbeeldvorming, wordt onderzocht. Deze techniek kan waarschijnlijk verbeterd worden door gebruik te maken van tracers gericht tegen specifieke tumoreigenschappen. De ontwikkeling en toepassing van fluorescent gelabelde antilichamen zijn onderzocht in muismodellen met een intra-operatieve camera. Hiervoor zijn de antilichamen bevacizumab en trastuzumab gelabeld met de nabij-infrarode fluorescente kleurstof IRDye 800CW. Bevacizumab is gericht tegen VEGF-A en trastuzumab tegen HER2. Tumoropname van de nieuw ontwikkelde fluorescente tracers is getest door ze te vergelijken met dezelfde antilichamen, maar dan met ^{89}Zr gelabeld voor PET beeldvorming. De nieuw ontwikkelde fluorescente antilichamen, toonden dezelfde specifieke tumoropnames als de radioactief gelabelde antilichamen. Met de fluorescente probes konden zelfs sub-millimeter tumorlaesies aangetoond worden. Microscopische analyses op het tumorweefsel ondersteunden deze bevindingen. Uit deze studie blijkt dat fluorescent gelabelde antilichamen, gericht tegen VEGF of HER2, gebruikt kunnen worden voor specifieke en sensitieve detectie van tumorlaesies. Mede op basis van verkregen resultaten wordt deze techniek momenteel bestudeerd in borstkankerpatiënten.

Samenvattend beschrijft dit proefschrift de preklinische ontwikkeling en toepassing van nieuw ontwikkelde tracers voor PET beeldvorming en het gebruik van deze tracers om de tumorstatus te monitoren tijdens behandeling met antikankergeneesmiddelen. Daarnaast zijn antilichamen fluorescent gelabeld, en kunnen ze gebruikt worden voor locale detectie van tumorlaesies. Het onderzoek voor dit proefschrift is onder andere uitgevoerd met een subsidie van KWF Kankerbestrijding.

Dr. O.R. Brouwer

28 juni 2013
Universiteit van Amsterdam

Promotores:
Prof. dr. A.J.M. Balm
Prof. dr. S. Horenblas

Co-promotores:
Dr. R.A. Valdés Olmos
Dr. F.W.B. van Leeuwen
Dr. O.E. Nieweg

Innovating image guided surgery: Introducing multimodal approaches for sentinel node detection

Sentinelnodes in complexe gebieden

In dit proefschrift wordt onderzoek beschreven naar nieuwe technieken en multimodale benaderingen die gebruikt kunnen worden om sentinelnodes in complexe gebieden beter te kunnen lokaliseren. Om met de sentinelnode procedure de juiste lymfeklieren te kunnen vinden is het van belang dat alle sentinelnodes zowel pre- als peroperatief zichtbaar worden gemaakt. Dit kan vooral lastig zijn indien er sprake is van atypische lymfedrainage patronen, wanneer sentinelnodes nabij de primaire tumor/injectieplaats gelegen zijn, of wanneer sentinelnodes niet blauw gekleurd zijn ten tijde van excisie. Het zijn juist deze moeilijke omstandigheden waarbij nieuwe technieken en multimodale benaderingen zoals beschreven in dit proefschrift van toegevoegde waarde kunnen zijn.

Optimale preoperatieve beeldvorming

SPECT/CT is een aanvullende beeldvormingsmodaliteit, waarbij de driedimensionale SPECT beelden gefuseerd worden met CT beelden. Het proefschrift beschrijft onder meer een onderzoek waarin SPECT/CT voorafgaand aan de

operatie werd toegepast in meer dan driehonderd patiënten. SPECT/CT visualiseerde in alle patiënten nauwkeurig de locatie van de sentinelnodes in hun anatomische context. Daarnaast bleek SPECT/CT beter atypische lymfedrainage patronen in kaart te kunnen brengen. Zo worden in hoofdstuk negen bijvoorbeeld de resultaten van een prospectieve multicenter studie gepresenteerd waarbij vijftig patiënten met twee tumoren in de borst werden geïncludeerd om na te gaan of lymfoscintigrafie in combinatie met SPECT/CT, na injectie in beide tumoren afzonderlijk, tot meer gevisualiseerde sentinelnodes leidt dan injectie in alleen de grootste tumor. Bij 64% van de patiënten werd additionele lymfedrainage gezien na injectie in de tweede tumor. Dit betrof zowel multifocale als multicentrische tumoren. Dit hoge percentage van aanvullend gevonden sentinelnodes suggereert dat het bepalen van het lymfedrainage patroon van iedere aanwezige tumor kan leiden tot een betere stadiëring.

Hybride tracer die zowel radioactief als fluorescent is

Om de sentinelnode zichtbaar te maken voor het oog wordt tijdens de operatie standaard een blauwe kleurstof toegediend: patentblauw. Deze procedure leidt echter niet altijd tot succesvolle sentinelnode visualisatie. In dit proefschrift wordt de waarde beschreven van het toevoegen van peroperatieve fluorescentie beeldgeleiding aan de gebruikelijke combinatie van visuele en radioactief gestuurde procedure. Hiervoor wordt de toepassing beschreven van indocyaninegroen 99mTc-nanocolloid (ICG-^{99m}Tc-nanocolloid), een nieuwe hybride tracer die zowel radioactief als fluorescent is.
De resultaten toonden aan dat het fluorescente element van ICG-^{99m}Tc-nanocolloid sentinelnode visualisatie significant verbetert vergeleken met de standaard gebruikte blauwe kleurstof.
Hoofdstuk zes beschrijft een grotere prospectieve studie naar de meerwaarde van het gebruik van ICG–^{99m}Tc-nanocolloid bij 104 patiënten met een melanoom in het hoofd-halsgebied, op de romp, of op de extremiteiten. In totaal werden 246 sentinelnodes preoperatief geïdentificeerd. Er werden geen bijwerkingen ten gevolge van de ICG–^{99m}Tc-nanocolloid injectie gezien. Peroperatief kon 97% van de sentinelnodes worden gevisualiseerd met de fluorescentiecamera (tot zelfs 27 uur na injectie), terwijl slechts 60% van de sentinelnodes gekleurd was na injectie van patentblauw ($p<0.05$).
In hoofdstuk zeven wordt de toepassing van ICG–^{99m}Tc-nanocolloid tijdens laparoscopische procedures geëvalueerd bij patiënten die een robotgeassisteerde prostatectomie ondergingen gevolgd door sentinelnode biopsie. Na echogeleide toediening van ICG–^{99m}Tc-nanocolloid in de prostaat werden de sentinelnodes preoperatief scintigrafisch in beeld gebracht. Het hybride karakter van ICG–^{99m}Tc-nanocolloid maakte peroperatieve optische identificatie van de sentinelnodes mogelijk met behulp een endoscopische fluorescentiecamera. Tijdens de ingreep bleken detectie van het radioactieve en fluorescente signaal complementair. Fluorescentie was van waarde in gebieden met een hoog radioactief achtergrondsignaal, waarbij geleiding op basis van radioactiviteit compenseerde voor de nog beperkte weefselpenetratie van het fluorescente signaal. Alle geëxcideerde klieren waren zowel radioactief als fluorescent. Dit bevestigt de hoge correlatie tussen het radioactieve en het fluorescente signaal wat betekent dat de hybride tracer dus stabiel blijft gedurende het gehele pre- en peroperatieve proces.

3D intraoperatieve beeldgeleide navigatie

Idealiter zou de gedetailleerde preoperatieve driedimensionale informatie die SPECT/CT verschaft ook gebruikt kunnen worden om de chirurg tijdens de operatie te helpen de sentinelnodes te lokaliseren. Het laatste deel van het proefschrift beschrijft de eerste stappen in het overbrengen van SPECT/CT naar de operatiekamer door middel van peroperatieve beeldgeleide navigatie (mixed reality). Het bleek dat intraoperatieve navigatie op basis van preoperatieve SPECT/CT beelden technisch haalbaar is, maar dat verdere ontwikkeling van een peroperatieve modaliteit om succesvolle sentinelnode lokalisatie te bevestigen (zoals een gammastralendetectieprobe of fluorescentiecamera) nog wenselijk blijft.

Conclusies

- SPECT/CT visualiseert preoperatief nauwkeurig de locatie van de sentinelnodes in hun anatomische context en kan ook atypische lymfedrainage patronen beter in kaart brengen
- intraoperatieve radio- en fluorescentiegeleiding zijn modaliteiten die elkaar complementeren en kunnen worden verenigd in de hybride tracer ICG-^{99m}Tc-nanocolloid
- de toevoeging van peroperatieve hoge resolutie beeldvorming met een mobiele gammacamera en een fluorescentiecamera verbetert sentinelnode detectie in patiënten met sentinelnodes nabij de injectieplaats of in een gebied met complexe anatomie
- het fluorescente element van ICG-^{99m}Tc-nanocolloid verbetert sentinelnode visualisatie vergeleken met de standaard gebruikte blauwe kleurstof
- de succesvolle klinische introductie van deze hybride benadering stimuleert de verdere ontwikkeling van tumorgerichte hybride tracers en (hybride) camerasystemen
- peroperatieve 3D beeldgeleide navigatie op basis van SPECT/CT is technisch haalbaar gebleken; deze techniek maakt optimaal gebruik van de beschikbare preoperatieve beeldvorming en biedt nieuwe perspectieven voor beeldgeleide chirurgie

Link naar de inhoud van het proefschrift:
http://dare.uva.nl/record/448097

Congres van de Belgische Vereniging van Nucleaire Geneeskunde (BelNuc)

Oostende (België), 24 tot en met 26 mei 2013

Staging patients with high risk prostate cancer: ^{18}F-methylcholine PET/CT can not replace PLND

van Os KJ[1], Trip EJ[2], van Melick HHE[2], Verzijlbergen JF[1], van Buul MMC[1]

Departments of [1]Nuclear Medicine and [2]Urology, St. Antonius Hospital Nieuwegein/Utrecht, The Netherlands

Purpose

The incidence of (advanced) prostate cancer (PCA) is increasing. In patients with high risk prostate cancer, lymph node (LN) metastases most commonly involve the internal iliac, external iliac, or obturator nodes. For LN staging, pelvic lymph node dissection (PLND) is the gold standard. In this study, it was evaluated if ^{18}F-methylcholine positron emission tomography/computed tomography (FCH PET/CT) can replace invasive PLND.

Materials and methods

A consecutive series of patients with high risk PCA according to D'Amico criteria (or cT3, or PSA>20, or Gleason ≥8), were prospectively included from May 2011 - July 2012. All patients underwent routinely laparoscopic pelvic lymph node dissection (LPLND) after FCH PET/CT. Acquisition started 5 min after injection of the radiotracer. The blinded reviewed imaging results were compared with histology. Sensitivity, specificity, positive- and negative predictive value (PPV, NPV) of FCH PET/CT were calculated.

Results

Sixteen patients were included with a mean age of 69 y (60-77 y), mean PSA 42,9µg/l (2.8-363µg/l), mean Gleason score 8.2, and a chance of ≥ 15% to have disseminated disease according to the MSKCC nomogram. Sensitivity, specificity, PPV and NPV were calculated as 63%, 88%, 83%, and 70% respectively. In none of the patients, distant metastases were found in this early stage of disease.

Conclusion

In patients with high risk prostate cancer, ^{18}F-Methylcholine PET/CT can not replace laparoscopic pelvic lymph node dissection in the staging procedure. These results are comparable with studies in literature in which FCH PET/CT was acquired 60 min. post-injection. This suggests that bladder activity is not the cause of the low sensitivity in lymph node staging.

The potential value of first-pass FDG PET imaging

Mertens J[1], De Man K[1], Van de Wiele C[1], Smeets P[2], Goethals I[1]

Departments of [1]Nuclear Medicine and [2]Radiology, Ghent University Hospital, Ghent, Belgium

Introduction

It was previously shown that first-pass FDG PET images could provide an index of tumor perfusion. A study was set up to assess the feasibility of first-pass PET images and to identify the different patterns of FDG uptake on these early images.

Methods

89 patients referred for oncological (re)staging underwent a dynamic PET acquisition. First-pass images (0-2 min. after injection) were compared to standard images.

Results

Twenty-four cases (27%) had no detectable lesions on standard and first-pass images in the selected field of view. In the remaining 65 cases, four different patterns of 18F-FDG distribution were identified. The first pattern consisted of a decreased uptake in the tumours in the early phase whereas increased uptake was noted on the standard images. This was observed in 14 patients (16%), mainly in liver metastases. In the second pattern, the tumoural lesions (n=12; 13%) could only be visualized on the standard images and were iso-intense compared to the background on the first-pass images. In the third pattern, both the first-pass and the standard images showed increased uptake in the tumours, but uptake was higher on the standard images. This was observed in the majority of tumours (n=38; 43%). The last pattern also showed an increased uptake on both the first-pass and the standard images, but uptake was relatively higher on the early images. This pattern was observed in only one case (1%).

Conclusion
First-pass PET images provide information that is visually different from that in the standard PET images. Further studies are needed to explore the relationship between first-pass FDG uptake and tumour perfusion as well as to assess the clinical relevance of these findings.

Nuclear imaging of mesenchymal stem cells using the human sodium iodide symporter

Wolfs E[1], Holvoet B[1], Gijsbers R[2], Debyser Z[2], Van Laere K[1], Verfaillie CM[3], Deroose CM[1]

[1]Division of Nuclear Medicine and Molecular Imaging (Department of Imaging and Pathology), [2]Leuven Viral Vector Core (LVVC), Centre for Molecular Medicine, and [3]Stem Cell Institute (Department of Development and Regeneration), KU Leuven, Leuven, Belgium

Introduction
Mesenchymal stem cells (MSCs) are of great interest in the field of regenerative medicine due to their extended differentiation capacity, their trophic effects on endogenous repair mechanisms and their immune regulatory capacity. However, more knowledge on the in vivo fate of these cells has to be acquired. Therefore, imaging reporter genes can be introduced into these cells for longitudinal and non-invasive imaging following engraftment. Human reporter genes have theoretical immunological advantages compared to the viral reporter genes. The aim of this study is the in vitro optimization of MSC expression of the human reporter gene sodium iodide symporter (hNIS).

Methods
As a proof of principle, several hNIS bearing constructs were used for transducing HEK293 cells and uptake experiments were performed using $^{99m}TcO_4^-$. Subsequently, the optimal promoter for driving the final construct for MSC targeting was assessed using GFP expression measured by FACS. From these data, the final multicistronic lentiviral vector was created encoding EF1α- 3flag-Fluc-T2A-hNIS-IRES-Puro, for bioluminescence imaging (BLI) and PET/SPECT. This system was validated with uptake experiments with $^{99m}TcO_4^-$ and in vitro BLI in MSCs. Furthermore, we performed blocking experiments using perchlorate.

Results
A significantly higher uptake of $^{99m}TcO_4^-$ in HEK 293 cells expressing hNIS was observed. Additionally, the optimal promoter for transducing MSCs was the EF1α promoter, as measured using FACS. First experiments using the final multicistronic lentiviral vector in MSCs, revealed that the uptake of $^{99m}TcO_4^-$ after puromycin selection was ~25 times higher than the uptake in controls or in non-selected hNIS expressing cells, with 55% of the tracer taken up per 1, 000,000 cells. Also, the expression of Fluc was confirmed using in vitro BLI. Perchlorate, used for blocking hNIS function, successfully inhibited the uptake of $^{99m}TcO_4^-$ in MSCs.

Conclusions
In this study, it was confirmed that a functional expression of the imaging reporter genes Fluc and hNIS is obtained in MSCs after the transduction of these cells with a lentiviral vector. In a next step, these cells will be used for in vivo validation of this system.

Prognostic value of the corrected absolute uptake (CAU) obtained using ^{99m}Tc-MAG3 renography within the 24h following renal transplantation.

Lemonnier F, Musuamba F, Mourad M, Jamar F

Department of Nuclear Medicine, UCL, Bruxelles, Belgium

Aim of study
Renography using ^{99m}Tc-MAG3 is commonly used as a non-invasive evaluation method in the follow-up of renal transplants. We studied the short and medium term prognostic value of the corrected absolute uptake (CAU) obtained using ^{99m}Tc-MAG3 renography within the 24h following renal transplantation.

Materials and methods
CAU is the uptake of ^{99m}Tc-MAG3 during the parenchymal transit time -90-150 sec- (corrected for attenuation, body surface area, expressed as % of injected activity). We performed a retrospective study on 208 consecutive kidney transplant patients in a University Hospital between 2007 and 2009. We took into consideration the following parameters of the donor (alive, heart-beating-donor (HBD) or non-heart-beatingdonor (NHBD), gender, age, BMI, serum creatinine level (Cr)) and of the receiver (gender, age, BMI, HLA match, total ischemia time). The following outcome parameters were analysed: the need for posttransplantation dialysis session(s), the time required to reach a Cr < 2mg/dl, Cr at day 14, 1 and 6 months, Cr, GFR according to MDRD, the survival of the graft and of the patient at one year. Univariate and multivariate analyses were performed to investigate the importance and influence of the CAU on the renal graft's function up to one year.

Results
The univariate analysis demonstrates that a CAU above 5.6% can forecast (NPV of 91%) a good graft's function at one year. Conversely, a low CAU does not indicate a bad function of the transplant at one year. From the multivariate analysis, we found that CAU is an independent prognostic parameter of graft's function on short term and up to one year.

Conclusion
The CAU measurement is an easy complementary information to offer. It turned out to be a good forecasting parameter on the short and medium (one year) term of the good functioning of the kidney graft.

Use of a portable gamma camera for preoperative lymphatic mapping in head/neck melanoma

Hellingman D[1], Vidal-Sicart S[2], de Wit-van der Veen L[1], van der Hiel B[1], Valdés-Olmos RA[1]

Department of [1]Nuclear Medicine, Netherlands Cancer Institute - Antoni van Leeuwenhoek hospital (NKIAVL), Amsterdam, The Netherlands and Department of [2]Nuclear Medicine (CDIC), University Hospital Clinic, Barcelona, Spain

Purpose
In head/neck melanoma lymphatic drainage may concern different node basins with sentinel nodes (SNs) often located near the primary lesion. We evaluated the feasibility of preoperative lymphatic mapping with a portable small high-resolution gamma-camera.

Methods
Preoperative lymphoscintigraphy with a 40×50cm field of view (FOV) conventional gamma-camera was firstly performed after ^{99m}Tc-nanocolloid injection on the basis of a 10min dynamic study, followed by anterior and lateral images (15min, 2h) and SPECT/CT (2h). Subsequently, anterior and lateral overview images were performed with a portable gamma-camera (Sentinella, Oncovision), with a 4mm pin-hole collimator, positioned at 15cm from the patient to obtain a FOV of 20×20cm. Additionally, high-resolution images of the injection site and hotspots found in the overview images were obtained with the portable camera positioned close to the skin . Lymphatic drainage as depicted on the 2h-conventional gamma-camera images was compared with the portable camera views concerning number of depicted nodes, localization, and acquisition time.

Results
In the first 10 patients the portable gamma-camera was able to detect SNs in 9 patients (90%), in 2 of them in the proximity of the injection. Conventional gamma-camera depicted SNs in 70% and SPECT/CT in 90%. Second-echelon nodes were visualized in 50% of the patients with the portable gamma-camera, and in 60% of the cases with the conventional gamma-camera and SPECT/CT. Average acquisition times (2h post injection) were 10 min (±2 SD) for the portable gamma-camera and 12min (±1 SD) for the conventional one.

Conclusion
Due to its better spatial resolution a portable gamma-camera fitted with a pinhole collimator may be of great value to preoperatively depict sentinel nodes near the injection site. This device may be useful in centres without the possibility to perform adequate preoperative image with conventional gamma-cameras.

Quantification of ^{11}C-NE40, a novel PET radioligand for CB2 receptor imaging

Postnov A[1], Ahmad R[1], Evens N[2], Versijpt J[3], Vandenbulcke M[6], Yaqub M5, Verbruggen A[2], Bormans G[2], Vandenberghe W[3], Van Laere K[1]

Departments of [1]Nuclear Medicine and Molecular Imaging, [2]Laboratory for Radiopharmacy, [3]Neurology, and [6]Old Age Psychiatry, University Hospital KU Leuven, Belgium; Department of [4]Neurology, University Hospital Brussels, Belgium and Department of [5]Nuclear Medicine, VUmc, Amsterdam, The Netherlands

Objective
The type 2 cannabinoid receptor (CB2R) is part of the endocannabinoid system and is expressed in tissues related to the immune system. CB2R upregulation has been reported in neurodegenerative disorders post-mortem and CB2R stimulation has anti-inflammatory properties. Here, we have performed initial brain kinetic modeling of the novel CB2R tracer ^{11}C-NE40 in healthy controls (HC), Alzheimer's disease patients (AD) and in Parkinson's disease patients (PD).

Material and Methods
Dynamic 90 min [11C]-NE40 PET scans were performed on 10 HC, 8 AD and 6 PD patients using a Siemens Biograph 16 PET-CT. Manual arterial blood sampling was done for input function determination including metabolite correction, and volumetric 1.5 T T1 MRI

images were acquired for grey matter segmentation and VOI delineation.

Results
^{11}C-NE40 was metabolized quickly leading to 50% of intact tracer 20 min p.i. and 20% at 90 min p.i. Uptake was generally low with the average K1 value around 0.05 ml/min/ml tissue. A relatively large intraindividual variability was observed in TAC shapes, response to the input function and thus in kinetic parameters (see table 1). AD patients had lower VT and BPND compared to HV and PD. Partial volume correction (Rousset) did not alter the results significantly.

Table 1. Kinetic modeling results. Between-group differences (p<0.05): AD-HC(*), AD-PD(**)

	VT 1T model	VT 2T model	BPND 2T model
HC	0.90±0.12 *	1.24±0.25 *	1.28±0.36 *
AD	0.70±0.07 *,**	0.90±0.13 *,**	0.77±0.21 *,**
PD	0.90±0.07 **	1.11±0.20 **	1.17±0.42 **

Conclusion
For ^{11}C-NE40, a 2T model fitted most of the TACs best and both BPND and Vt parameters can be used. We did not observe a significant increase in PD or AD patients compared to controls in vivo.

The prognostic value of preoperative FDG PET-CT in hepatocellular carcinoma treated by liver transplantation

Govaerts L, Detry O, Blétard N, Verset G, Honoré P, De Roover A, Delwaide J, Hustinx R

CHU de Liège, Belgium

Objectives
To evaluate the prognostic value of pretreatment FDG PET-CT in patients from occidental population with hepatocellular carcinoma (HCC) treated by liver transplantation and to compare it with established prognostic factors.

Methods
Retrospective observational analysis which includes patients with HCC treated by liver transplantation that had an FDG PET-CT before the transplantation with no neoadjuvant treatment prior the FDG PET-CT and no history of other malignancy. We measured the maximal standardized uptake value and the mean standardized uptake value of the tumour (TSUVmaxand TSUVmean) and the normal liver (LSUVmax and LSUVmean) and the ratio TSUVmax/LSUVmax and TSUVmean/LSUVmean were tested as prognostic factors and compared to conventional prognostic factors.

Results
28 patients met de inclusion criteria (25 men and 3 women, mean age 58 years ± 9 years, mean follow-up 26 ± 17 months). The ratio TSUVmax/LSUVmax and TSUVmean/LSUVmean were tested with established prognostic factors including MILAN, CLIP, OKUDA, TNM stage, alphafoetoprotein, size of the biggest nodule, degree of tumour invasion in the liver. The ratio TSUVmax/LSUVmax was significant for recurrence and death in an univariate analysis and particularly for the 1.15 cut-off with sensibility, specificity, negative predictive value and positive predictive value respectively 80%, 83%, 95% and 50%. Among the conventional prognostic factors, only the size of the biggest nodule was significant for the risk of recurrence and death.

Conclusions
The ratio TSUVmax/LSUVmax seems to be the best short-term prognostic factor for recurrence and death in patients with HCC treated by liver transplantation with a cut-off value of 1.15 and it should be used in the preoperative assessment.

A systematic review of the predictive value of ^{18}FDG-PET in oesophageal and oesophagogastric junction cancer after neo-adjuvant treatment on the SURVIVAL outcome stratification

Pascaline Schollaert MD[1], Ralph Crott MPH, PhD[4], Claude Bertrand, MD[2], Lionel D'Hondt MD, PhD[3], Thierry Vander Borght, MD, PhD[1] and Bruno Krug, MD, PhD[1,4].

Divisions of Nuclear [1]Medicine, [2]Surgery and [3]Oncology, CHU UCL Mont-Godinne-Dinant, Yvoir, and [4]Institute of Health and Society, Université Catholique de Louvain, Belgium

Background
Although radical surgery preceded by neo-adjuvant chemoradiation or chemotherapy is the most common approach for treating patients with advanced oesophageal and oesophagogastric junction cancer, predicting clinical outcome remains difficult.

Objective
We studied the predictive value of ^{18}FDG-PET for

assessing disease-free (DFS) and overall survival (OS) in advanced oesophageal and oesophagogastric junction cancer.

Data sources
A literature search (PUBMED/MEDLINE, EMBASE, Cochrane) until April 2012 was performed to identify full papers with ^{18}FDG-PET and survival data, using indexing terms and free text words.

Study selection
Studies with >10 patients, to present sequential or at least one post-treatment ^{18}FDG-PET data and Kaplan-Meier survival curves with >6 months median follow-up period.

Main Outcome Measures
We performed a meta-analysis for disease-free survival (DFS) and overall survival (OS) data using the hazard ratio (HR) as outcome measure. Sources of study heterogeneity were explored.

Results
We identified 26 eligible studies including a total of 1544 patients (mean age 62 years, 82% males). The TNM distribution was as follows: stage I 7%, II 24%, III 53% and IV 15%. The pooled HRs for complete metabolic response versus no response were 0.51 for OS (95%CI, 0.4 to 0.64; P<0.00001) and 0.47 for DFS (95%CI, 0.38 to 0.57; P<0.00001), respectively. No statistical heterogeneity was present. To explore other sources of heterogeneity we realised subgroup and regression analyses. Taken into account the moderate correlation between OS and DFS (rho 0.54), we used joint bivariate random regression model. These analyses did not show a statistically significant impact of study characteristics and PET modalities on the pooled outcomes.

Conclusion
Despite methodological and clinical heterogeneity, complete metabolic response on ^{18}FDG-PET is a significant prognostic predictor for long-term survival outcomes.

Sentinel node procedure for lymph node staging in prostate cancer

Van den Bergh L, Joniau S, Lerutm E, Isebaert S, Ameye F, Van Poppel H, Haustermans K, Deroose CM

University Hospitals Leuven, Leuven, Belgium

Introduction & objectives
The objective of this study was to investigate the feasibility of a sentinel node (SN) procedure and to compare it to different lymph node dissection (LND) templates in prostate cancer (PCa) patients at high risk for lymph node (LN) involvement.

Materials & methods
A total of 74 patients with a risk ≥10% for LN metastases (Partin tables) who were N0 at contrast-enhanced CT-scan, were prospectively enrolled. Three transrectal ^{99m}Tc-nanocolloid injections were performed per prostate lobe under ultrasound guidance. Two hours later, patients underwent planar and SPECT-imaging. The SPECT images were fused to CT images to facilitate localisation of the SN during surgery. Intraoperatively, a gamma probe was used to detect the LN that had taken up the radionuclide and SN were removed separately. After SN dissection, all patients underwent a super-extended (se)LND (internal, external and common iliac, obturator fossa and presacral regions), followed by radical prostatectomy. All retrieved LN were sectioned and histopathologically examined.

Results
In total, 470 SN (median 6) were scintigraphically detected of which 371 (median 4) were located and removed during surgery. In 3 patients, no SN were detected intraoperatively of which 1 patient had negative SPECT images as well. Histopathology confirmed LN metastases in 34 patients (46%) with 91 affected LN in total (median 2). Fortysix metastatic LN were SN (51%). Twenty-eight node positive (N+) patients had at least 1 N+ region containing a SN, which was affected in 96% (27/28). When taking the 6 additional N+ patients into account in whom no SN were detected in the affected region the sensitivity of the procedure decreased to 79% (27/34). These results are inferior to results obtained with a standard extended LND which would have correctly staged no less than 94% of these patients (32/34).

Conclusion
Although the SN procedure was technically feasible, its sensitivity was too low to offer a valuable alternative to the standard extended LND for nodal staging in this setting.

The role of ^{18}FDG-PET/CT for response assessment after (chemo)radiotherapy for head and neck squamous cell carcinoma

Roothans D, Van Den Heuvel B, Helsen N, Van den Wyngaert T, Van Den Weyngaert D, Carp L, Stroobants S

Department of Nuclear Medicine, UZ Antwerpen, Belgium

Purpose
To evaluate dedicated FDG-PET/CT for the assessment of treatment response in patients with head and neck squamous cell carcinoma (HNSCC).

Patients and methods
Patients with histologically proven HNSCC treated with (concomitant chemo-)radiotherapy were studied retrospectively. Histopathology or clinical follow-up (≥12 months) provided the reference standard. Sensitivity, specificity, positive (PPV) and negative predictive value (NPV), and accuracy were calculated on a patient level. The impact of the imaging interval post-treatment was analysed using logistic regression. For survival outcomes, Kaplan Meier-analysis and adjusted Cox regression were used.

Results
104 patients were included (median age 60y; male n=84). Median follow-up was 28.3 months (range 0.4 - 60.7 months). FDG-PET/CT was performed at a median of 13 weeks post-treatment (range 5.4-28.9 weeks). Sensitivity, specificity, PPV, NPV, and accuracy were 89% (95% CI 73% – 97%), 90% (95% CI 80% – 96%), 82% (95% CI 66% – 92%), 94% (95% CI 85% – 98%) and 89% (95% CI 82% – 95%), respectively. FDGPET/ CT was significantly more accurate when performed >11 weeks after treatment (p=0.01), due to a higher specificity (97% vs 50%, p<0.001). The odds of FDG-PET/CT correctly identifying complete responders increased with 34% for every additional week between end of therapy and imaging (OR 1.34; 95% CI 1.07 – 1.68; p=0.01). A complete response on FDG-PET/CT was associated with a significantly longer median overall survival (50.7 vs 10.3 months; p<0.001). In an adjusted Cox model, residual disease on FDG-PET/CT after therapy was associated with a 7-fold higher risk of death (HR 7.11; 95%CI 3.58 - 14.12; p<0.001).

Conclusion
FDG-PET/CT has a high diagnostic value to detect residual disease after (chemo)radiotherapy, with significantly higher accuracy when performed >11 weeks after end of therapy. Furthermore, FDG-PET/CT can be used to identify patients with poor prognosis.

Transient ischemic dilation in patients evaluated for coronary artery disease with adenosine SPECT and coronary angiography.

Janssen J, Danad I, Knaapen P, Raijmakers PG

VU Medical Centre, Amsterdam, The Netherlands

Introduction
Changes in left ventricular volume (LV) can be quantified using myocardial stress/rest SPECT imaging, and are expressed as the Transient Ischemic dilation (TID) ratio. The TID measurement provides additional diagnostic information for patients evaluated for coronary artery disease (CAD). However, different stress and scanning protocols with varying tracers may have different cut-off values for normal/ abnormal TID ratios. Data regarding normal limits of TID values for adenosine tetrofosmin SPECT imaging are scarce.

Methods
In this prospective study we compared SPECT derived TID values with the findings of a coronary angiogram, performed within a week from SPECT imaging. In all patients Fractional Flow Reserve (FFR) measurements of the coronary vessels was performed.

Results
We included 68 patients (male/female 62%/38%, and mean age 58.1+/-9.8 year). All patients had an intermediate risk for CAD. All patients had a two day stress/rest ^{99m}Tc-Tetrofosmin SPECT protocol, with a standardized adenosine stress protocol. The mean TID for patients without a significant stenosis in the coronary arteries, defined as a FFR value of >080, was 1.01+/-0.094. Hence, the upper normal limit for TID was 1.20. Patients with severe CAD, defined as significant 3 vessel disease and/or significant left main stenosis, had a significant higher TID of 1.08+/-0.13 (p<0.05). However, only 33% of the patients with severe CAD had a TID > 1.20.

Conclusion
The upper normal limit of TID is 1.20 for a 2 day adenosine tetrofosmin SPECT protocol. TID has a limited accuracy for the detection of severe CAD.

Optimal projections subset determination for the reconstruction of ^{99m}Tc-DMSA SPECT studies after motion correction.

Hesse M[1], Demonceau G[2], Walrand S[1], Jamar F[1]

Departments of Nuclear Medicine [1]Cliniques Universitaires Saint-Luc, Brussels and [2]Sint-Elizabeth Ziekenhuis, Zottegem, Belgium

Aim
Most ^{99m}Tc-DMSA studies are done on children, and are so often prone to patient motion. Motion correction in pinhole SPECT is quite challenging due to the pinhole magnification

that is strongly spatially dependent. Using a previously validated motion correction technique, we investigated whether the reconstruction of a projection subset could be better than using all the projections.

Methods
Six hours after a weight-dependent injection of ^{99m}Tc-DMSA, a 25min-pinhole SPECT was performed in 110 patients from 1 month old to 47 years old. First, a motion-free orbit subset was determined, reconstructed and re-projected at all acquisition angles. Then the acquired projections were shifted to match as well as possible those re-projections. This process was repeated on the corrected projections until the orbit subset free of residual motions increased no longer. To define the projection subsets to reconstruct, we used various criteria based on the kidney's position on the motion corrected acquisition, and we selected projections for which these positions were closer to a fitted sinogram or to the re-projected kidney's position. The final reconstruction quality was visually assessed, based on the presence of high background and double contours.

Results
The selected set of projections differed from the full orbit in more than half the patients. However, no significant improvement with respect to the full orbit reconstruction was observed. This was probably due to the fact that the subsets differed in general only in a few isolated angles, whose effect was reduced by the averaging in the reconstructed image.

Conclusion
Contrary to what could be expected, using some criteria to limit the set of incidences to be reconstructed after our motion correction in PHS did not provide any visual improvement of the final image.

Preoperative radioguided tumour-related injection with freehand-SPECT for sentinel lymph node mapping in non-palpable breast cancer

Pouw B, de Wit - van der Veen L, Stokkel M, Brouwer OR, Valdés Olmos RA

Department of Nuclear Medicine, the Netherlands Cancer Institute, Amsterdam, the Netherlands

Purpose
This study was designed to explore the feasibility of replacing conventional ultrasound (US) guided ^{99m}Tcnanocolloid injections by radioguided tumour-related ^{99m}Tc-nanocolloid administration using freehand-SPECT in patients with non-palpable breast cancer scheduled for Sentinel Lymph Node Biopsy (SLNB). The freehand-SPECT procedure was based on the detection of an iodine-125 (^{125}I) seed, which was implanted a few weeks before SLNB. This approach aimed to decrease the workload for the Radiology Department, avoiding a second US-guided procedure.

Materials and Methods
In 10 patients in supine position the implanted ^{125}I seed was firstly localized using freehand-SPECT and subsequently by conventional US. For both techniques the perpendicular ^{125}I seed depth was determined to guide ^{99m}Tc-nanocolloid injection. The following 21 patients were injected using only freehand-SPECT localisation, the distance between the ^{99m}Tc-nanocolloid injection and the ^{125}I seed was evaluated by means of SPECT/CT.

Results
The average depth difference measured by US and freehand-SPECT in the first 10 patients was 1.6 mm (SD 1.6 mm, Range 0-5 mm). In the following 21 patients the average difference between the ^{125}I seed and the centre of the ^{99m}Tc-nanocolloid injection-depot was 11.6 mm (SD 7.0 mm, range 0-26 mm). In a control group of 21 patients with only US-guided injections an average difference of 8.7 mm (SD 4.6 mm, range 2-21 mm) was measured.

Conclusion
Minimal differences for ^{125}I seed guided injections between conventional US and freehand-SPECT in patients with non-palpable breast tumours were observed in the present study. Additionally, when comparing the ^{99m}Tc-nanocolloid and ^{125}I localisations on SPECT/CT, the concordance was clinically acceptable. It is concluded that freehand-SPECT guided ^{99m}Tc-nanocolloid injections in patients with non-palpable breast cancer, scheduled for SLNB and with an implanted ^{125}I seed, are feasible and appear to be reliable.

Transient Changes in the Endocannabinoid System after Acute and Chronic Ethanol Exposure and Abstinence in the Rat: a Combined PET and Microdialysis Study

Ceccarini, Casteels C*, Koole M, Bormans G, Van Laere K*

University Hospital Leuven, Leuven, Belgium
** equal contribution*

Objective
Recent evidence suggests involvement of the endocannabinoid system in alcohol drinking behavior. Using

^{18}F-MK-9470 small-animal PET imaging, we first evaluated type 1 cannabinoid receptor (CB1R) binding changes in rats subjected to several ethanol conditions: (i) at baseline, (ii) after acute ethanol administration (4g/kg), (iii) after 7-days of forced chronic ethanol consumption, and (iv) after 7 and 14-days of abstinence. Secondly, levels of brain anandamide (AEA) in the nucleus accumbens (NAcc) were investigated in the same animals using microdialysis and correlated to the CB1R binding changes.

Methods
In total, twenty-eight male Wistar rats were investigated. Small-animal PET was done on a FOCUS-220 with ~12 MBq of ^{18}F-MK-9470. Images were normalized to Paxinos space and analyzed voxel-wise using SPM8. AEA content was quantified using HPLC with tandem mass spectrometry detection.

Results
Acute ethanol administration increased CB1R binding in the NAcc (+7.7%) that positively correlated to the change in AEA level of that region (r=0.99). Chronic ethanol exposure decreased CB1R binding in the hippocampus (-5.2%) and caudate-putamen (-5.7%), whereas same regions were increased by +8.9% and +14.2% after 7-14 days of abstinence. Also, after 7-14 days of abstinence, CB1R binding additionally decreased in the orbitofrontal cortex (>-20.1%). The magnitude of these hippocampal and frontal changes was highly correlated to daily ethanol intake (r=0.99 and r=-0.99, respectively).

Conclusion
This study provides evidence that acute ethanol consumption is associated with an enhanced endocannabinoid signaling in the NAcc. In addition, chronic ethanol exposure points to regional dysfunctions in CB1R levels, incorporating hippocampus and caudate-putamen that are reversible within two weeks in this animal model.

Energy spectrum and point spread function comparison of pinhole and parallel-hole collimators for ^{90}Y bremsstrahlung imaging

Walrand S[1], Hesse M[1], Seret A[2], Demonceau G[3], Jamar[1]

[1]UCL, [2]Ulg, [3]SEZH, Belgium

Aim
Recent studies prove pinhole being superior to parallel hole collimator for ^{90}Y bremsstrahlung SPECT. We analyzed their energy spectra and PSF.

Methods
A camera (1/2"-thick NaI), successively equipped with a medium energy general purpose (MEGP) parallel hole and a 9mm-diameter aperture medium energy pinhole (MEPH) collimator was used. A ^{90}Y point source surrounded by 1cm-thick perpex wall and a 1cm-diameter ^{99m}Tc source, both located at 10 cm far away the collimator, were acquired.

Results
MEGP ^{90}Y energy spectrum matched published Monte Carlo (MC) simulations. Compared to MEGP, the lead fluorescence x-rays were reduced by 4 in the MEPH 90Y energy spectrum which displayed an exponential decrease pattern. The MEPH collimator sensitivity was 1.5 times higher than that of the MEGP one, but for a FOV area 6 times smaller. The FWHM (FWTM) in the object space for 90Y were 1.2 (2.0) and 1.5 (3.1) cm for the MEPH and MEGP collimators, respectively. Farther than 3 cm, the MEGP PSF was typically 6 fold higher than the MEPH one. By subtracting from the 90Y PSF the 99mTc one, the geometric to total x-rays ratios in a [50-150] keV window were 68% and 31% for the MEPH and MEGP collimators, respectively. This last value is in line with MC simulations.

Conclusions
For ^{90}Y, the MEPH collimator displayed a twice better geometric to total x-rays ratio and a sharper PSF with 6 fold lower tail than the MEGP ones explaining the better spatial resolution and quantification accuracy obtained by helical pinhole bremsstrahlung SPECT. MEPH collimator MC modelling will assess the different components contribution: tungsten insert, lead housing, camera compartments.

TSH measurement is not an appropriate screening test for autonomous functioning thyroid nodules: a retrospective study of 368 patients

Chami R[1], Moreno-Reyes R[2], Corvilain B[1]

Departments of [1]Endocrinology and [2]Nuclear Medicine Hôpital Erasme, Université Libre de Bruxelles, Brussels, Belgium

Objective
Based on the assumption that a normal TSH concentration rules out the presence of autonomous functioning thyroid nodules (AFTNs), nearly all clinical guidelines on the management of thyroid nodules only recommend performance of a thyroid scan if TSH concentration is subnormal. Our objective was to

determine the proportion of AFTNs with a normal TSH level to ascertain whether a normal TSH really rules out the presence of an AFTN.

Design
Retrospective study on 368 patients with a final diagnosis of AFTN.

Setting
Academic hospital in Brussels (Belgium).

Participants
All the thyroid scans with a diagnosis of AFTN were reviewed retrospectively by one of us (R.M-R), unaware of the clinical data. The diagnosis of unique AFTN was confirmed in 368 patients. Among them we secondarily selected 217 patients on the basis of the absence of another thyroid nodule greater than 10 mm, the absence of medical conditions able to interfere with thyroid function and the completeness of the data.

Main outcome measures
Proportion of patients with a diagnosis of AFTN and a normal TSH level.

Results
In our population the proportion of AFTNs with normal TSH was 49%. This proportion increased to 71% if we considered only those patients for whom thyroid scan was performed in the workup of a thyroid nodule. This proportion decreases as the size of the nodule increases. A normal TSH was observed in 97% of AFTNs between 10 and 19 mm, 77% between 20 and 29 mm, 59% between 30 and 39 mm and 40% above 40 mm.

Conclusions
Our data suggest that serum TSH measurement is not an effective screening tool to diagnose an AFTN. On the basis of a "TSH only" screening, as recommended by the vast majority of international guidelines, 71% of our patients would have undergone unjustified fine needle aspiration cytology (FNAC) in the workup of a thyroid nodule leading to unnecessary surgery for some of them. Thyroid scan remains the gold standard for detecting AFTN and should be considered before performing FNAC.

Human brain PET imaging of PDE10A in Parkinson's and Huntington's disease

Ahmad R[1], Bourgeois S[1], Postnov A[1], Schmidt ME[2], Bormans G[1], Vandenberghe W[1], Van Laere K[1]

[1]University Hospital Leuven and [2]Janssen Pharmaceutica, Beerse, Belgium

Objective
Phosphodiesterase 10A (PDE10A) is an enzyme that hydrolyzes cAMP and cGMP. PDE10A is strongly expressed in striatal medium spiny neurons and is assumed to be involved in several brain disorders. We have used the novel tracer ^{18}F-JNJ-42259152 and Positron Emission Tomography (PET) to evaluate PDE10A activity in patients with Huntington's (HD) and Parkinson's (PD) disease in vivo.

Methods
Five patients with PD and 5 patients with HD were compared to 11 healthy controls (CON). Patients were clinically evaluated using the Unified Parkinson's Disease Rating Scale (UPDRS), and Unified Huntington's Disease Rating Scale (UHDRS), respectively. All subjects received a slow bolus of 168.3±11.5 MBq 18F-JNJ-42259152, were scanned dynamically for 90 minutes with full arterial sampling. Dynamic VOI analysis of the striatum and substantia nigra was done on individual volumetric MRI data. Distribution volume VT, obtained with a two tissue compartment model (2TCM) and binding potential (BPND) using a Reference Tissue Model (MRTM) with frontal cortex as a reference region was used with partial volume correction.

Results
HD patients showed a strongly reduced VT and BPND in the striatum compared to CON. After PVC BPND values where significantly different between HD en CON for putamen (PT) and caudate nucleus (CNc) ($p=0.02$ and $p<0.001$ respectively), but not for ventral striatum (VSt) or substantia nigra (SN). There was no significant difference between PD and CON (PT $p=0.77$; CNc $p=0.79$; VSt $p=0.23$; SN $p=0.46$).

Conclusion
In vivo, PDE10A activity is severely reduced in PT and CNc of patients with HD, whereas it is preserved in PD. Modulation of PDE10A activity may be of interest in HD as potential novel target.

Correlation of dynamic ^{68}Ga-DOTATOC PET/CT parameters with static image parameters in neuroendocrine tumor patients during PRRT

Van Binnebeek S[1], Koole M[2], Baete K[1], Vanbilloen B[1], Clement PM[3], Haustermans K[4], Mortelmans L[1], Bogaerts K[5], Van Cutsem E[6], Verslype C[6], Verbruggen A[7], Mottaghy FM[8,9], Deroose CM[1]

Department of [1]Nuclear Medicine, [2]Medical Oncology,

[4]Radiation Oncology, [5]Department of Public Health and primary Care (I-BioStat), [6]Digestive Oncology, [7]Laboratory for Radiopharmacy, University Hospitals Leuven, Leuven, Belgium and Department of [2]Nuclear Medicine, University Medical Centre Groningen, Department of [8]Nuclear Medicine, Maastricht University Medical Center, Maastricht, The Netherlands and Department of [9]Nuclear Medicine, University Hospital Aachen, Germany

Aim

Our aim was to investigate the relationship between dynamic-imaging parameters (Ki) and static imagederived parameters of ^{68}Ga-DOTATOC PET to determine which static parameter best reflects the underlying somatostatin receptor expression levels on neuroendocrine tumors (NETs) during peptide receptor radionuclide therapy (PRRT).

Methods

19 patients with metastasized NETs underwent a dynamic and static ^{68}Ga-DOTATOC PET before PRRT, at 7 and 40 weeks after the first therapy cycle. In total, we analyzed 172 lesions on both dynamic and static scans. Kinetic modeling was performed using the software package PMOD on 1 to 5 prospectively chosen target lesions per patient. Maximum standard uptake value (=SUVmax) and mean SUV (=SUVmean) of the tumoural lesions were assessed on each of the 6 scans, the input function was retrieved from image data. In addition, Ki, corresponding to the influx of tracer in the tumor, was calculated using PMOD and the Patlakplot. Finally, 4 regions for normalization of the SUVtumor (spleen(S), pituitary gland (PG), muscle (M) and bone marrow (BM)) were delineated on the static scans determining 4 ratios: SUVT/S, SUVT/PG, SUVT/Mu and SUVT/BM.

Results

A good correlation was found between SUVmax and SUVmean of the tumoral lesions on the dynamic and SUVmax and SUVmean of the lesions on the static 68Ga-DOTATOC PET (SUVmax: ICC=0.57; SUVmean: ICC=0.59). Also SUVmax, SUVmean and Ki showed a good linear correlation; SUVratios and Ki had a poor correlation. Ki and SUVtumor showed a significantly better correlation than Ki and all the SUVratio ($p<0.0001$ for all).

Conclusion

As the golden standard dynamic parameter Ki correlates best with the absolute SUVtumour, underlying somatostatin receptor expression levels in NETs is best reflected by SUVtumour. This parameter can be used to select PRRT-candidates and for (early) response assessment.

Prevention of severe kidney function deterioration post-PRRT through individualized dosimetry-based ^{90}Y-DOTATOC activity reduction

Van Binnebeek S[1], BaeteK[1], Vanbilloen B[1], Terwinghe C[1], Koole M[2], Mottaghy FM[3,4], Clement PM[5], Mortelmans L[1], Haustermans K[6], Van Cutsem E[7], Verbruggen A[8], Bogaerts K[9], Verslype C[7], Deroose CM[1]

Departments of [1]Nuclear Medicine, [5]Medical Oncology, [6]Radiation Oncology, [7]Digestive Oncology, [8]Laboratory for Radiopharmacy, [9]Public Health and primary Care (I-BioStat), University Hospitals Leuven, KU Leuven, Leuven, Belgium. Department of [2]Nuclear Medicine, University Medical Centre Groningen, the Netherlands. Department of [3]Nuclear Medicine, Maastricht University Medical Center, Maastricht, the Netherlands. [4]Department of Nuclear Medicine, University Hospital Aachen, Germany

Aim

Aiming to assess the evolution of kidney function after ^{90}Y-DOTATOC-PRRT, an extended biological effective dose (BED) estimation with a threshold of 37Gy BED to the kidneys was used.

Methods

In a prospective phase-II study, 22 patients with metastasized neuroendocrine tumours were evaluated for therapy using 185 MBq ^{111}In-pentetreotide with amino acid co-infusion. Planar whole-body images were acquired at 4 time-points post-injection and kidney volumes were measured using CT or MRI. The BED to kidney was estimated with an extended BED formula using a bi-exponential renal clearance. Based on published BED dose-toxicity relationships, we allowed the maximal kidney BED to be 37Gy; if the calculated BED >37Gy, treatment activity was reduced. Kidney function was assessed at baseline and 18 months predominantly using ^{51}Cr-EDTA. The rate of renal function decline was expressed as annual GFR loss (aGFRL).

Results

No rapid deterioration of kidney function was observed in the follow-up interval of 18 months. For all patients, the median aGFRL after ^{90}Y-DOTATOC-PRRT was 8%, with IQR25-75% 2-14. Looking at the change in kidney toxicity score between baseline and 18 months, 17 (=77%) patients maintained their toxicity grade, 3 (=14%) patients increased with 1 grade; 1 (=4.5%) patient improved with 1 grade; 1 (=4.5%) patient developed a grade-2 toxicity, starting from grade-0. No significant correlations between kidney volume ($p=0.35$), baseline GFR ($p=0.18$), risk

factors for renal function loss (p=0.74) and aGFRL were observed. No patients with aGFRL >30% were noticed.

Conclusion
Prospective dosimetry, using a BED of 37Gy as threshold for kidney toxicity is a good guide for 90YDOTATOC-PRRT and results in a low risk of rapid renal function deterioration and evolution to severe nephrotoxicity. Kidney size as such is not a risk factor, but should be implemented in the dosimetry-analysis.

Comparison between motion corrected pinhole and parallel hole SPECT in ^{99m}Tc-DMSA studies

Demonceau G, Hesse M, Walrand S

Sint-Elizabeth Ziekenhuis, Zottegem, Belgium and Cliniques Universitaires Saint-Luc, Brussels, Belgium

Aim
Pinhole SPECT studies (PHS) were previously demonstrated to be of general better quality than parallel-hole SPECT for Tc-DMSA studies. Motion correction is particularly challenging in renal pinhole SPECT, due the pinhole magnification that is strongly spatially dependent, unlike what happens in parallel-hole collimation. We wonder if, after motion correction, the advantage of pinhole SPECT would still remain.

Methods
Six hours after a weight-dependant injection of ^{99m}Tc-DMSA, four 5min-dynamic views and two 25min-SPECT were performed in 25 patients (pts). On both SPECT imaging, the acquired projections were shifted to match as well as possible the re-projections of a first reconstruction of the set of good incidences only. Reconstruction of both SPECT was made with an OSEM algorithm with, in the case of PHS, geometric correction and adaptive filters. Criteria for the visual comparison of both SPECT were the blurring of the contours, the cortex/cavity contrast and the depth and volume of the cortical defects. In case of doubt, the motion-corrected planar imaging was used as gold standard.

Results
Compared to parallel-hole SPECT, pinhole SPECT had a better quality of imaging in 13 pts, the same in 6 pts and a lower quality in 6 pts. A significant relation was observed with the registered counts for PHS: a large number of counts (i.e. above 150.000) is associated with a greater chance to be superior to parallel-hole SPECT. The amount of registered counts is depending on the injected dose, the body attenuation and the kidney-pinhole distance. The superiority of PHS was thus clearer for patients with age between 2 and 18 years.

Conclusion
In conclusion, the difficulty to correct for motion in PHS doesn't preclude the superiority of this method on parallel-hole SPECT for children. In adults, both techniques seem equal, probably due to the higher kidney pinhole distance and attenuation.

Slower thyroid clearance of ^{99m}Tc-MIBI in case of Hashimoto's thyroiditis

Demonceau G, Hesse M, Walrand S

Sint-Elizabeth Ziekenhuis, Zottegem, Belgium and Cliniques Universitaires Saint-Luc, Brussels, Belgium

Introduction
Focal Hashimoto's thyroiditis is sometimes difficult to differentiate on scintigraphy using ^{99m}Tc-pertechnetate or iodine from other hypoactive lesions like carcinoma, cyst or some adenomas. The shape of the lesion obtained by pinhole SPECT (PHS) helps, but is not sufficient in this purpose. We investigate if ^{99m}Tc-MIBI, a cellular marker not directly related to endocrine secretion, could still improve the differentiation.

Methods
We retrospectively studied 40 patients. Ten of them were suffering from extended Hashimoto disease at different stages, as proved by the clinical data (specially the time evolution) and the high amount of antithyroglobulin antibodies. The remaining 30 patients used as controls, had various thyroid pathologies, chiefly multinodular disease and cysts. Immediately after injection of 740 MBq of 99mTc-MIBI, 3 PHS of 5' each were successively performed. The PHS software uses an OSEM reconstruction algorithm and adaptive filters, and enables the absolute quantification of the reconstructed images. A Student t-test was used to compared in both series the value of the clearance index ((early SPECT –late SPECT)/early SPECT).

Results
The clearance index between the 1st and the 3th SPECT of the patients with thyroiditis (10.0%) was significantly lower ($p = 0.03$) than the control group (14.8%), also between the 1st and the 2nd SPECT (7.6 vs 11.6%; $p = 0.04$). We found no influence of the hormonal status in both series.

Conclusions
These preliminary results suggest a early clearance of ^{99m}Tc-MIBI slower than normal in patients suffering from Hashimoto disease, at least in its extended form. If this could be transposed to its focal form, than it could become a parameter of differential diagnosis. This also should be kept in mind in case of thyroid lesions with increasing activities of ^{99m}Tc-MIBI with time.

Lesion size effect on variability in PET quantification in multicenter trials

Guiot T[1], Vanderlinden B[1], Seret A[2], van Elmbt L[3], Bol A[3], Trotta N[4], Keppens J[5], George J[6], Lambrechts M[7], Lavent F[8], Pareyn J[8], Alberty J[9], Destine M[10], Bernard C[11], Greffe JL[12], Garcia C[1], Flamen P[1]

[1]Nuclear Medicine, Jules Bordet Institute, Brussels; [2]Clinique St-Joseph, Liège; [3]Clinique Université St-Luc, Brussels; [4]Hôpital Erasme, Université Libre de Bruxelles, Brussels; [5]UZ Gent, Gent; [6]CU UCL Mont-Godinne, Yvoir; [7]UZ Antwerp, Edegem; [8]AZ Groeninge, Kortrijk; [9]GZA, Wilrijk; [10]Clinique Ste Elisabeth, Namur; [11]CHU Liège, Liège; [12]CHU Charleroi, Belgium

Introduction
In multicenter trials, the various capabilities of different PET/CT systems impact the SUV quantification between centers. The lesion size is known to affect SUV. We performed a phantom study to assess its role in the inter-center variability of quantification.

Materials & Methods
The NEMA NU2-2007 phantom was used. The background was filled with 2.6 kBq/ml of ^{18}F-FDG and the spheres (A=26.5, B=11.5, C=5.6, D=2.6, E=1.2, and F=0.5 ml in volume) with 3, 6 and 9 times the background activity. Each center applied its routine acquisition and reconstruction settings. The recovery coefficients (RC) were measured in spherical VOIs matching the phantom spheres. We assessed the variability in quantification with: a. the coefficient of variation (CoV) in the RC distribution, b. the standard deviation (SD) in the distribution of SUV differences (ΔSUV) between two spheres of same volume and different contrasts. The RC's and ΔSUV were between two groups: the three largest (ABC) and the three smallest (DEF).

Results
The CoV for all contrasts and centers are 12.9% (group ABC) and 35.8% (DEF) (Levene's test: p<1e-5). The SD for relative ΔSUV for 3 contrasts comparisons are:

	9 to 9	9 to 6	9 to 3
ABC	5.8	4.7	4.0
DEF	12.3	9.1	7.2

The difference is also significant (p<1e-5).

Conclusions
Our study shows that the well known lesion size effect on PET quantification can be reduced to an acceptable level of variability in a multicentre setting, even with poor knowledge of the lesions volume. This can be achieved both for RC and ΔSUV by considering only lesions with a size above 2 cm.

^{18}F-18 FDG PET, MRI or PET/MRI: which method is best for discriminating high-grade from low-grade gliomas?

Acou M[1], D'Asseler Y[2], Deblaere K[1], Van den Broecke C[3], Hallaert G[4], Okito Kalala JP[4], Achten E[1], Goethals I[2]

Departments of [1]Radiology, [2]Nuclear Medicine, [3]Pathology, and [4]Neurosurgery, Ghent University Hospital

Aim
To investigate which of 5 methods - visual interpretation of PET images at conventional and delayed intervals, MRI and PET/MRI or SUV calculation at the site with the highest tumour grade according to MRI - is best for differentiating high-grade from low-grade gliomas.

Methods
Twenty-five patients with gliomas undergoing a stereotactic biopsy underwent PET scanning at conventional and delayed intervals, and multimodal MR examinations. On the PET, MR and PET/MR images, tumours were visually classified in 5 categories (definitely high-grade, probably high-grade, inconclusive, probably not high-grade, and definitely not high-grade). SUV of the voxel with the highest tumour grade according to MRI was calculated. Validity of the visual reading and the quantitative approach, this is SUV calculation, was investigated by performing a receiver-operating-characteristic (ROC) analysis with the pathological diagnosis as the gold standard.

Results
Area under the ROC curve (AUC) values (± SE) of the visual reading of PET images at conventional and late intervals was 0.64 ± 0.12 and 0.89 ± 0.07, of MRI was 0.91 ± 0.06, and of PET/MRI was 0.90 ± 0.06. AUC values (± SE) of SUV, calculated on the conventional and late PET images, were 0.94 ± 0.06 and 0.97 ± 0.04 respectively (difference between AUC values, not

significant except AUC of PET at conventional intervals versus other AUCs).

Conclusion
Our results indicate that for discriminating low-grade from high-grade gliomas combined PET/MRI with a quantitative approach, this is SUV calculation at the voxel with the highest tumour grade according to MRI, is preferred.

^{18}F-FDG PET: changes in uptake as a method to assess radium-223 dichloride (^{223}Ra) response in bone metastases of breast cancer patients with bone-dominant disease

Flamen P[1], Coleman R[2], Garcia C[1], Ghanem G[1], Vanderlinden B[1], Aksnes A-K[3], Gaye J[1], Guiot T[1], Wimana Z, Muylle K[1], Piccart M[1]

[1]Institut Jules Bordet, Brussels, Belgium; [2]Weston Park Hosp, Sheffield, UK; [3]Algeta ASA, Oslo, Norway

Background
^{223}Ra, a first-in-class α-emitting agent, targets bone mets with high-energy α-particles of very short range (<100 µm). ^{18}F-FDG uptake reflects tumor activity of bone mets in BC, and sequential PET can provide information on response of bone mets to therapy.

Methods
The study included MBC pts with BDD who had progressed on endocrine therapy (ET) and were not candidates for further ET. ^{223}Ra was given as add-on to existing bisphosphonate therapy. Osteoblastic lesions detected on bone scan with standardized uptake value (SUVmax) > twice normal liver uptake and diameter >15 mm on PET CT were defined as target lesions. Sequential ^{18}F-FDG PET was done at baseline, before the third study drug administration (wk 9), and at Tx discontinuation (wk 17).

Results
23 pts were to receive 4 ^{223}Ra IV Tx (50 kBq/kg) q4wk. 15/23 pts received all 4 ^{223}Ra Tx, 19/23 pts had 3, and all 23 pts had 2. 20 pts had ^{18}F-FDG PET that showed a total of 155 bone target lesions at baseline (3 pts had no PET). 1/3 of target lesions showed significant metabolic decrease (≥25% reduction of SUVmax from baseline) after 2 ^{223}Ra Tx (32.3% response rate [RR] at wk 9), persisting after 4 Tx (41.5% RR at wk 17).

Conclusions
^{223}Ra targets areas of increased bone metabolism caused by BC bone mets, and response in osteoblastic lesions from MBC can be assessed using sequential ^{18}F-FDG PET.

Diagnostic accuracy of ^{111}In-pentetreotide SPECT versus ^{68}Ga-DOTATOC PET: a lesion-by-lesion comparative analysis in PRRTpatients

Van Binnebeek S[1], Vanbilloen B[1], Baete K[1], Terwinghe C[1], Koole M[2], Mottaghy FM[3,4], Clement PM[5], Mortelmans L[1], Bogaerts K[6], Haustermans K[7], Van Cutsem E[8], Verslype C[8], Verbruggen A[9], Deroose CM[1]

Departments of [1]Nuclear Medicine, [5]Medical Oncology, [6]Department of Public Health and primary Care (IBioStat), [7]Radiation Oncology, [8]Division of Digestive Oncology and [9]Laboratory for Radiopharmacy, University Hospitals Leuven and Department of Imaging & Pathology, KU Leuven, Leuven Belgium -
Department of [2]Nuclear Medicine, University Medical Centre Groningen, The Netherlands
Department of [3]Nuclear Medicine, Maastricht University Medical Center, Maastricht, The Netherlands
Department of [4]Nuclear Medicine, University Hospital Aachen, Germany

Introduction
In this prospective study, the detection efficiency of metastatic lesions using ^{111}In-pentetreotide-SPECT or ^{68}Ga-DOTATOC-PET, in patients with neuroendocrine tumours (NET), was compared. We specifically looked for incremental lesions, defined as lesions only observed on one modality even after extensive retrospective evaluation of the other modality.

Methods
Twenty patients with a metastasized NET underwent 185MBq ^{111}In-pentetreotide-SPECT 24h post-injection and 185MBq whole-body ^{68}Ga-DOTATOC-PET/CT 30min post-injection. As all patients had liver metastases, the SPECT-images were acquired from the liver downward. For the SPECT-PET comparison, only the field of view of the SPECT was taken into account on the PET-images (=PETFOVSPECT). A lesion-by-lesion analysis was performed for all tumour foci on both somatostatin-receptor-imaging methods whereby total lesions as well as incremental lesions were determined for both modalities.

Results
^{111}In-pentetreotide-SPECT was performed within 2

days of ^{68}GA-DOTATOC-PET, except for patient 15 in whom scintigraphy was performed 3 months after PET/CT. Significantly more lesions were detected on PETFOVSPECT compared to SPECT, 398 (range: 5-47, median: 18.5) versus 240 (range: 0-34; median: 10) respectively (p=0.0002 (paired t-test)). In one patient (=5%), one single incremental lesion was detected on SPECT. In the remaining 19 patients (=95%), 159 incremental lesions were noticed on PETFOVSPECT. When expressed as fraction of all lesions seen on PET, the incremental lesions on PETFOVSPECT represented on average 44% (median: 34%; IQR: 24-66%).

Conclusion

^{68}Ga-DOTATOC-PET is superior for the detection of NET metastases, compared to ^{111}In-pentetreotide-SPECT, picking up a significantly higher number of tumoural lesions. PETFOVSPECT detected hereby, in 95% of the patients, an average of 8 incremental lesions per patient, which represents 44% of all the lesions detected on PETFOVSPECT. One must therefore be aware of the potential higher clinical impact of ^{68}Ga-DOTATOC-PET due to its higher sensitivity for tumour detection.

^{99m}Tc-labelled S-HYNIC-Certolizumab for selecting patients for anti-TNFα treatment: a biodistribution and dosimetric study.

Lambert B[1], Carron P[2], D'Asseler Y[1], Bacher K[3], Van den Bosch F[2], Elewaut D[2], Verbruggen G[2], De Vos F[4]

Departments of [1]Nuclear Medicine, [2]Rheumatology, UZ Gent and the Department of [3]Basic Medical Sciences and [4]Faculty of Pharmaceutical Sciences- Radiopharmacy, UGent, Gent, Belgium

Introduction

Biologicals targetting Tumor Necrosis Factor have proven their efficacy in rheumatoid arthritis and spondyloarthritis. We initiated a clinical study to verify whether the therapeutic effect of Certolizumab pegol, a humanized Fab-fragment directed against TNFα, could be predicted by a pretherapeutic scintigraphy with radiolabelled Certolizumab pegol.

Aim

To perform a biodistribution and dosimetry study of ^{99m}Tc-labelled S-HYNIC-Certolizumab.

Methods

First, an attenuation map was obtained from a WBscan using a ^{57}Co floodsource. WBscans and blood sampling were performed immediately pi, at 1h, 4-6h and at 24h with a standard activity ^{99m}Tc placed in the FOV. Urinary excretion of the tracer was measured in urine collections up to 24h pi. All visualized organs as well as ROIs for the WB, background and standard activity were delineated on the 4 geometric mean WB images. Residence times in the WB and organs were estimated using mono-exponential fitting and absorbed doses computed by OLINDA/EXM.

Results

We analyzed 8 patients, suffering rheumatoid arthritis(1), psoriatic arthritis(2) or spondyloathritis(5). High tracer uptake was observed in the bloodpool, liver, spleen and kidneys, with mean absorbed doses in kidneys, spleen and liver of 56.1, 34.0, 32.7 µGy/MBq. The WB effective dose was 6.2mSv for a mean IA of 690MBq ^{99m}Tc-labelled S-HYNIC-Certolizumab. The urinary excretion was 15.1% IA at 24h. Blood samples were fitted to a two-compartment model with a distribution half-life of 1.2h and an elimination half-life of 26.9h.

Conclusion

Following an injection of 690MBq ^{99m}Tc-labelled Certoluzimab an effective WBdose of 6.2mSv was estimated. The organs receiving the highest absorbed doses are the kidneys, spleen and liver. Urinary excretion was 15.1% at 24h. The elimination half-life in blood was estimated to be 26.9h.

Cost-Effectiveness of FDG-PET/CT for Cytologically Indeterminate Thyroid Nodules

Vriens D[1], Adang EMM[2], Netea-Maier RT[3], Smit JWA[3], de Wilt JHW[4], Oyen WJG[1], de Geus-Oei LF[1]

Departments of [1]Nuclear Medicine, [2]Health Evidence, [3]Medical Endocrinology and [4]Surgical Oncology, Radboud University Medical Centre, Nijmegen, the Netherlands

Rationale

Screening for malignancy in a thyroid nodule (TN) is performed using ultrasonography guided fine-needle aspiration cytology (FNAC). In about 3/4th of patients FNAC cannot lead to a diagnosis and hemithyroidectomy is needed. A benign TN is found in approximately .th of operated patients and surgery was therefore unbeneficial. This leads to unnecessary costs, complaints and complications. Our recent meta-analysis, found a very high negative predictive value for FDG-PET/CT in these patients. We therefore proposed that incorporation of FDG-PET/CT in the work-up of an FNAC-indeterminate TN may lead to better and costeffective patient care. Via

a decision analytic approach we synthesize the available evidence to provide answers concerning the efficacy and economics.

Material and Methods
We developed a 13-state Markov decision model. Based on literature, reimbursement rates and expert panel opinion we attributed distributions to the transition probabilities, costs (€) and utility scores (health related quality of life, HRQoL) throughout the model. Analysis of the model was performed by probabilistic sensitivity analysis over a duration of 5 years. Average costs and utility (QALYs) were determined. The mean 5-year incremental cost effectiveness ratio (ICER) was determined stochastically. One-way sensitivity analysis of the major impact parameters with respect to the ICER was performed.

Results
Implementation of FDG-PET/CT lead to a negative average discounted cost estimate while increasing the QALYs modestly. It therefore was the dominant procedure.

Conclusion
Markov decision modeling showed the high likelihood of FDG-PET/CT being cost-effective. Prospective randomized studies must be undertaken to validate this finding in practice.

Tuberculosis on FDG PET-CT: the great imitator

Castaigne C[1,2], Garcia C[2], Flamen P[2]

Departments of [1]Nuclear Medicine, Saint Pierre Hospital and [2]Unit of Positron Emission Tomography, Institut Jules Bordet, Université Libre de Bruxelles, Brussels, Belgium

Objective
The aim of this retrospective study was to describe patterns and the added value of whole-body ^{18}Ffluorodeoxyglucose positron emission tomography/computed tomography (FDG PET/CT) in guiding the diagnosis of tuberculosis (TB) in patients without clinical suspicion.

Methods
Whole-body FDG PET/CT was performed in 15 immuno-competent patients. A diverse clinical presentation was de reason to perform the metabolic examination. Seven patients presented clinical lymphadenopathies, five clinical suspicion for peritoneal carcinomatosis , two patients with fever of unknown origin and only one with deterioration of general status.
Definitive diagnosis of TB was proven either on bacteriological or histopathological studies.

Results
PET/CT showed misleading imaging mimicking neoplasia in almost all cases. Abnormal hypermetabolic foci were found in 14/15 patients. Pathological foci were also identified in lymph nodes (87% of patients), peritoneum (40% of patients), pleura (27% of patients), lungs (20 % patients), bone/articular sites (20% of patients), soft tissues (13% of patients), liver (7% of patients) and spleen (7% of patients). In 13/15 patients. FDG PET/CT helped in the final diagnosis guiding the biopsy Diagnosis was confirmed by lymph nodes biopsy (n=5), peritoneal biopsy (n=5), pleural biopsy (n=2), sputum cultures (n=2) and lumbar disk biopsy (n=1). All of the 13 biopsy proven sites of tuberculosis were correctly identified by PET/CT.

Conclusion
Whole-body FDG PET/CT appears to be a valuable tool in the work up of tuberculosis diagnosis. PET/CT can bring accurate and easy localization for biopsy, in particular lymph nodes and peritoneum which are the most common site of the involvement as well as providing a full image of the extent of the disease.

^{11}C and ^{18}F radiolabeled imidazo-triazin derivatives: a potential radioligand for in vivo visualization of phosphodiesterase type 5 (PDE5) in myocardium

Chekol R[1], Gheysens O[2], Cleynhens J[1], Janssens S[3], Verbruggen A[1], Bormans G[1]

Departments of [1]Laboratory of Radiopharmacy, [3]Departement of Nuclear Medicine, and [3]Department of Cardiovascular Diseases, UZ Leuven, Leuven, Belgium

Objective
Evidence is accumulating that patients with end-stage heart failure exhibit significantly higher phosphodiesterase type 5 (PDE5) expression in the myocardium. The aim of this study was to investigate different imidazo-triazin derivatives labeled with either ^{11}C or ^{18}F as potential radioligands for in vivo visualization of PDE5 expression in cardiomyocytes.

Methods
^{11}C-1, ^{11}C-2 and ^{18}F-3 were prepared by alkylation of the precursor with ^{11}C-H3OTf and ^{18}F-EtOTf respectively.

Biodistribution was studied in NMRI mice and microPET imaging was performed in transgenic mice with cardiomyocyte-specific PDE5 over-expression (PDE5 TG). To address specificity, blocking and chase experiments were done using the structurally unrelated PDE5-specific inhibitor tadalafil.

Results

Biodistribution study showed that the highest uptake was observed in the lungs of NMRI mice (8.0±1.9 and 8.9±0.8 SUVs for ^{11}C-1 and ^{18}F-3 respectively) at 30 min post injection, in agreement with reported PDE5 expression in rodents. However, ^{11}C-2 showed lower retention than the other two (3.8±1.2 SUV). Lung retention of 11C-1 was blocked to 1.0±0.2 SUV at 30 min p.i. (87 % reduction, $p < 0.0001$) by pretreatment with tadalafil. The tracers were cleared from blood mainly via the hepatobiliary pathway. In vivo dynamic microPET imaging studies in PDE5 TG mice, showed a high myocardial uptake for ^{11}C-1 and ^{18}F-3 but not for ^{11}C-2. Radioactivity in myocardium was displaced by intravenous injection of tadalafil and pretreatment with tadalafil resulted in absence of retention in myocardium.

Conclusions

Among the imidazo-triazin derivatives, ^{11}C-1 and ^{18}F-3 are found to be promising tracers for in vivo visualization of PDE5 and further studies are underway to employ ^{11}C-1 in clinical practice.

A nuclear medicine approach to treat metastatic or locally advanced evolutive radio-iodine "resistant" differentiated thyroid carcinomas (DTC) using 13-cis-retinoic acid; report of 7 cases

Bourgeois P, Ahmed B, Vanderlinden B

Brussels

Introduction

Redifferenciation approach using retinoic acids (RA) represents an old one but now the single therapeutic option which can be practically proposed to patients with metastatic or locally advanced evolutive DTC resistant after ^{131}I treatment. We report here our results of 7 patients treated "simply" using 13-cis-RA.

Methods

The protocol (approved by our institutional ethical committee) is as follows:

1. the "metabolic" status and the iodine metabolism of patient's lesions were evaluated using ^{18}F-FDG and ^{124}I PET-CT under rh-TSH stimulation.
2. they were thereafter treated (RAT) using 13-cis-RA (Ro-Accutane ®: 1 mg/kg) during 2 months and Tg was controlled every 2 weeks.
3. after and under RAT, their metabolic responses were evaluated as in 1.
4. if metabolic changes were observed, patients were treated by ^{131}I (7400 MBq) and thereafter maintained under RAT.
5. they were followed biologically (Tg: every two weeks) and metabolically (^{18}F-DG PET-CT: one and three months).

Results

- 4 patients showed (3 to 4 folds) increase in iodine uptake thus improving the radio-biological effects of administered ^{131}I activities with transient biological and/or metabolic responses.
- 1 patient with a non-surgically resectable pulmonary metastasis showed before any ^{131}I administration a biological and RECIST response allowing a surgical approach of for her lesion.
- 1 patient showed a complete response at the level of some of his lesions.

Conclusion

Despite our limited number of cases, these results are encouraging. Also based on the past and recent literature supporting our results, the therapeutic approach proposed here (the administration of one inexpensive commercially available drug) represents today a valuable and rationale option for these patients.

Indirect assessment of regional ventilation derived from SPECT/CT

Mathey C, George J, De Nizza D, Cavus H, Meurisse H, Pirson AS, Krug B, Vander Borght T

Department of Nuclear Medicine, CHU UCL Mont-Godinne Dinant, Université Catholique de Louvain, Yvoir, Belgium

Introduction

Ventilation-perfusion imaging (VQ scan) is a well-established diagnostic tool for clinically suspected pulmonary embolism (PE). Although perfusion images alone own all the sensitivity, ventilation ones may be required to increase specificity, especially in a patient with respiration disease. The respiratory phase of imaging is, however, often difficult to obtain. In the current study, we evaluated if the regional movement of lung parenchyma may provide an indirect assessment of regional lung ventilation.

Material and methods
Sixteen patients (66±14 years, mean±SD), referred for suspected PE were prospectively included in this study. All patients underwent planar V/Q scintigraphy, V-SPECT and two low-dose CT (20mAs) acquired at inhale (iBH) and exhale (eBH) breath-hold. By a deformable image registration algorithm, we determined tridimensional displacement vector fields between the iBH and eBH CT. The resulting 3D images were segmented to include only the air-density lung area; then, compared with the standard SPECT ventilation imaging using Technegas.

Results
The preliminary results suggest, most of the time, similar regional distribution on CT-derived and SPECT ventilation images. The former can be obtained currently in less than 60min on a quad-core 2.6 GHz computer. Improvement of the acquisition as well as the reconstruction process is underway.

Conclusions
In addition to provide alternative diagnosis, deformable registration of inhale and exhale thoracic CT images may potentially serve as an indirect measure of regional ventilation. It could be associated with a perfusion scan in a patient with respiratory disease to improve our diagnostic accuracy of PE, at a reasonable increase of radiation exposure (0.8±0.1 mSv).

CT based splenic index versus FDG PET derived spleen/liver ratio in lymphoma patients

De Man K, Smeets P, Maes A, Sathekge M, Verstraete K, Van de Wiele C

Department of Nuclear Medicine, Ghent University Hospital, Ghent, Belgium

Patients and Methods
Sixty-seven FDG PET/CT data sets derived from 48 lymphoma patients who were not on rhG-CSF treatment were included for analysis. CT images covered a wide range of spleen volumes and revealed no focal spleen abnormalities. On all data sets, the spleen index (Lackner index, normal values < 480 ml), defined as W x L x T was calculated. Spleen and liver SUV mean values were calculated and divided by each other yielding the spleen/liver ratio.

Results
Spleen index values proved significantly correlated with mean SUV spleen (p=0.0001) and spleen/liver ratio's (p=0.0001). Mean SUV spleen values and spleen/liver ratios proved not significantly correlated with WBC count (p=0.988 and p=0.903 respectively) whereas a correlative trend was found between mean SUV spleen values and spleen/liver ratios with CRP values (p=0.09). Mean SUV spleen values and spleen/liver ratios proved significantly higher in the abnormal spleen index group versus the normal spleen index group (p = 0.002 and p = 0.0001 respectively). Using a cut-off value of > 2.15 for mean SUV spleen and of 1 for spleen/liver ratio's, patients with a spleen index > 480 ml could be separated from those with a spleen index < 480 ml with a sensitivity of 77% and 75 % and a specificity of 74 % and 96% (areas under the curve, respectively 0.83 and 0.88).

Conclusion
In this population FDG uptake by the spleen equal to or greater than that of the liver is nearly 100% specific for spleen enlargement, the most relevant independent prognostic factor for spleen involvement. Furthermore, the impact of associated inflammatory changes on FDG uptake by the spleen is likely minimal.

SPECT-CT imagings of the thyroid and/or parathyroid glands: reflexions around Mr Hounsfield's contributions

Bourgeois P and Vanderlinden B

Brussels, Belgium

SPECT-CT imaging is now the standard approach for some organs and/or investigations in nuclear medicine. The interest of the SPECT-CT approach has been largely stressed to image and localize the para-thyroid glands. In the case of the thyroid glands, SPECT-CT allows also to define « cold » and/or « hot » nodules better than with planar imagings. However, the informations present in the CT are underused. In fact, (Dr) Hounsfield's units (HU) define the « densities » of the tissues on the classical CT scale and, of interest, normal thyroid tissues contain their « own » specific « contrast agent »… the iodine-127 which HU are +100 to +110. Consequently, when displaying SPECT-CT results, if you apply on your CT slides a scale between 0 and +110 HU, you put directly in relation the tissue uptake of your radio-tracer (^{123}I, ^{99m}TcO4, ^{99m}Tc-MIBI) with the naturally « iodinated » thyroid tissue. The application of such a scaling to the thyroid and/or parathyroid glands imagings is simply fascinating. The nodules described by the echographist are now on « our » display: around 0 HU, these are cysts : around 40-70 HU, they are solid : but if they are around 100-110 HU, this is normal thyroid tissue. The « structure » of the thyroid tissues may now be said homogenous or

heterogeneous. In contrats, some tissues with a normal iodine « content » may appear scintigraphically hypo-funtional whereas « hot » nodules may show either a normal, or a decreased iodine content. In one patient with hyper-para-thyroidy, if your MIBI spot does not contain iodine, that is your adenoma. Several examples illustrating these Hounsfield's contributions will be shown on the poster.

A dosimetric method for neuroendocrine tumors (NET) treatment with octreotate labelled with lutetium

Marin G, Vanderlinden B, Guiot T, Flamen P

Department of Nuclear Medicine and Medical Physics, Institut Jules Bordet, Université libre de Bruxelles, Brussels, Belgium

Purpose
The aim of this work was to provide a dosimetric method for NET's treatment quantification. Based on phantom imaging, we determined optimal settings to quantify ^{177}Lu activity by investigating quantification capabilities of SPECT and planar images.

Material and methods
The phantom defined in the protocols IEC 61675-1 and NEMA NU2-2007 was used. The activities put in the main compartment, the central cylinder and the spheres were chosen to obtain the same SUV than in the liver, kidneys and lesions of patients who underwent diagnostic PET-CT imaging with ^{68}Ga-octreotate. The phantom was acquired throughout five ^{177}Lu half-lives on a Siemens Symbia T3/8'' with high energy collimators with SPECT and planar whole body imaging. SPECT images were reconstructed using 3D OSEM with different sets of parameters by varying the number of subsets, iterations and the FWHM of post-filter Gaussian smoothing kernels. The optimal reconstruction settings were assessed by:

- Quantitative measurements comparing standard deviation (SD) to recovery coefficient (RC)
- Qualitative visual assessment by a nuclear medicine physician.

Results
The quantitative and qualitative assessments found the best trade-off between SD and RC with 16 subsets and 16 iterations. However, they chose different kernel sizes of 12 and 14.4 mm FWHM, respectively. The calibration factor is independent of the count rate (no dead-time correction needed) and was set at 20.9kBq/kcps with the chosen reconstruction parameters. The half-life was evaluated with an error of 2.5% with planar whole body images. No count rate dependency could be observed.

Conclusion
It was then concluded that octreo-therapy quantification is achievable with SPECT with ^{177}Lu and does not depend on count rate or geometry. The clinical implementation of the treatment actually started in Jules Bordet Institute.

Hepatocellular carcinoma (HCC) treatment with intra-arterial radiolabelled Lipiodol versus Ytrium-90-microspheres: a retrospective survival analysis

De Man K, Defreyne L, Delanghe E, Dhondt E, Van Vlierberghe H, Geerts A, Verhelst X, Troisi R, Lambert B

UZ Gent, Ghent, Belgium

Introduction
At the UZ Gent, we switched in 2005 from radiolabelled Lipiodol to ^{90}Y-microspheres for intra-arterial treatment of HCC, because of radioprotective issues. In this study we investigated a potential impact of the switch from radiolabelled Lipiodol to ^{90}Y-microspheres on overall survival.

Methodology
We retrospectively analyzed HCC patients who were not eligible for curative treatment, had no extrahepatic disease, Child-Pugh C cirrhosis, Karnofsky score <70% neither bilirubin >2 mg/dL. 52 patients treated with ^{131}I- or ^{188}Rh-Lipiodol were compared with a more recent series of 64 patients treated with ^{90}Y-microspheres (TheraSphere). Patients' characteristics were compared by Chi-Square and survival was calculated using Kaplan-Meier and compared by LogRank and CoxRegression.

Results
Distribution of age, gender, Child-Pugh score, portal vein thrombosis and Barcelona Clinic Liver Cancer classification did not vary significantly between groups. However, according to the CLIP score (Cancer of the Liver Italian Program) a less favorite distribution of this prognostic index was present in the group treated with ^{90}Y-microspheres. Mean survival time in the Lipiodol group was 14.4 months since first radionuclide treatment versus 12.3 months in the 90Y group (p 0.71). In the ^{90}Y group 6 patients were downstaged and transplanted versus 2 in the Lipiodol group.

Conclusion
Survival in HCC patients treated with ^{90}Y-microspheres does not significantly differ from those who

underwent treatment with ^{131}I- or ^{188}Rh-Lipiodol in our hospital, despite a less favourable distribution of the CLIP prognostic index in the group treated with ^{90}Y-microspheres. The shorter observation time available for the ^{90}Y patients could cause an underestimation of the survival in a subgroup of patients, especially patients who were downstaged to undergo transplantation.

The classification of non demented patients attending a Memory Clinic according to the NIA&AA guidelines on Alzheimer's disease related biomarkers

Ivanoiu A, Dricot L, Gilis N, Grandin C, Lhommel R, Quenon L, Hanseeuw B

Background
The National Institute of Aging & Alzheimer Association (NIA&AA) experts recently issued new diagnostic criteria for the preclinical and predemential stages of Alzheimer's disease (AD) including the use of biological markers. However, the use of biomarkers in clinical practice has not clearly been defined. The present study attempted to document whether the biomarkers in the combination recommended by the NIA&AA are useful in the classification of a clinical population of non-demented patients.

Method
Forty-three non-demented patients attending our Memory Clinic have been included in the study and compared with thirty-one healthy elderly subjects. All participants were examined by a trained neurologist and they underwent a full neuropsychological examination. The patients' cognitive performance on memory, language, visuospatial and executive domains below pc10 compared to controls classified them as mild cognitive impairment (MCI). All participants carried out 3T brain MRI, brain PET ^{18}F-FDG and 18F-flutemetamol. The hippocampus volume (HV) assessment with FreeSurfer software, the 18F-FDG AD index (Herholtz et al., 2002) and the SUVr Neocortex/ Cerebellum uptake of ^{18}F-flutemetamol (Vandenberghe et al., 2010) were considered abnormal if they had scored below pc10 compared with scores of the controls. Participants with normal cognition (above pc 10) were classified according to the NIA&AA preclinical stages. MCI patients were applied the NIA&AA levels of certainty for the diagnosis of MCI due to AD.

Results
Among the referred patients, twenty-nine (67%) were classified into the MCI group (90% amnestic, 10% non-amnestic). The remaining fourteen patients were considered as subjective complainers (SC) with normal cognition (33%). Among the MCI patients, 52% were likely due to AD, 28% unlikely due to AD and 21% unclassifiable. According to the NIA&AA classification, the percentage of stage 0/stage1 to 3/SNAP/ unclassified in the SC group was of 64%/21%/14%/0% whereas in the controls group it was 61%/10%/ 16%/13%. On the whole, the biomarkers method classified 86% of the patients, among whom 30% had to be reclassified in comparison with the clinical diagnosis.

Conclusion
Classification accuracy is improved by using the three biomarkers, compared with the results obtained by using the clinical and neuropsychological diagnosis alone.

Hippocampus subfields atrophy in preclinical and predemential Alzheimer's disease is different from atrophy observed in patients suffering from non-Alzheimer pathology

Hanseeuw B, Dricot L, Gilis N, Grandin C, Lhommel R, Quenon L, Ivanoiu A

Background
Hippocampus volume has proved to be reduced in various neurodegenerative diseases including Alzheimer's disease (AD). The new diagnostic criteria for the preclinical and predemential stages of AD allow distinguishing between AD and non AD pathology since the earliest stages. In this study, we inquired whether hippocampus subfields atrophy may arise differently in AD and non-AD pathology.

Method
Seventy-four non-demented elderly subjects (71.2y +/- 6.9) were included in this study: Forty-three patients complaining about their memory attended our Memory Clinic and 31 not complaining volunteers were recruited by advertising. All participants underwent a full neuropsychological examination and carried out 3T brain MRI, brain PET ^{18}F-FDG and ^{18}F-flutemetamol. Subjects were consequently classified in three groups, whatever how they were initially recruited:

- Preclinical and predemential AD (pAD) (n=22) had amyloid deposits on the ^{18}F-flutemetamol scan (above pc90 of volunteers).
- Patients suffering from non-AD pathology (non-AD) (n=18) had no amyloid deposits but global
- hippocampus atrophy or ^{18}F-FDG hypometabolism (below pc10 of volunteers).
- Healthy elderly (HE) (n=26) had normal cognition and none of the 3 biomarkers positive.

- Eight subjects could not be classified as they had abnormal cognition without evidence of neurodegeneration. Global hippocampus and subfields volumes were assessed using FreeSurfer.

Results
Non-AD (3054 +/- 497 mm3 - p=0.000) and pAD (2841 +/- 447 mm3 - p=0.000) had both global hippocampus atrophy when compared to HE (3583 +/- 321 mm3). Global hippocampus atrophy in pAD was not significantly more important than in non-AD (p=0.162). Right and left subiculum and right and left presubiculum were atrophic in non-AD as in pAD (all p-values < 0.000). Similarly, right (p=0.028 in non-AD - p=0.000 in pAD) and left (p=0.009 in non-AD - p=0.000 in pAD) fimbria were atrophic in both groups. However, right CA1 (p=0.029), right (p=0.001) and left (p=0.002) CA2-3 and left CA4-DG (p=0.001) were atrophic in pAD while they were not in non-AD.

Conclusion
Although both pAD and non-AD present reduced global hippocampus volumes, CA subfields atrophy seems to be specific of preclinical and predemential AD. Hippocampus atrophy in non-AD seems to be mainly driven by reduced presubiculum and subiculum volumes.

Validation of ^{68}Ga-NOTA-Anti-HER2 Nanobody probe for iPET Imaging of HER2 Receptor Expression in Cancer and First in Human Results

Xavier C[1], Vaneycken I[1], D'huyvetter M[1,2], Keyaerts M[1,3], Heemskerk J[3], Devoogdt N[1,4], Muyldermans S[4], Lahoutte T[1,3], Caveliers V[1,3]

Departments of [1]In vivo Cellular and Molecular Imaging Lab, ICMI, Vrije Universiteit Brussel, Brussels, [2]Radiobiology Unit, Molecular and Cellular Biology Expert Group, Belgian Nuclear Research Center (SCK•CEN), Mol, [3]Nuclear Medicine Department, UZ Brussels, Brussels, and [4]Laboratory of Cellular and Molecular Immunology, VUB, Brussels, Belgium

Introduction
Non-invasive in vivo molecular characterization of disease using imaging is an emerging method for the selection of patients that can profit from targeted therapies and for measuring early therapeutic response. In this study, we labelled the previously selected anti-HER2 nanobody (single-domain antibodies) with ^{68}Ga via a NOTA derivative bifunctional chelator, as a probe for HER2 PET imaging.

Methods
The lead GMP grade 2Rs15d nanobody was conjugated with a NOTA derivative (p-SCN-Bn-NOTA) to enable ^{68}Ga labelling at room temperature and within a short period of time. Biodistribution and PET/CT studies were performed in HER2-positive and -negative tumour xenografts. The effect of mass (0.1, 1, 10 µg of NOTA-2Rs15d) on biodistribution was evaluated. The biodistribution data were extrapolated to calculate radiation dose estimates for the adult female using OLINDA software. A single dose extended toxicity study for NOTA-2Rs15d was performed in healthy mice up to a dose of 10 mg/kg.

Results
Radiolabelling was quantitative (>97 %) after 5 min at RT. Biodistribution studies showed fast and specific uptake in HER2 positive tumours (4.34 ± 0.90 % IA/g) and high T/M (28.49 ± 0.25) and T/B (14.11 ± 3.24) ratios at 1h p.i. High contrast PET-CT images showing high specific tumour uptake were obtained. The injected mass has an effect on the general biodistribution, increasing the NOTA-2Rs15d mass from 0.1 to 10 µg increased specific tumour uptake while non-specific uptake decreased. The calculated effective dose was 0.0218 mSv/MBq, which is comparable with a FDG PET scan. In the toxicity study there were no adverse effects observed after injection of 10 mg/kg NOTA-2rs15d.

Conclusion
A new GMP grade anti-HER2 PET tracer, 68Ga-NOTA-2Rs15d, was synthesized via a rapid procedure under mild conditions. Preclinical validation showed favourable biodistribution, high specific contrast imaging of HER2 positive tumours and no toxicity was observed in a single dose toxicity study. 68Ga-NOTA-2Rs15d is currently in human clinical trial and preliminary results will be present.

Current situation and perspectives of the ^{99}Mo/^{99m}Tc supply

Ponsard B

SCK•CEN, BR2 Reactor, Mol, Belgium

The worldwide supply of ^{99}Mo relies on a limited number of research reactors and processing facilities. Its production is essential for nuclear medicine as ^{99m}Tc, distributed in the form of ^{99}Mo/^{99m}Tc generators, is used in about 80% of diagnostic nuclear imaging procedures. These applications represent approximately 30 million examinations worldwide every year. Therefore, a weekly ^{99}Mo production of about 10.000 Ci '6- day' calibrated is required to supply North America (53%), Europe (23%),

Asia (20%) and the rest of the world (4%). The supply chain consists of uranium target manufacturers, nuclear reactors for target irradiation, processing facilities to dissolve the irradiated targets and extract the ^{99}Mo, of ^{99}Mo/^{99m}Tc generators manufacturers, radiopharmacies to elute ^{99m}Tc from the ^{99}Mo/^{99m}Tc generators and prepare radiopharmaceutical doses to be injected to the patients for diagnosis, and of course transport companies. The whole manufacturing process along the supply chain must be carried out in a 'just-in-time' manner because of the short half-lives of the radioisotopes involved. Historically, there were only five research reactors involved in the large scale production of ^{99}Mo, i.e. NRU (Canada), HFR (The Netherlands), BR2 (Belgium), OSIRIS (France) and SAFARI (South Africa). Highly enriched uranium (HEU) targets were irradiated for the production of about 95% of the available ^{99}Mo by four processing facilities: AECL/MDS NORDION (Canada), COVIDIEN (The Netherlands), IRE (Belgium) and NTP (South Africa). Several severe shortages are experienced since 2008 in the supply of ^{99}Mo and ^{99m}Tc. The supply chain has to face unexpected shutdowns of ageing research reactors or extended maintenance periods required to ensure safe operation. However, the situation improved since the creation of the High-Level Group on the Security of Supply of Medical Radioisotopes (HLG-MR) in 2009. Practical measures have been identified for a reliable supply, including significant changes in the economic structure. Additional irradiation capacity has been implemented in existing reactors (+50% in the BR2 reactor) and a few research reactors joined the supply chain, i.e. MARIA (Poland), LVR-15 (Czech Republic) and OPAL (Australia). The optimal coordination of the operating schedules of these eight research reactors within the AIPES Reactors and Isotopes Working Group – together with processing facilities and generator manufacturers – is increasing the reliability of ^{99}Mo supply. The HLG-MR established six principles to address the key issues for a secure supply of ^{99}Mo/^{99m}Tc, including the implementation of full-cost recovery and reserve capacity. Different scenarios for future supply and demand of ^{99}Mohave been investigated, taking into account several projects that are currently in various stages of development. Europe is planning to develop replacement irradiation capacity based on conservative production technologies, involving the challenging conversion to LEU targets by 2015, i.e. FRMII (Germany), JHR (France), MYRRHA (Belgium) and PALLAS (Netherlands). In the US, where there is currently no ^{99}Mo production capacity, funding has been awarded to several projects aiming the development of alternative ^{99}Moproduction routes, under which the photonuclear reaction route 100Mo(γ,n)^{99}Mo in high-power electron accelerators, the development of Aqueous Homogeneous Reactors (AHR) to irradiate low enriched uranium (LEU) fuel in solution and extract regularly the ^{99}Mo fission product, Canada is developing an alternative production route using cyclotrons for the direct production of ^{99m}Tc by the reaction 100Mo(p,2n)^{99m}Tc. However, these projects are subject to technical feasibility and economical viability, and will therefore not all be materialized.

WHERE OTHERS SEE COMPLEX PROBLEMS, MALLINCKRODT SEES UNIQUE SOLUTIONS

The new, independent Mallinckrodt Pharmaceuticals combines more than 145 years of expertise with the determined focus needed to solve the complex pharmaceutical challenges of today. Whether it's the production of medicines for pain or development of state-of-the-art imaging technology, we are working to make complex products simpler, safer, and better for patients.

Learn more at www.mallinckrodt.com

Mallinckrodt Pharmaceuticals

Tijdschrift voor Nucleaire Geneeskunde
ISSN 1381-4842, nr. 3, oktober 2013
Uitgever

KLOOSTERHOF
ACQUISITIE SERVICES - UITGEVERIJ

Kloosterhof acquisitie services - uitgeverij
Napoleonsweg 128a
6086 AJ Neer
T 0475 59 71 51
F 0475 59 71 53
E info@kloosterhof.nl
I www.kloosterhof.nl

Hoofdredacteur
prof. dr. J. Booij
j.booij@amc.uva.nl

Redactie
mw. drs. B. Bosveld
mw. drs. F. Celik
dr. J. van Dalen
dr. E.M.W. van de Garde
drs. A.W.J.M. Glaudemans
mw. dr.C.J. Hoekstra
dr. P. Laverman
A. Reniers
dr. H.J. Verberne
dr. O. de Winter

Bureauredactie
Yvonne van Pol-Houben
T 0475 60 09 44
E nucleaire@kloosterhof.nl

Advertentie-exploitatie
Kloosterhof Neer B.V.
acquisitie services – uitgeverij
Eric Vullers
T 0475 597151
E. eric@kloosterhof.nl

Vormgeving
Kloosterhof Vormgeving
Marie-José Verstappen
Sandra Geraedts

Adviesraad
prof.dr. F.J. Beekman
prof.dr. O.C. Boerman
prof.dr. J. Booij
prof.dr. E.F.I. Comans
prof.dr. R.A.J.O. Dierckx
prof.dr. A.A.M.S. van Dongen
prof.dr. B.L.F. van Eck-Smit
prof.dr. P.H. Elsinga
prof.dr.ir. M.de Jong
prof.dr.I. Goethals
prof.dr. O.S. Hoekstra
prof.dr. E.P. Krenning
prof.dr. A.A. Lammertsma
prof.dr. L. Mortelmans
prof.dr. W.J.G. Oyen
prof.dr. A.M.J. Paans
prof.dr. P.P. van Rijk
prof.dr. G.J.J. Teule
dr. R.A. Valdes Olmos

Abonnementen
Leden en donateurs van de aangesloten Leden en donateurs van de aangesloten beroepsverenigingen ontvangen het Tijdschrift voor Nucleaire Geneeskunde kosteloos. Voor anderen geldt een abonnementsprijs van € 45,00 per jaar; studenten betalen € 29,00 per jaar (incl. BTW en verzendkosten).
Voor buitenlandse abonnementen gelden andere tarieven. Opgave en informatie over (buitenlandse) abonnementen en losse nummers (€ 13,50) bij Kloosterhof acquisitie services - uitgeverij, telefoon 0475 59 71 51.
www.tijdschriftvoornucleairegeneeskunde.nl

Verschijningsdata, jaargang 35
Nummer 3: 1 oktober 2013
Nummer 4: 24 december 2013

Verschijningsdata, jaargang 36
Nummer 1: 1 april 2014
Nummer 2: 1 juli 2014
Nummer 3: 30 september 2014

Aanleveren kopij, jaargang 35
Nummer 4: 1 oktober 2013

Aanleveren kopij, jaargang 36
Nummer 1: 1 januari 2014
Nummer 2: 1 april 2014
Nummer 3: 1 juli 2014
Nummer 4: 1 oktber 2014

Cursus- en Congresagenda

Lustrumcongres 2013 NVKF
3 – 5 October, 2013. Twente, The Netherlands. www.lustrumnvkf.nl

Jaarlijks congres Nederlandse Vereniging voor Technische Geneeskunde NVvTG)
11 October, 2013. Utrecht, The Netherlands. www.nvvtg.nl/congres/

MRI guided Focused Ultrasound
18 October, 2013. Utrecht, The Netherlands. www.umcutrecht.nl/subsite/radiotherapy-research/Symposium/

EANM '13
19 – 23 October, 2013. Lyon, France. www.eanm.org

Lustrum NVNG
8 November, 2013. Rotterdam, The Netherlands. www.nvng.nl

EANM Dosimetry Course, advanced
14 – 15 November, 2013. Vienna, Austria. www.eanm.org

EANM/ESTRO Educational Seminar on PET in Radiation Oncology
22 – 23 November, 2013. Vienna, Austria. www.eanm.org

EANM Course on PET/CT in Oncology, advanced
28 – 30 November, 2013. Vienna, Austria. www.eanm.org

RSNA 2013
1 – 6 December, 2013. Chicago, USA. www.rsna.org/Annual_Meeting.aspx

Imaging infections and imflammation, 1st European course
12 – 14 December, 2013. Rome, Italy. www.eanm.org

2014
TOPIM 2014 – ESMI Winter Conference
19 – 24 January, 2014. Les Houches, France. www.e-smi.eu

3rd Tübingen PET/MR Workshop
17 – 21 February, 2014. Tübingen, Germany. www.pet-mr-tuebingen.de

NuklearMedizin 2014
26 – 29 March, 2014. Hannover, Germany. www.eanm.org

EMIM 2014 – European Molecular Imaging Meeting
4 – 6 June, 2014. Antwerp, Belgium. www.e.smi.eu

SNMMI Annual Meeting
7–11 June, 2014. St. Louis, Missouri, USA. www.snmmi.org/am2014

Adreswijzigingen

Regelmatig komt het voor dat wijzigingen in het bezorgadres voor het Tijdschrift voor Nucleaire Geneeskunde op de verkeerde plaats terechtkomen. Adreswijzigingen moeten altijd aan de betreffende verenigingssecretariaten worden doorgegeven. Dus voor de medisch nucleair werkers bij de NVMBR, en voor de leden van de NVNG en het Belgisch Genootschap voor Nucleaire Geneeskunde aan hun respectievelijke secretariaten.
De verenigingssecretariaten zorgen dan voor het doorgeven van de wijzigingen aan de Tijdschrift adresadministratie.
Alleen adreswijzigingen van betaalde abonnementen moeten met ingang van 1 januari 2011 rechtstreeks aan de abonnementenadministratie van Kloosterhof Neer B.V. worden doorgegeven: Kloosterhof Neer B.V., t.a.v. administratie TvNG, Napoleonsweg 128a | 6086 AJ Neer of per E-mail: nucleaire@kloosterhof.nl

Oldelft Benelux Medical Solutions

...Het hele spectrum aan gamma camera's...

AnyScan

X-Ring-R

CardioDESK

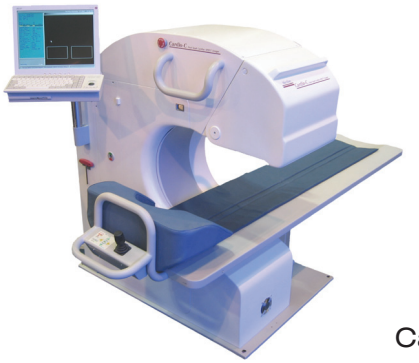

Cardio-C

X-Ring 4R

Nucline TH

...van kleine enkelkops tot geavanceerde SPECT-PET-CT combinaties.

Met Mediso levert Oldelft Benelux het hele spectrum aan gamma camera's; van kleine enkelkops, tot geavanceerde SPECT-CT-PET combinaties.

Oldelft Benelux heeft reeds meer dan 80 jaar ervaring in de verkoop en service van diagnostische apparatuur en innovatieve healthcare ICT systemen. Zij heeft zich ontwikkeld van producent van apparatuur naar System Integrator en Service Provider voor ziekenhuizen en zorginstellingen.

Voor meer informatie omtrent de Mediso oplossingen kunt u contact opnemen met uw accountmanager, of stuur een e-mail naar info@oldelftbenelux.nl.

Oldelft Benelux
MEDICAL SOLUTIONS

Oldelft Benelux B.V. Wiltonstraat 41 3905 KW Veenendaal The Netherlands
T +31 318 583 400 F +31 318 583 401 E info@oldelftbenelux.nl I www.oldelftbenelux.nl

GE Healthcare

Improving Heart Failure Risk Assessment

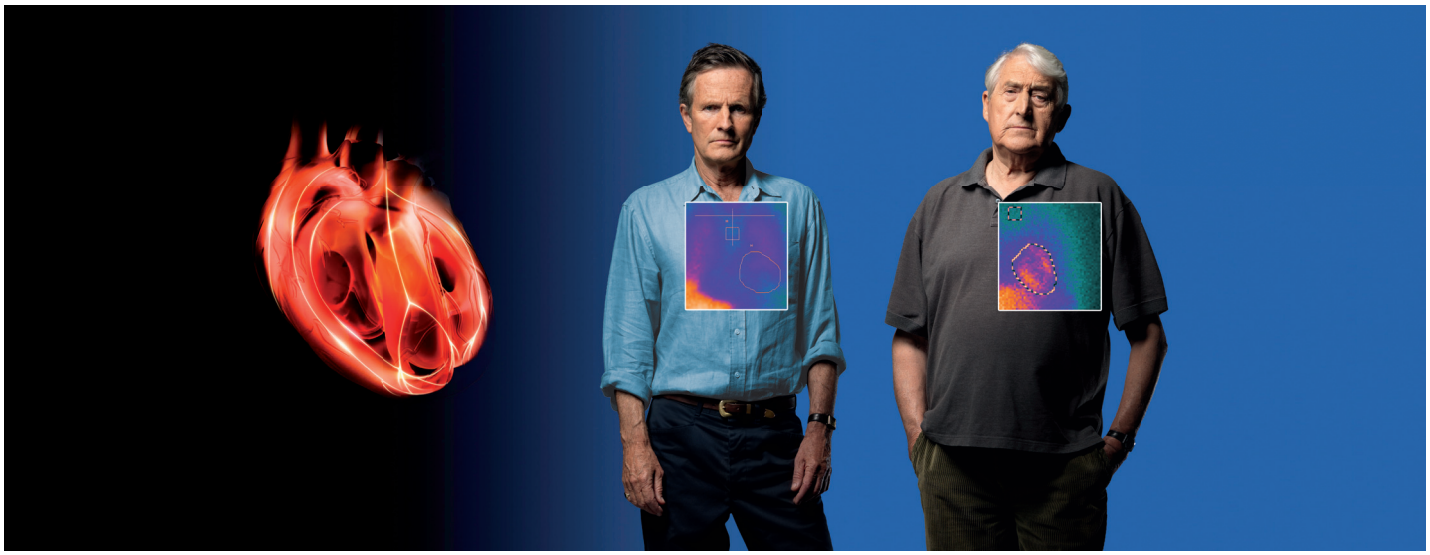

AdreView is a diagnostic agent providing a powerful prognostic insight into heart failure[1]

- Assesses cardiac sympathetic innervation[1]
- Helps predict patients who are at greater or lower risk of heart failure progression, arrhythmias & cardiac death[1]
- Provides a Negative Predictive Value (NPV) of 96% for arrhythmia likelihood & an NPV of 98% for cardiac death likelihood over 2 years[1]
- Provides superior prognostic information in combination with LVEF or BNP compared to LVEF or BNP alone[1]
- Improves heart failure patients' risk assessment and may help clinicians' management decisions[1]

GE imagination at work

AdreView™ Iobenguane I 123 Injection

AdreView is authorised for marketing in the following European countries: Germany, France, Spain, Italy, the United Kingdom, Denmark, Norway, The Netherlands and Belgium.

PRESCRIBING INFORMATION AdreView, Iobenguane (^{123}I) Injection 74 MBq/ml solution for injection
Please refer to full national Summary of Product Characteristics (SPC) before prescribing. Indications and approvals may vary in different countries. Further information available on request.
PRESENTATION Vials containing 74 MBq/ml [^{123}I]Iobenguane at calibration date and hour. Available pack size: 37 to 740 MBq. **DIAGNOSTIC INDICATIONS** • Assessment of sympathetic innervation of the myocardium as a prognostic indicator of risk for progression of symptomatic heart failure, potentially fatal arrhythmic events, or cardiac death in patients with NYHA class II or class III heart failure and LV dysfunction. • Diagnostic scintigraphic localisation of tumours originating in tissue that embryologically stems from the neural crest. These are pheochromocytomas, paragangliomas, chemodectomas and ganglioneuromas. • Detection, staging and follow-up on therapy of neuroblastomas. • Evaluation of the uptake of iobenguane. The sensitivity to diagnostic visualisation is different for the listed pathological entities. The sensitivity is approximately 90% for the detection of pheochromocytoma and neuroblastoma, 70% in case of carcinoid and only 35% in case of medullary thyroid carcinoma (MTC). • Functional studies of the adrenal medulla (hyperplasia). **DOSAGE AND METHOD OF ADMINISTRATION** Cardiology: For adults the recommended dosage is 370MBq. Children under 6 months: 4 MBq per kg body weight (max. 40 MBq), the product must not be given to premature babies or neonates. Children between 6 months and 2 years: 4 MBq per kg body weight (min. 40 MBq). Children over 2 years: a fraction of the adult dosage should be chosen, dependent on body weight (see SPC for scheme). No special dosage scheme required for elderly patients. Oncology: For adults the recommended dosage is 80-200 MBq, higher activities may be justifiable. For children see cardiology. No special dosage scheme required for elderly patients. Administer dose by slow intravenous injection or infusion over several minutes. **CONTRAINDICATIONS** Hypersensitivity to the active substance or to any of the excipients. The product contains benzyl alcohol 10.4 mg/ml and must not be given to premature babies or neonates **WARNINGS AND PRECAUTIONS** Drugs known or expected to reduce the iobenguane(123-I) uptake should be stopped before administration of AdreView (usually 4 biological half-lives). At least 1 hour before the AdreView dose administer a thyroid blockading agent (Potassium Iodide Oral Solution or Lugol's Solution equivalent to 100 mg iodine or potassium perchlorate 400 mg). Ensure emergency cardiac and anti-hypertensive treatments are readily available. In theory, iobenguane uptake in the chromaffin granules may induce a hypertensive crisis due to noradrenaline secretion; the likelihood of such an occurrence is believed to be extremely low. Consider assessing pulse and blood pressure before and shortly after AdreView administration and initiate appropriate anti-hypertensive treatment if needed. This medicinal product contains benzyl alcohol. Benzyl alcohol may cause toxic reactions and anaphylactoid reactions in infants and children up to 3 years old. **INTERACTIONS** Nifedipine (a Ca-channel blocker) is reported to prolong retention of iobenguane. Decreased uptake was observed under therapeutic regimens involving the administration of antihypertensives that deplete norepinephrine stores or reuptake (reserpine, labetalol), calcium-channel blockers (diltiazem, nifedipine, verapamil), tricyclic antidepressives that inhibit norepinephrine transporter function (amitryptiline and derivatives, imipramine and derivatives), sympathomimetic agents (present in nasal decongestants, such as phenylephrine, ephedrine, pseudoephedrine or phenylpropanolamine), cocaine and phenothiazine. These drugs should be stopped before administration of [123I]iobenguane (usually for four biological half-lives to allow complete washout). **PREGNANCY AND LACTATION** Only imperative investigation should be carried out during pregnancy when likely benefit exceeds the risk to mother and foetus. Radionuclide procedures carried out on pregnant women also involve radiation doses to the foetus. Any woman who has missed a period should be assumed to be pregnant until proven otherwise. If uncertain, radiation exposure should be kept to the minimum needed for clinical information. Consider alternative techniques. If administration to a breast feeding woman is necessary, breast-feeding should be interrupted for three days and the expressed feeds discarded. Breast-feeding can be restarted when the level in the milk will not result in a radiation dose to a child greater than 1 mSv. **UNDESIRABLE EFFECTS** In rare cases the following undesirable effects have occurred: blushes, urticaria, nausea, cold chills and other symptoms of anaphylactoid reactions. When the drug is administered too fast palpitations, dyspnoea, heat sensations, transient hypertension and abdominal cramps may occur during or immediately after administration. Within one hour these symptoms disappear. Exposure to ionising radiation is linked with cancer induction and a potential for development of hereditary defects. For diagnostic nuclear medicine investigations the current evidence suggests that these adverse effects will occur with low frequency because of the low radiation doses incurred. **DOSIMETRY** The effective dose equivalent resulting from an administered activity amount of 200 MBq is 2.6 mSv in adults. The effective dose equivalent resulting from an administered activity amount of 370 MBq is 4.8 mSv in adults. **OVERDOSE** The effect of an overdose of iobenguane is due to the release of adrenaline. This effect is of short duration and requires supportive measures aimed at lowering the blood pressure. Prompt injection of phentolamine followed by propanolol is needed. Maintain a high urine flow to reduce the influence of radiation. **CLASSIFICATION FOR SUPPLY** Subject to medical prescription (POM).**MARKETING AUTHORISATION HOLDERS.** DE: GE Healthcare Buchler GmbH & Co. KG, 18974.00.00. DK: GE Healtcare B.V., DK R. 1013. FR: GE Healthcare SA, NL 18599. NL: GE Healthcare B.V., RVG 57689. NO: GE Healthcare B.V., MTnr. 94-191. **DATE OF REVISION OF TEXT** 9 August 2010 .

GE Healthcare Limited, Amersham Place, Little Chalfont, Buckinghamshire, England HP7 9NA
www.gehealthcare.com

References: 1. Jacobson AF *et al.* Myocardial Iodine-123 *Meta*-Iodobenzylguanidine Imaging and Cardiac Events in Heart Failure. Results of the Prospective ADMIRE-HF (AdreView Myocardial Imaging for Risk Evaluation in Heart Failure) Study. J Am Coll Cardiol 2010;55.

10-2010 JB4260/OS INT'L ENGLISH